PROPAGATION CHANNEL MODELS FOR 5G MOBILE NETWORKS

Simulation and Measurements of 5G Propagation Channel models for Indoor and outdoor environments covering both LOS and NLOS Scenarios

WAQAS MANAN

BCS (Hons), MSc.

Submitted for the Degree of

Master of Philosophy

Faculty of Engineering and Informatics,

University of Bradford

2018

ABSTRACT

PROPAGATION CHANNEL MODELS FOR 5G MOBILE NETWORKS

Simulation and Measurements of 5G Propagation Channel models for Indoor and outdoor environments covering both LOS and NLOS Scenarios

Keywords
Propagation Channel, 4G, 5G, Indoor and Outdoor Propagation, Path Loss, Delay spread, Line of Sight (LOS), Non-LOS (NLOS), Wireless Communications, Shooting and Bouncing Ray (SBR)

At present, the current 4G systems provide a universal platform for broadband mobile services; however, mobile traffic is still growing at an unprecedented rate and the need for more sophisticated broadband services is pushing the limits on current standards to provide even tighter integration between wireless technologies and higher speeds. This has led to the need for a new generation of mobile communications: the so-called 5G. Although 5G systems are not expected to penetrate the market until 2020, the evolution towards 5G is widely accepted to be the logical convergence of internet services with existing mobile networking standards leading to the commonly used term “mobile internet” over heterogeneous networks, with several Gbits/s data rate and very high connectivity speeds. Therefore, to support highly increasing traffic capacity and high data rates, the next generation mobile network (5G) should extend the range of frequency spectrum for mobile communication that is yet to be identified by the ITU-R. The mm-wave spectrum is the key enabling feature of the next-generation cellular system, for which the propagation channel models need to be predicted to enhance the design guidance and the practicality of the whole design transceiver system.

The present work addresses the main concepts of the propagation channel behaviour using ray tracing software package for simulation and then results were tested and compared against practical analysis in a real-time environment. The characteristics of Indoor-Indoor (LOS and NLOS), and indoor-outdoor (NLOS) propagations channels are intensively investigated at four different frequencies; 5.8 GHz, 26GHz, 28GHz and 60GHz for vertical polarized directional, omnidirectional and isotropic antennas patterns. The computed data achieved from the 3-D Shooting and Bouncing Ray (SBR) Wireless Insite based on the effect of frequency dependent electrical properties of building materials. Ray tracing technique has been utilized to predict multipath propagation characteristics in mm-wave bands at different propagation environments. Finally, the received signal power and delay spread were computed for outdoor-outdoor complex propagation channel model at 26 GHz, 28 GHz and 60GHz frequencies and results were compared to the theoretical models.

ACKNOWLEDGEMENT

First and foremost, I would like to thank **ALLAH (S.W.T)** for giving me this opportunity to take on this journey. I wish to express my sincere appreciation who have supported and contributed to the success of this research.

I offer my sincerest gratitude to my Supervisor, *Prof Raed A. Abd-Alhameed*, who supported me throughout my research thesis for MPhil with his patience and knowledge. The completion of this thesis would not have been possible without a source of his suggestions, encouragement and efforts. Also, I would like to thank, *Prof Fun Hu* and *Dr. SMR Jones* for their valuable ideas, guidance and support throughout this work.

In addition, I would like to extend my thanks and appreciations for the faculty of engineering, staff, administration and all lab fellows of the University of Bradford for their great support and help.

I wish to express my deepest thanks to my lab fellows *Huthifa Obeidat* and *Ali Abdullah* for their endless support throughout my research.

Finally, special thanks are also given to my beloved parents for their financial support and encouragement through all my pursuits over this period.

TABLE OF CONTENTS

Chapter 3

Chapter 4

Chapter 5

Chapter 6

Chapter 7

LIST OF FIGURES

LIST OF TABLES

ACRONYMS

1G	First generation
NMT	Nordic Mobile Telephones
TACS	Total Access Communication Systems
2G	Second generation
TDMA	Time division multiple access
CDMA	code division multiple access
GSM	Global system for mobile communication
BSS	Base station subsystem
BTS	Base transceiver station
BSC	Base station controller
NSS	Network switching subsystem
MSC	visitor location register
VLR	Visitor location register
SMSC	Short message service centre
VMS	Voicemail service
GPRS	General packet radio services
SGSN	Serving GPRS Support Node
3G	Third generation

WCDMA	Wideband code division multiple access
LTE	Long-term evolution
4G	Fourth generation
OFDM	Orthogonal frequency division multiplexing
QoS	Quality of service
QoE	Quality of experience
SBR	Shoot and Bouncing ray
FIT	Finite integration techniques
5G	Fifth generation
MIMO	Multiple input and Multiple Output
LOS	Line of Sight
NLOS	Non-Line of Sight
mm-wave	millimetre wave
EHF	extremely high frequency
VHF	very high frequency
ITU-R	International telecommunication union- Radio communication
GHz	GigaHertz
3D	Three dimensions
3GPP	3rd Generation partnership Project

AP	Access Point
METIS	Mobile and wireless communications Enablers for the Twenty-twenty Information Society
ISI	Intersymbol Interference
UE	User Equipment
MS	Mobile Station
Tx-Rx	Transmitter to Receiver
dB	Decibels
FDTD	Finite-difference time-domain
MTOA	Mean time of arrival
TOA	Time of arrival
AOA	Angle of arrival
DOA	Direction of arrival
RSS	Received signal strength
ITU	International telecommunication union
dBm	decibel-milliwatts
DSO	Digital storage oscilloscope
FPGA	Field-programmable gate array

1. INTRODUCTION:

1.1 Background

In the last decade, there is remarkable developments, advancement and phenomenal growth in the telecommunication industry which acts an important role in our daily life. Generally, mobile communication is the transmission of a signal over a very large distance for information sending for which Mobile networks have experienced a huge growth in the telecommunication industry and it is differentiated from each other by generations. Mobile network generations concept started early in the 1980s, have faced massive challenges, changes and proven extensive growth.

Cellular coverage improvement is a major and important research area in a wireless communication industry. Over the last few years, wireless communications have been experienced by demanding higher data rates, large capacity and good quality of services. Minimizing the distance between transmitter and receiver can achieve the high data rate benefits to the end users, which is economically challenging by demanding more base stations in a network. First, in the start, wireless communication system was been designed for voice calls and transmission of data (and messages), while now wireless equipment required high data rate applications such as fast video streaming and file transfer which is the real challenge for the system to be achieved.

First generation mobile network called 1G used analogue transmission for speech services. Nordic Mobile Telephones (NMT) and Total Access Communication Systems (TACS) were the most popular analogue system in terms of cellular mobile networks. This analogue system offered handover and roaming capabilities that were unable to interoperate between countries and one of the inexorable disadvantages of the first-generation mobile network.

Then the second-generation mobile network (2G) introduced, that used digital multiple access technologies, time division multiple access (TDMA) and code division multiple access (CDMA) with high spectrum efficiency, better data services and advanced roaming. GSM (Global system for mobile communications) used TDMA to support various users. The main component of GSM system is the Base station subsystem (BSS), Base transceiver station (BTS), Base station controller (BSC), network switching subsystem (NSS), Mobile switching centre (MSC), visitor location register (VLR), Authentication centre (AC) and Equipment Identity Register (EIR). All of these elements are able to provide services of up to 9.6kbps and the base station services was able to reduce the load on the first-generation mobile network. The new advancement in GSM technology was by adding two important platforms called short message service centre (SMSC) and the second one was voice mail service (VMS).

Further new services were added to the GSM system called (SGSN) servicing GPRS and (GGSN) gateway to GPRS to make possible by sending data through the packet core network. The 2.5G network starts with GPRS (General packet radio services). GPRS is defined as the radio technology for GSM that consist of

packet switching protocols that set the time shorter for ISP. Packet switching is the technique that in which the information to be sent is broken into packets than routed the data within each packet. GPRS is an important way to towards 3G [9]. During this period of 2G, research was already going on 3G.

UMTS (Universal mobile telecommunication system) is for 3rd generation mobile network that provides telecommunication services like voice, low and high data, multimedia etc. used to improve spectral efficiency [10]. 3G (Third generation mobile network) system's structure has many protocols and complicated work structure like WCDMA (Wideband code division multiple access) and cdma2000 to cover system architecture. To cover and solve these Problems, 4G (Fourth generation mobile network) introduced to create an All-IP based packet switched system, as to IP backbone. Figure 1.1 shows the time period of mobile networks generations and its specification.

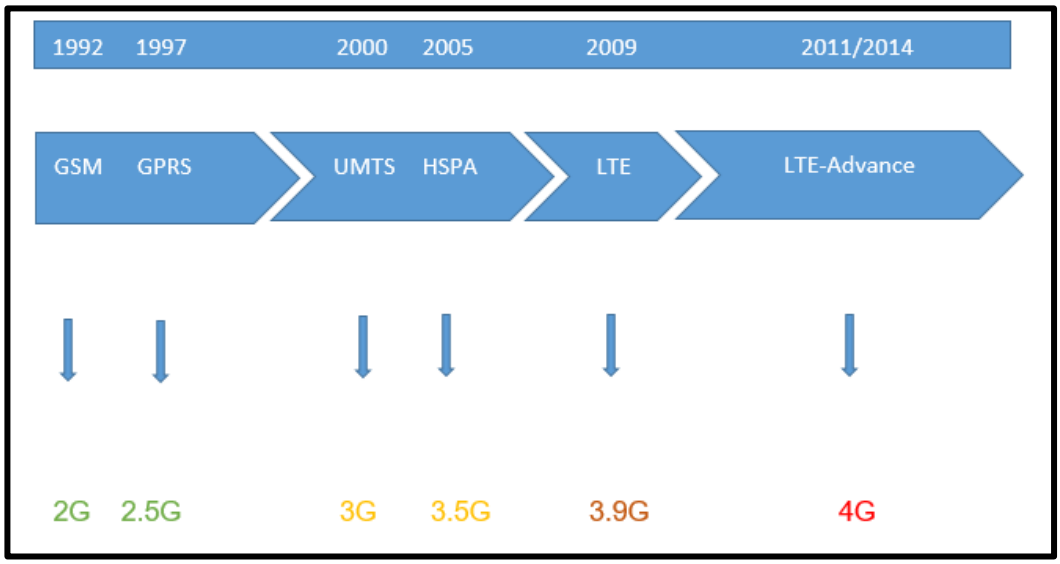

Figure 1.1: Mobile networks time-period and specification

In order to increase the demand of data rate, enhancing system capacity, 3GPP initiate LTE-Advance (LTE-A) for 4th generation (4G) that introduces the speed of 100 Mb/s for the downlink and 50 Mb/s for the uplink. The most important goal of LTE-A is to provide cell edge performance in networks, which was ignored by the previous generation in a particular area. The main function of 4G network technology is orthogonal frequency division multiplexing (OFDM) that divide the spectrum into orthogonal subcarriers.

By providing wireless services at any time and anywhere stated in [11], terminal mobility is an important and must in 4G infrastructure and have faced two main issues: hand-off management and location management. Hand-off management maintains communication when terminal roams while on the other hand location management handles the information about the roaming terminals.

1.2 Overview and Motivations:

In the field of the wireless communication system, models, methodologies, and even measurements are being designed to process precise channel modelling of real-world wireless systems. The percentage of indoor wireless data traffic has been increased in the communication system, which involves radio links partially indoor and outdoor environment.

Macro cells, mostly called large cells, with wide range are not efficient to provide indoor coverage, experience the attenuation through walls, floors, objects and ceiling resulting weak signal strength. Small cells are low powered base station with smallest coverage range in meters typically designed and installed inside the

buildings to provide better coverage, as when there is poor macro cells coverage. Using limited radio resources is one of the key challenges for network planners to achieve coverage and capacity requirements. Network operators integrate small cells inside the macro cell's network by reusing the spectrum to spread traffic load and maintain the quality of service (QoS) that bring a set of challenges, which requires accurate measurement of signal strength and path loss.

The whole computing systems technology into a detailed deterministic or site-specific model has been one of the most important fusions over the last century for planning tools. The software packages and tools run simulated channel models in pragmatic designed environments by doing prediction to where and how the wireless communication equipment will be able to attain the higher accomplishments.

For the utilization of radio propagation predictions and modelling, 3D (the three dimensional), ray-tracing model (SBR) is one of the most promising techniques [12], Some low-level computational effort needs for a standard PC to allow analysis, which normally requires greater processing time, high speeds and memory availability. Many methods and techniques have been successfully applied in the research field to model propagation channels, but not all reproduce, all attributes of the real channel models, which are required to accurately estimate for the production of complex broadband systems to make full use of both time and frequency.

Some previous research work presented and explained propagation models that are developed to predict the loss of signal strength or coverage at a specific location, path loss measurement with a simulation using finite integration techniques (FIT) to obtained accurate results which need high computational efforts. Thus, more scientists used mathematical tools to plan wireless communication systems. In wireless communication, the losses are between transmitter and receiver are called propagation path loss in [13]. The recent active interest for research work is the use of multiple antennas in wireless communication is called MIMO (Multiple Input and Multiple Output) where multiple antennas used both at transmitter and receiver. MIMO requires a propagation channel model to achieve a wireless communication performance in a particular environment [14]. The most favourable method to evaluate MIMO propagation model in wireless communication is the deterministic, 3-D shoot and bouncing ray-tracing model (SBR) because it only requires middling computing endeavour (efforts) [15]. This can acceptably give accurate divination over an indoor and outdoor environment.

1.3 Aim and Objectives of the Research Project:

The aim of this research is to investigate and discuss the properties of wireless propagation channel in a new environment that entail buildings and scenarios of indoor-indoor, indoor-outdoor and outdoor-outdoor propagation in a wireless communications system. Different types of antenna radiation patterns with a waveform from a lower frequency to higher frequencies are investigated, which is the requirements of the next generation network (5G).

The objectives of work are identified to:

- Understand the current approaches for the next-generation mobile network, mm-wave and the propagation channel models in the literature review and able to model and simulate ongoing broadband wireless communication system.

- Develop the propagation model for small cell scenario includes indoor, indoor-outdoor and outdoor-outdoor and simulate channel modelling for performance assessment.

- Characterise the wireless channel by examining channel parameters with lower to higher frequencies, using different antennas, and polarisation to compare the individual parameters in different environments including LOS and NLOS. The simulation results were then tested for practical analysis in a real-time environment.

- Obtain the performance of the system using the propagation channel model with path loss, received signal power, delay spread, mean direction of arrival.

- Contribute fully to the new techniques which enhance the performance of the system. To investigate the Channel impulse response power density

and delay for both simulation and measurements of indoor real environment in mm-wave spectrum.

The simulation model for multi-storey office environment was created using wireless insite to evaluate the channel propagation for indoor LOS, NLOS and indoor to outdoor (NLOS) scenarios. The model includes the details of the building and its materials used where the signal strength at the receiver, path loss and delay spread were evaluated. In addition, the mean direction of arrival and mean arrival time were also investigated. This was done for four frequencies including mm-wave spectrum with different antennas radiation patterns.

The simulation results for indoor channel propagation of mm-wave were tested for practical analysis in a real environment of third floor B wing of Chesham building at University of Bradford for complex impulse response power density against delay and the simulated results and measured results were computed for LOS and NLOS.

Second simulation model is for city centre which represents many tallest buildings with different heights, dimensions and structures were modelled, to evaluate the channel propagation for outdoor-outdoor scenario. This gives the general framework for MIMO configuration with mixed LOS and NLOS for three different spectrums. In mixed LOS and NLOS MIMO transmission, multipath richness exists depending on the size, height and location of the buildings, where received signal strength and delay spread evaluated.

1.4 Organization of the thesis:

The thesis is organized by the following chapters:

Chapter 2: This chapter presents an introduction to next-generation mobile network (5G) and channel propagation model. It explains the basics of wireless channel propagations and the requirements of the new channel model supporting 5G. Also, this chapter gives the description of multipath propagation mechanism to differentiate LOS and NLOS.

Chapter 3: This chapter provides a brief introduction of propagation prediction models to overcome the challenges of propagation phenomenon. Two types of approaches that can be used for channel models are presented. Finally, different channel parameters to characterize the behaviour of the channel with expressions for research work are presented.

Chapter 4: A simulation model for the multi-storey office environment is developed to evaluate the channel propagation for indoor-indoor and indoor-outdoor scenarios with different frequencies and different antennas radiation pattern, the model includes the details of the building in term of dimensions and materials used, where path loss, received signal power, delay spread, and mean direction of arrival were evaluated.

Chapter 5: Applying a 3-D SBR technique of the ray paths, an indoor multipath channel propagation for mm-wave was simulated using Wireless Insite and the

results accuracy compared to the results obtained from measurements of the complex channel impulse response power and delay(s).

Chapter 6: The simulation for urban city model is developed to evaluate the channel propagation for the outdoor-outdoor scenario of different mm-wave frequency bands. The model includes many buildings with different structures, faces and dimensions where received signal strength and mean delay spread were evaluated for mixed LOS and NLOS.

Chapter 7: The overall conclusion of the research work and further extensions of the work are discussed in this chapter.

2. LITERATURE REVIEW

2.1 Introduction:

In this chapter, the next generation mobile network (5G), millimetre wave (mm-wave), recent channel modelling activities, basics of wireless propagation channels, new channel requirements and propagation mechanisms are briefly overviewed. The mobile data services lead the improvement from 3G to 4G mobile networks to increase the data rate. The high growth of data traffic in mobile networks are due to the high access to data communication system anywhere, any time and the demand for high data rates.

This drove the research to design the next generation of mobile communication. It is stated in [16] that to meet the expected growth of wireless communications traffic, both efficient transmission schemes and additional spectrum allocations are needed. The transmitted signal is not only in the direct path but follow a various number of propagation paths commonly known as multipath propagation. High frequencies of the mm-wave ranges are the most promising prospects for additional spectrum and the corresponding extensions of propagations are needed.

2.2 Next Generation mobile network (5G):

The telecommunication industry players are preparing a time frame to introduce the fifth-generation mobile network (5G) for the wireless telecommunication by

around 2020. Fifth generation 5G will need to deliver much improvement in cell capacity to accommodate the increasing traffic demands. As 5G will be the new technology that will enable networks and devices for better spectrum resources and it is expected to reach several Gbits/s data rates in supporting the mobile and wireless applications. The usage scenarios proposed by ITU-R are grouped into three categories: enhanced mobile broadband, massive machine type communications, reliable and low-latency communications. Energy efficiency, peak data rate, traffic capacity, mobility and spectrum efficiency etc is a key performance indicator, referred as a technical requirement [17].

It is well known that mobile data consumption is increasing with the passage of time, by increased penetration of smart devices like smartphones, tablets, better hardware, better user interface design and the design for anywhere, anytime high-speed connectivity. About more than 70% of data usage is indoor in homes, offices, malls, train stations and public places. If the mobile data traffic is increasing, then the signalling traffic is increasing by 50 % than the data traffic.

To support highly increasing traffic capacity and to enable the transmission bandwidths needed to support very high data rates, 5G will extend the range of frequencies used for mobile communication. Spectrum for mobile communication in higher frequency bands is yet to be identified by the ITU-R. Wireless communication industry remains challenger about particular choices, and the entire frequency range up to approximately 100GHz is under consideration at this stage [18]. It means that the mm-wave bands will be used for the fulfilment of 5G

mobile networks systems, which needs the propagation channel models to design the system.

2.2.1 Technical Requirements for 5G:

The new technical requirements were suggested to overcome the limitations of 4G mobile network and the requirements of 5G networks in terms of wireless technologies to provide for each service are summarized in Table 1[17]. In table 2.1 there are seven wireless technologies required included with a detailed description. The first three requirements are needed in the scenario of IoT and put it in the first tier, while the remaining requirements mentioned are placed in the second and third tiers because of its limited scenarios.

Table 2.1: Technical Requirements for 5G

Technical Requirements	Description
Ultra-high speed	• Tens of Gbps peak data rate • Up to 1 Gbps user experienced data rate • Areal capacity of 10 Mbps per square meter
Massive connection	• Identify all devices (maximum of one trillion devices) over the world. • Services to a million terminals per square kilometre.
High reliability	• 99.999% service availability even in an extreme situation. • Guarantee a single packet transmission failure per 10,000 or 100,000 transmissions.
Ultra-low latency	• Less than 1ms latency over the radio interface
High mobility	• seamless connectivity to moving terminal at speed of 500 km/h
High energy efficiency	• Improvement of 100 times energy efficiency per bit.
High cost-effectiveness	• Improve cost-effectiveness in network side even handling the huge volume of traffic Reduction of devices

The eight major requirements of the next-generation 5G system in educational and industrial research as stated in [19, 20] are identified as:

1. *1 - 10 Gbps data rates in real networks:* This is almost 10 times increase from traditional LTE network's theoretical peak data rate of 150 Mbps to provide ultra-high speed.

2. *1 ms round-trip latency:* Almost 10 times reduction from 4G's 10 ms round trip time.

3. *High bandwidth in the unit area:* It is needed to enable a massive number of connected devices with higher bandwidths for longer durations in a specific area and deliver services to a million terminals per square kilometre.

4. *An enormous number of connected devices:* In order to realize the vision of IoT, emerging 5G network needs to provide connectivity to a thousand devices.

5. *Perceived availability of 99.9%*: The next generation envisions that wireless network should practically be always available.

6. *Almost 100% coverage for 'anytime anywhere' connectivity*: 5G wireless networks need to ensure complete coverage irrespective of users' locations.

7. *Reduction in energy usage by almost 90%*: Development of green technology is already being considered by standard bodies. This is going to be even more crucial with high data rates and massive connectivity of 5G wireless.

8. *High battery life:* Reduction in power consumption by smart devices is fundamentally important in emerging 5G mobile networks.

2.2.2 5G Mobile Network Challenges:

However, telecommunications companies and the International Telecommunication Union (ITU) have been working on requirements for the next generation since the last standardization of the International Mobile Telecommunications. In this section, we will overview the open major research challenges relating to a 5G mobile network that is being addressed categorically.

1. **Computations and Complexity:**

As 5G network devices are being proposed, supporting high data rates at any time and anywhere. To achieve this, the wireless communication nodes will be intelligent and have the ability of sensing by selecting the appropriate channels without forming any harmful interference to the other users. These type of functions require a high complex number of implementation [21].

2. **Capacity and Data rate:**

Before 2020 mobile networks will have a need to support a 1000-fold rise in traffic relative to 2010 levels, and from 10- to 100-fold increase in data rates even at

high mobility and in crowded areas if current trends for wireless devices continue. The higher spectrum, 3D MIMO and new air interface, small cells, local offload are some of the key enablers to address this challenge in the radio access network (RAN) [22].

3. Massive Number of Connecting devices:

Devices need to be able to range from sleeping until needed to always-on yet get the connectivity when required. Handling an increasing number of devices that may pop in and out of connection constantly will be a challenge for next-generation mobile network. Fourth generation (4G) is not an ideal mobile network to handle a massive number of connectivity because current systems are disconnected. A combination of advances in air interface design, signalling optimization, and intelligent clustering and relaying techniques can all contribute to support hyperconnectivity as stated in [23]

4. Quality of Experience (QoE):

Quality of experience and quality of services[24] describes the subjective perception of the user as to how well an application or service is working. The applications of the video are entirely depending on the quality of the delivered video in the context of the display on which the video is shown. Delivering the video application with a very low QoE leads it to user dissatisfaction. As a challenge for 5G is to support quality services with a consistent level of (QoE) anywhere and anytime[23].

5. **Cost:**

It is important to lower the infrastructure cost as well as associated with their deployment, sustainability, management, and operations to make connectivity available universally, affordable. The challenge for the design of 5G is that huge improvement is needed to address the new requirements that address all the new requirements at the cost which will make the service maintainable. There is one way to reduce the cost that is to minimise the number of functionalities by implementing one-layer functionality in the base station to a high layer functionality of a network cloud which will serve many base stations. This will reduce the operation cost [25]. Energy-efficient hardware design, low-power backhaul, and intelligent energy management techniques, especially in ultra-dense networks, to put base stations to sleep when not in use can all contribute to reducing the cost of operating a network.

2.3 Millimetre wave (mm-wave):

Millimetre-wave, referred to as mm-Wave, is the band of spectrum between frequencies of 30 GHz and 300 GHz. The wavelength for mm-wave is very short ranging from 10mm to 1mm and has high atmospheric attenuation, even absorbed by the gases in the environment which reduces the strength and the range of the wave. A small wavelength allows implementation of a large number of antenna elements in the current size of radio chips. Use of the proper beamforming, the large antenna array delivers high antenna gain for both transmitter and receiver, which can recompense for the high path-loss without any extra amount of transmission power. In addition the direct transmissions, mm-Wave communication encounters a directed channel, for which, a communication

link will be established in a particular direction within a range that varies according to the directionality level [26, 27].

Millimetre wave is also known as extremely high frequency (EHF) or very high frequency (VHF) by the International Telecommunications Union (ITU). Millimetre wave is a band of spectrum that can be used in a large range of products and services such as, high speed, wireless local area network (WLAN) and broadband access. In wireless communication, a millimetre wave is used for a variety of services on mobile and wireless networks, as it allows for higher data rates up to 10 Gbps. Due to its small range of about a kilometre, mm-wave travels by LOS, so its high-frequency wavelengths can be blocked by objects like buildings and trees. Millimetre-Wave will be used for access channels in 5G cellular networks and will operate in a different manner from conventional cellular systems below 6 GHz [28].

Radio wave propagation is affected by diverse physical mechanisms as explained in section 2.4.1. The frequency dependence of reflections, which are the main reason for multipath propagation, is mainly related to surface roughness. The roughness of typical exterior building materials only moderately affects propagation in the lower GHz range. However, in the mm-wave band it may decide between receiving a beneficial near-specular reflection path and none. Diffraction effects decrease rapidly as frequency increases. In the millimetre-wave band, they are typically only relevant if the size of the obstacle is quite small as in the order of tens of cm [29].

2.3.1 The Role of mm-wave in 5G:

Millimetre-wave is being actively followed by academia, standard organizations, regulatory commissions, and industry insiders as a key enabler of 5G by allocating higher bandwidth to provide faster, higher-quality video, and multimedia content and services. Today, mm-wave spectrums are mainly used for indoor applications. Mobile networks have avoided the high-frequency bands because of its high propagation loss and poor building penetration, while on the other hand, the advanced technology has made mm-wave commercially feasible prospects [30].

The main objective of the mm-wave based Mobile radio Access network for fifth Generation Integrated Communications project is to develop and design new concepts for mobile Radio Access Technology (RAT) for deployment in the frequency range 6–100 GHz. The key aim is to develop validated advanced channel models, should base on statistically significant measurement data from different scenarios and in multiple frequency bands within the entire range from 6–100 GHz. The radio channel measurement campaigns at various locations in Europe are currently being carried out. The main objective is to lay out the basis for a new modelling approach of mm-wave-specific propagation behaviour and a unified statistical channel model for system level simulations, which is valid over the entire frequency range [31].

With the high growth of mobile data demand, the next generation mobile network (5G) would exploit the enormous amount of spectrum in the mm-wave bands to increase communication capacity. The main differences between the mm-wave

wireless communication and the other existing wireless system are especially in terms of propagation losses, directivity and sensitivity to blockage. With high bandwidth in the millimetre wave (mm-wave) band from 30GHz-300GHz, mm-wave communications have been proposed to be an important part of the 5G to provide multi-gigabit wireless services. For 60GHz band, there are two standards for mm-wave communication; IEEE 802.15.3c and IEEE 802.11ad.

2.3.2. Research Challenges of mm Wave in 5G Network:

The emerging mm-wave frequencies for 5G raised many new challenges in mobile wireless communications. The primary challenge is un-availability of any standard channel model. The key research challenges of millimetre wave in terms for the 5G mobile network is mentioned in as below:

1. 5G is expected to introduce mm-wave spectrum ranging from 30-300 GHz and the propagation characteristics of mm-waves are very less conducive for a wireless communication system, as compared to the current “beach-front spectrum”. However, the first main challenge is to examine the physics behind mm-waves, such as atmospheric absorption, diffraction, propagation, scattering, refraction, reflection, multipath and attenuation [19].

2. Mm-waves propagation is commonly dependent on environmental conditions, receiver and transmitter locations. Thus, specific cell design can be a key feature of 5G deployment. As this challenge is not much

investigated in legacy cellular systems and it requires further research[32].

3. Mm-wave mobile communication for the development of 5G requires a fundamental understanding of radio channels. The researchers are mainly focused on channel models for indoor, outdoor and fixed mm-wave communications. There is still needing to deeply investigate the mm-wave channels in outdoor environments to identify the effects of path loss, angular spread, delay time, NLOS beamforming and blocking issues [33].

4. Mm-wave frequencies have a smaller wavelength that allow placement of hundreds of antenna elements in an array. Large antenna arrays are capable to direct the beam energy and collect it coherently. One of the focus of on-going research is directional narrow beam communications. It changes the whole cell concept. The Cell concept depends on the C-plane/U-plane splitting. The C-plane is provided by eNodeBs (eNBs) for all the users within the network, while the U-plane is for mm-wave small cells only for the users within the ultra-capacity coverage. Hence, the radio resource control (RRC) connection phase between the user equipment and the mm-wave small cells, e.g., channel establishment and release operations, are directly controlled by the eNB. Although mm-wave small cells do not provide cell identification signals, they might be directly accessed through the eNB signalling. [34]. There are a number of research challenges for architecture design of both BS and mobile device to achieving the desired directivity.

5. The design of real-time baseband modem, mm-wave radio frequency (RF) circuitry and related software to provide beamforming technologies are interesting areas of research[35].

6. As discussed in the 5G requirement section (2.2.1) a round-trip latency of 1ms is identified as a requirement of 5G. However, a very little research work defining ways of achieving this important requirement. Low latency is also crucial for achieving a high quality of experience. QoE presents a number of many research challenges due to its subjective nature.

7. There is a vast scope for discussion on overall 5G architectural requirements with a massive deployment of LTE, the possibility of 5G architecture in any backward compatible would be greatly useful and vital. Along with standalone 5G systems, research work has utilised the feasibility for integration of 5G with legacy 4G/3G networks[19].

8. Also, mm-Wave systems will be inherently built of small cells, which means that path losses and cell association also change rapidly. From a systems perspective, this implies that connectivity will be highly intermittent, and communication will need to be rapidly adaptable. The channel will change in the order of hundreds of microseconds, much faster than today's cellular systems.

2.4 Radio propagation:

The phenomenon in which the radio waves propagates and transmitted from one point to another point and affected by various parts of the atmosphere. Building structures such as houses, flats, and offices in suburban areas with different size ranging from a few meters to tens of meters, influence the wireless propagation channels. Size of the structures can be larger in urban areas, so the features of these structures are same or even greater than the wavelength of the transmitted signal. This may block the radio wave causing diffusion. As a result, the mobile station (MS) may receive a signal via multiple paths instead of the direct signal.

In the multipath channel propagation, the transmitted signal from the transmitter reaches at the receiver points via multiple echoes due to the propagation mechanisms such as reflections, diffraction and scattering briefly explained in Section (2.5). These echoes, in some cases, make it feasible that enough power reaches to the receivers, so that the communication links are also feasible, especially when the direct signal is blocked. One important effect is characterised in mobile propagation is multipath where two level in the state of change of received signal as a function of Tx-Rx separation distance, namely, very slow variation due to the range and fast or short-term variations due to multipath. Multipath is a very important factor in wireless communication at which the receiver (MS) is normally at low height surrounding by obstructions [36].

2.4.1 Propagation Model Mechanisms:

Propagation introduces the dissimilarity of signal or ray amplitude and stage with respect to distance covered by propagation wave. Free space communication, a

line of sight (LoS), transmission, reflection and diffraction are the several estimated propagation mechanisms.

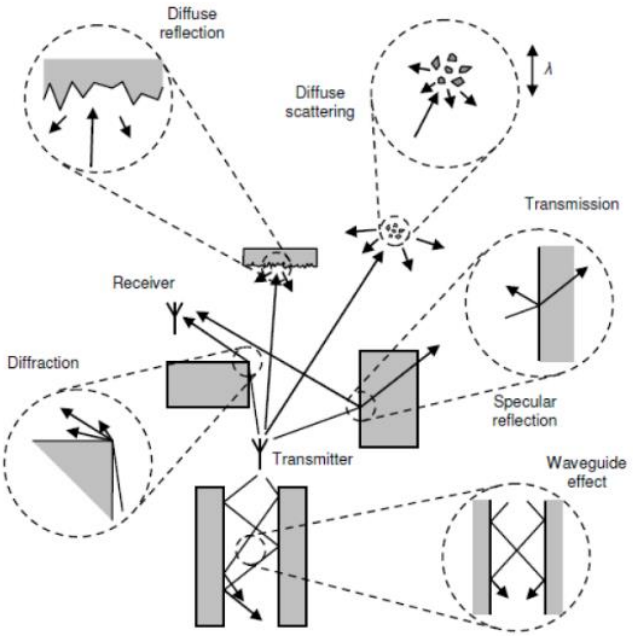

Figure 2.1: Multipath propagation mechanisms

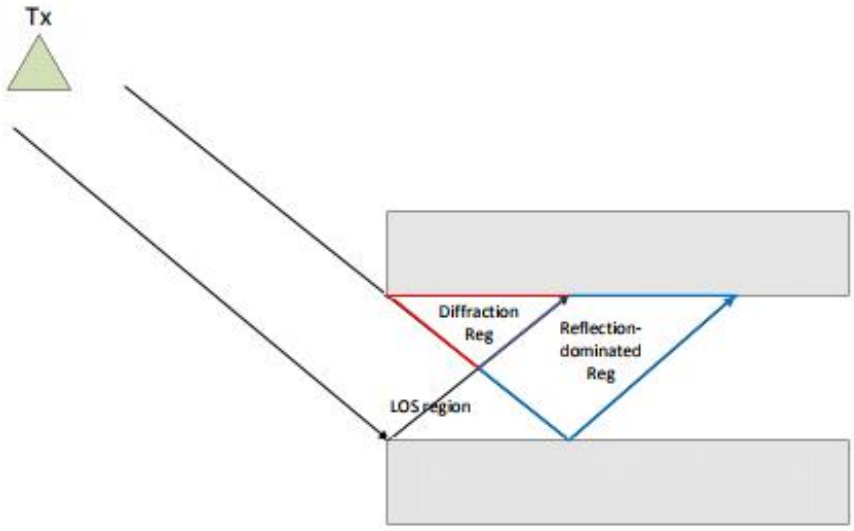

Figure 2.2: Reflection and diffraction dominated region [11]

It is common that transmission of the signal is not only in the direct path but also in a various number of propagation paths. The line of sight (LOS) is not available all the time so, in the case of Non-line of sight (NLOS), indirect paths are very

important for efficient communication explained in [37]. Multipath propagation concept can be illustrated in Figure 2.1. Figure 2.2 represents the reflection dominated and the diffraction dominated region in an idealised scenario.

The phenomenon of radio wave propagation is as:

- **Reflection:** When the radio wave hits to an object in front of it which is very large compared to its wavelength, then the wave gets reflected by that object. In such case, the direction of the reflected ray is ruled by the Snell's law of reflection. When a ray is reflected at many angles other than one angle because of surface roughness, the reflection is called diffuse reflection.

- **Diffraction:** When a ray hits an untrodden or edge of the large size object compared to its wavelength, the ray bends at the edges of the object, propagating in different directions governed by Fresnel principle.

- **Diffusion:** As clearly shown in Figure 2.1 when a wave hit the group of small objects or obstacles with respect to its wavelength, then the wave corresponds as like as the phenomenon of random diffraction. In this case, the incident wave handled in a statistical way is called diffusion. This happens mostly in indoor environments, may occur on a group of small objects.

- **Transmission:** The mechanism in which the ray reflected from the material and part of the incident wave travels inside the material is called transmission.

The radio propagation mechanisms based on the above phenomenon and the medium can be affected by three parameters: permittivity ε, conductivity σ, and permeability μ. These parameters are called constructive parameters of medium [38].

When plain radio wave propagates from a medium with physical properties, having a permittivity ε_1, conductivity σ_1 and permeability μ_1 to other medium having different permittivity ε_2 , conductivity σ_2 and permeabilityμ_2, the refraction can be happened at the boundary of the media with the same frequency as the incident wave, follows Snell's law of reflection.

From (Figure: 2.3) K_i is the incident wave arrives at angle θ_i and after reaches the interface, it breaks into two sections, K_r the reflected wave and K_t the transmitted wave. The transmitted wave here at this position is also called the refracted wave. This reflected and refracted waves travel in direction with θ_r and θ_t respectively [2].

According to Snell's law of reflection and refraction, we have the following expression:

$$\theta_i = \theta_r \qquad (2.1)$$

$$K_i Sin\theta_i = K_t Sin\theta_t \quad (2.2)$$

From Eq. (2.2) the incident angle and reflected angle are the same depending on the physical properties of each medium.

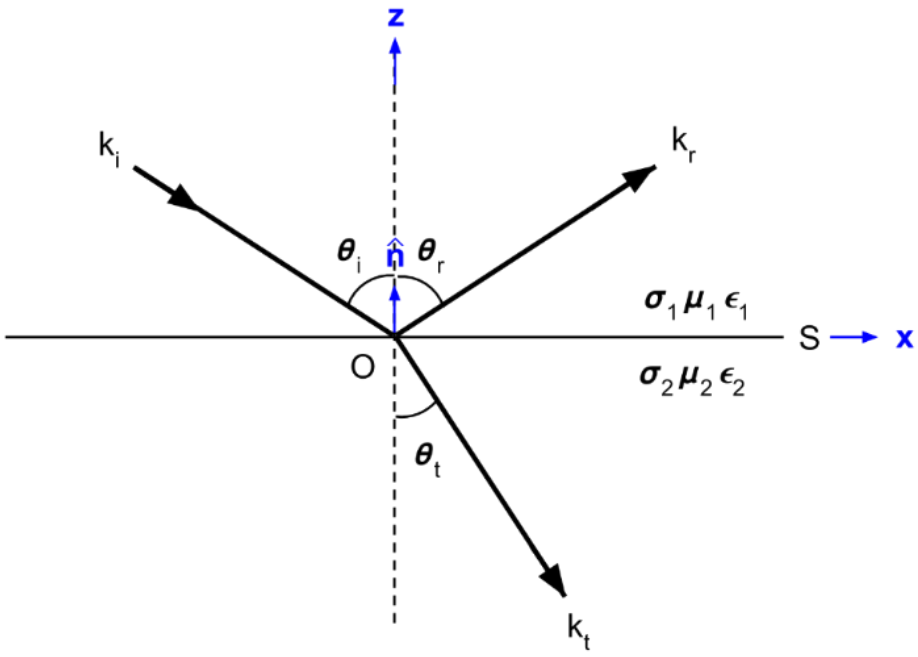

Figure: 2.3 Reflection and refraction*[2]*

The above is for smooth surface but when the surface is very rough and irregular, there will be a large number of scattered waves of the main reflected wave, which is a special case in reflection phenomenon. This means that the radio wave can be reflected in many non-uniform and uneven objects or surfaces and spread in a small opening is called diffraction. Diffraction defines the leakage of the field in the shadow region behind the edge of the objects. Single knife-edge model is the acceptable predicted model of diffraction in some cases to give the position of the knife-edge collision of the diffracted waves [39]. The typical obstructions for

5G[40] involve common building separation which is simple in nature, with dimensions that appear at such small wavelengths, like a wall and building edges can be justified simple diffraction models.

2.5 Propagation Channel Modelling:

Wireless channel models depend on channel parameters including carrier frequencies, bandwidth, the 3D separation distance between the transmitter (TX) and receiver (RX) and local environmental effects, needed to create a standardised system. The common challenge for 5G channel model is to provide a basic physical basis, while flexible and accurate across a large frequency range 0.5GHz – 100GHz [41]. Recently the research work in propagation channel modelling is to understand the mechanisms of the propagation and the behaviour of the channel at frequencies above 6GHz been published in [33, 42, 43]. In the referenced work, the specific type of antennas and many measurements collected vary widely.

Signals are transmitted from the transmitter as stated in [44] less than 10GHz not experiencing any remarkable impact from the atmosphere as compared to the mm-wave bands. Therefore, in a 5G network system, the effects of the local environments must be taken into account. Multipath propagation is included in the local environmental effects as well as the large-scale effects (free space loss). The penetration losses of buildings for indoor to outdoor are also different as compared to the 3GHz bands. So, the propagation channel effects, need to be modelled theoretically with experiments.

Wireless communication industry gets benefits in defining path loss for LOS and NLOS in different conditions. It predicts that when a user equipment (UE) is within the clear LOS of the Transmitter (TX) or in an NLOS part due to obstructions. The LOS channel propagation provides more reliable performance in an mm-wave communication system as compared to the NLOS environment, given the diffraction loss at higher frequencies comparatively at 6GHz, where the diffraction is the dominant propagation mechanism and provide high path loss component as compared to LOS [41].

2.5.1 5G Channel Modelling activities:

In 2015, many numbers of researchers including universities and industry partners published a paper about 5G channel model for up to 100 GHz frequency bands and have discussed different relevant aspects for 5G channel modelling[45]. This white paper has proposed a 3GPP 3-D as a good starting for modelling channel from 2GHz up to 100GHz and in addition, also stated that modification of existing steps to a new step may be needed.

There are several projects and groups whose ongoing activities are for the development of channel models named METIS, MiWEBA, ITU-R, COST2100, IEEE 802.11 and NYU wireless. Their work on channel modelling is briefly explained as:

Mobile and wireless communications Enablers for the Twenty-twenty Information Society (METIS) identified 5G requirements and performed channel measurements for different bands such as 2GHz and 60 GHz as well as provided

different channel model methodologies and their focus is on outdoor, indoor cafeteria and shopping mall scenarios. MiWEBA addressed various challenges for channel modelling such as environment dynamics, spherical wave modelling, Shadowing, spatial consistency, dual mobility Doppler model, the ratio between diffuse and specular reflections, polarization and performed channel measurements at 60 GHz. The ITU-R is focused to address the propagation loss on mm-wave and their focused scenarios are an urban environment for high data rate services such as indoor malls, home and mobility in the city. The COST2100 channel model based on the geometry of a stochastic channel model which provide the properties of MIMO over time, frequency and space [46].

The New York University (NYU) wireless channel models were also published in the year 2015 [5] and in 2016 [47]. These papers are based on the channel measurements for 28, 38, 60, and 73 GHz frequency bands and the model had three new features as compared to the 3GPP 3-D model, namely LOS/NLOS, power and angular profile and free space path loss model. In 2016, another white paper was published for channel measurements and 5G networks modelling in the frequency above 6GHz[48] for both fix and mobile links in indoor and outdoor environments. 802.11 ad/ay channel models conducted the ray tracing methodology on 60 GHz band for indoor channels such as for the scenario like a living room, conference room and proposed parameters in terms of ray delay and ray power distribution[46].

Further, the 3GPP extended the 3-D standardized models at 2GHz for higher frequency bands. The model was based on the same framework as the model at

2GHz frequency range but included the updated path loss models and frequency dependent parameters. Therefore, after modelling components were also introduced.

2.5.2 New Channel Models Requirements:

The new channel model requirements that will support 5G operation frequency bands are summarised below.

1. Increasing the wireless capacity due to advances in hardware is by reaching toward highest frequency bands with available bandwidth. The new channel model should be able to accommodate a higher frequency range and at different frequency bands will have needed to be evaluated for multi-band operation (e-g carrier aggregation configurations for low band and high band). The Mobile and wireless communications Enablers for the Twenty-twenty Information Society (METIS) has described the frequency bands from the current cellular spectrum up to 86 GHz. In [49] the medium and high priority bands are 10 GHz, 28GHz – 29 GHz, 32GHz – 33 GHz, 43 GHz, 46GHz – 50 GHz, 56GHz – 76 GHz, and 81GHz – 86 GHz.

2. The new channel model may support single channel bandwidths in the range of 100MHz to 2GHz. The channels may be spread out and assigned a range of several GHz.
3. In wireless communication, the movement goes in the direction to increase the number of antennas, which will open some new technological

possibilities. The channel models should use the existing models but to use 5G requirements and scenarios such as antenna arrays at high-frequency range at the transmitter (AP) and receivers (UE) will have needed to be properly modelled and direction of departure and arrival of multipath components. Each antenna will have antenna radiation patterns for directional performance gains.

4. The new channel must be structuring the models that should be suitable for mobility and rotation to support scenarios such as the mobility of 350 km/h from device to device (D2D) and vehicle to vehicle (V2V). It is most vital to model the links in a consistent manner. The consistent model can also inherently support mobility of users. The term spatial consistency means that the channel evolves smoothly without discontinuities when the TX and/or RX moves or turns.

5. To ensure the frequency consistencies for the second order statistics of the channels and channel states for a line of sight (LOS) and non-line of sight (NLOS) for indoor/outdoor propagation scenarios.

6. Spectral efficiency increases by using multiple antennas at the transmitter and receivers side and the trend goes in massively increasing the number of antennas. A large number of antennas will enable precise beamforming and targeting without interference creation[50]. The new channel models should support a large range of antenna arrays with high directivity and angular resolution of the channel down to 1 degree. Different arrays type

will be linear, spherical and cylindrical arrays having random polarization [51].

2.6 Multicarrier modulation:

Multicarrier modulation main idea is simple to strive for high data rates and intersymbol interference (ISI) free channels. To have a channel with free ISI, the channel delay spread *(τ)* has to be smaller than the symbol time (T_s). As for widethe band channel providing high data rates for modern applications, the desire symbol time is much smaller than the delay spread as a result inter symbol interference is severe. The principle of multicarrier modulation (MCM) is to divide higher transmitting data T_s by the lower data rate sub stream *L* and is greater than delay spread τ of which is $T_s/L \gg \tau$ by sending the sub stream to parallel sub channels, maintaining overall data rate to prevent ISI. Sub channel data rate is quite less than the entire data rate to communicate with bandwidth of sub channel which is comparatively less than the bandwidth of the total system. In simple words MCM divides the wideband data stream into narrowband data sub stream by transmit it over orthogonal frequency sub channels.

Multicarrier technique has an interesting ability to explain time domain and frequency domain in which the symbol duration in time domain increased to T = LT_s , ensures to that the channel delay spread exceeds $T \gg \tau$, while on the other hand frequency domain, subcarrier bandwidth will be $BL \ll B_c$ that lead to flat fading [3].

.

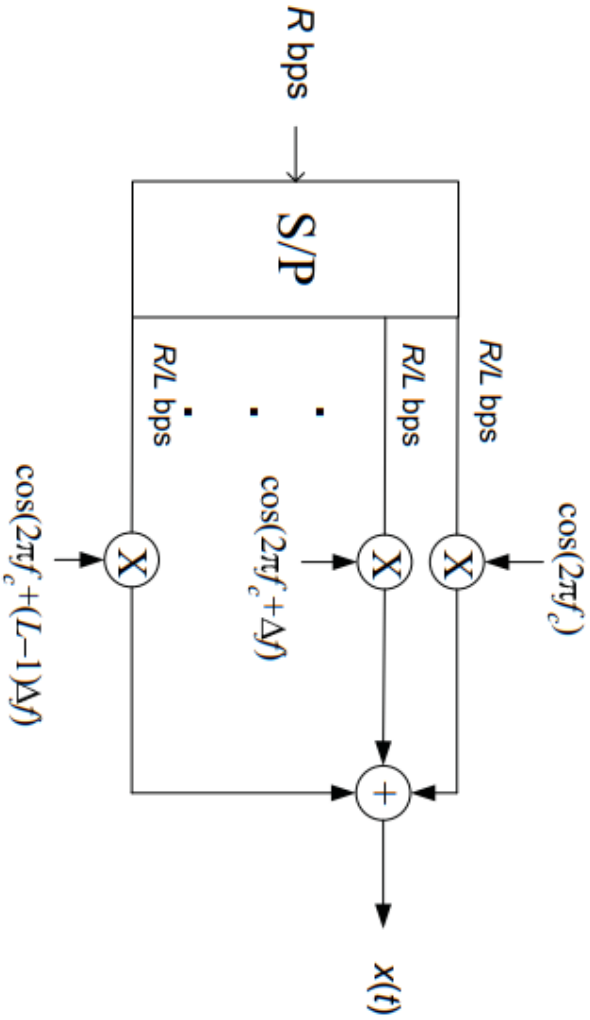

Figure 2.4. A basic multicarrier transmitter: A high-rate stream of R bps is broken into L parallel streams, each with rate R/L and then multiplied by a different carrier frequency[3]

Figure 2.4 illustrates the multicarrier transmitter, the data rate represented by R bps divided into L parallel sub-stream represented by *R/L* bps and bandwidth *B/L.* The number of the subcarrier is to ensure that the bandwidth of the subcarrier will be much lesser than the coherence bandwidth, which is $BL \ll B_c$ and the orthogonal signal can be detected.

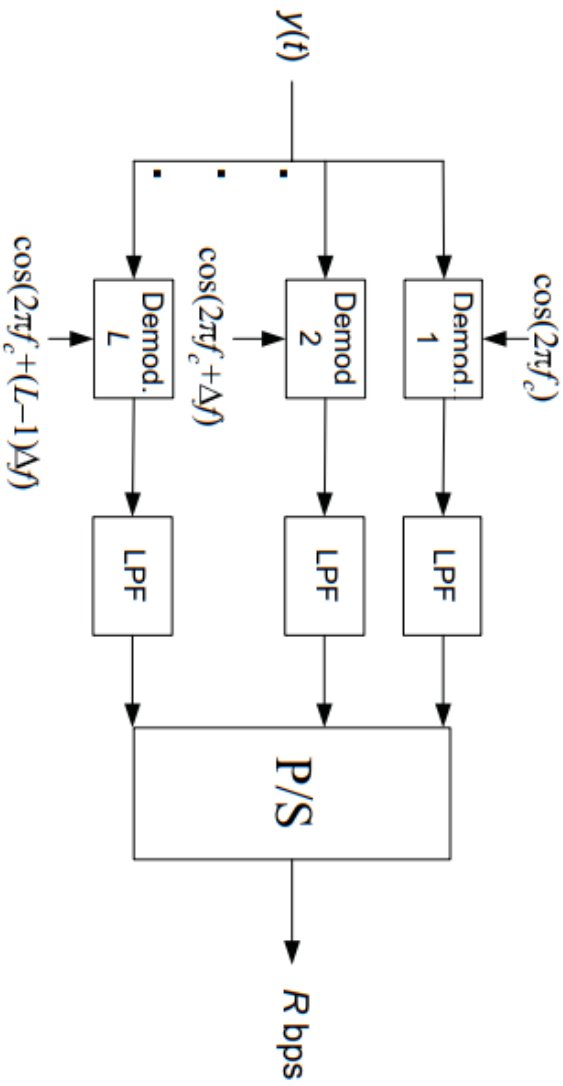

Figure 2.5. A basic multicarrier receiver: Each subcarrier is decoded separately, requiring L independent receivers.

Figure 2.5 shows the multicarrier receiver, similarly, the R bps is the data rate and subcarrier are decoded separately requiring L independent receiver.

2.7 Conclusions:

Next generation mobile network (5G) and its challenges, mm-wave and its challenges, channel modelling and its requirements are presented in this chapter. In addition, the propagation channel and its mechanisms are briefly explained. Mm-wave is used for a high speed of wireless local area network (WLAN) and for the diversity of services on wireless network s for up to the data rates of 10Gbps. Universities and industry research partners have discussed many aspects about channel modelling for up to 100GHz frequency bands. It has been reviewed that the new channel models should be able to accommodate a high frequency, the increasing number of antennas, suitable for mobility and increase spectral efficiency.

3. PROPAGATION PREDICTION MODELS AND CHANNEL CHARACTERISTICS

3.1 Introduction:

Radio propagation is the behaviour of radio waves as they propagated from source to destination. The models for radio propagation is developed usually to predict the nature of propagation in a different environment and based on large collection of data for the different specific scenarios. For propagation models, data collection has to be abundant to provide scope to all types of situations, which allows useful predictions on the characteristics of the signal at the receivers [52].

Next-generation cellular network (5G) will focus on frequencies from 5GHz to around 100GHz for which the development of 5^{th} generation network system needs a precise propagation model to use a frequency band above 6 GHz. As the previous generations were designed to operate the highest frequencies at 6GHz and is not enough to meet the multi-gigabyte data rate requirements of the proposed 5G network system. It is a challenge for the next generation cellular system to introduce a new channel model which operates at higher frequencies. This will allow the accurate system performance evaluation for indoor environments [51].

3.2 State of The Art and General Consideration of Propagation Channel Models:

Generally, the radio propagation models are more convenient and efficient when the most effective phenomenon are taken, such as in wireless communication, the nature of mobile radio environment provides a range of challenges for the investigation of propagation phenomenon:

- Providing indoor coverage and data services to the consumers located inside the building is crucial to maximising data capacity and network quality in such type of strategic areas. This is the complex challenge as the signal strength is to be insufficient in lower floors due to propagation losses.

- The distance between transmitter and receivers greatly changes, in a range of few meters to several kilometres at indoor and outdoor environments.

- The height of the antennas may vary from the rooftop of residential houses and offices to above multi-storey buildings.

- The size of man-made and natural objects in the environment in the range of smaller than a wavelength to numerous orders of wavelengths to influence radio wave propagation.

3.2.1 Review of Propagation Models:

There are many radio propagation models for different wireless services that specifically mark different propagation environments and frequency bands. The emerging technology is needed to enable the next generation wireless network, for which developing new propagation model is also essential. The reliable propagation models and its associated software tools are important for the successful implementation of the future wireless system. Solutions to overcome the above challenges in section (3.2) come from the following approaches.

3.2.1.1 Experimental Approach:

Empirical models which are based on measurements in a real world is known as an experimental approach, thus represents the physical geometry of the propagation environments. The main advantage of experimental models is their computational efficiency and simplicity. The accuracy depends on the accuracy of the measurement and likeness between the environments where the prediction and measurements are taking place to which results in weaker control on the environment and general models [53].

There are two categories for empirical models, namely non-time dispersive and time dispersive. Time dispersive gives information about the time of the channel characteristics during multipath like delay spread [54].

i. Free Space Propagation Model

In free space propagation model, the transmitter and receiver are located in the empty environment and neither absorbing and nor reflecting surfaces are

considered. This means that free space propagation is to predict the strength of the received signal when there is a clear and non-obstructed line of sight (LOS) between the transmitter and the receiver. The power receives by the receiver from the transmitter antenna by a distance is explained by the Friis transmission equation:

$$Pr(d) = \frac{P_t G_t G_r c^2}{(4\pi d)^2 f^2} \qquad (3.1)$$

Where $Pr(d)$ is the received power of the Tx-Rx separation distance$d$, P_t is transmitter power in dBm, G_t and G_r is the transmitter and receiver antenna gains in dBi and λ is the wavelength. Where λ =c^2/f^2, c= speed of light and f= frequency in megahertz.

In logarithmic form the equation (3.1) can be written as:

$$P\,r(d) = P_t + G_t + G_r + 20\log\left(\frac{\lambda}{4\pi d}\right) \qquad (3.2)$$

The free space path loss model is expressed as without antenna gain:

$$PL(d) = 20log\left(\frac{4\pi d}{\lambda}\right) = 20log\left(\frac{4\pi}{\lambda}\right) + 20\log(d) \qquad (3.3)$$

The $20\log(d)$ represents here in equation (3.3) that the path loss increases 20 dB in the distance between transmitter and receiver.

ii. Motley Keenan model:

The semi-empirical model in which the path loss obtained due to the penetration loss from the walls. As compared to the deterministic models explained in the next section, it does not count the effect of propagation mechanisms (reflection, diffractions and scattering) described in the previous section. This is designed for an indoor path loss environment for the treatment of walls, which do not provide accurate results when using outdoor scenarios [55]. The model [56] is mathematically expressed as:

$$L = 20log_{10}\ \frac{4\pi f}{C} + 20log_{10}d + nA_w \qquad (3.4)$$

In equation (3.4) we have d= the distance between transmitter and receivers in meter (m), n = the number of walls between transmitter and receiver and A_w = is the attenuation factor for wall the in (dB).

iii. Multiwall Model (COST231):

COST231 Multiwall model is one of the empirical models used for the enhancement of the Motley Keenan model as discussed above and was developed based on real measurements for 900MHz and 1800MHz bands in the cities of Europe. The floor loss also considers due to the floor presence by the multiwall model, adding parameters to the wall loss model and the type of material of each obstruction; the path loss can be expressed as [57]:

$$\text{PL} = L_{FS} + L_c + \sum_{i=1}^{T} L_{wi}\, W_{wi} + L_f W_f^{\left(\frac{W_f+2}{W_{f+1}} - b\right)} \qquad (3.5)$$

Where

- L_{FS} Represents the free space loss between transmitter and receiver.
- L_c is a loss constant.
- L_{wi} is the penetration loss for wall type i , while W_{wi} is the number of walls involved.
- T is the number of walls type, W_f is the number of floors and L_f is the per floor penetration loss.

It has been predicted that COST231 Multiwall models are easy to use and provides better prediction results and more accurate than other empirical models not considering wall loss, but there is a lack of accuracy for particular environments and applied some kind of restrictions such as a couple of walls type are considered for its thickness [57] [55].

3.2.1.2 Theoretical Approach:

Theoretical approach of propagation models is based on software simulation or mathematical studies and not examine as a reality itself but the simplified form of reality. This approach has full control over its environment to easily explain because of its simplification. The associated type of model for this approach is *Deterministic Models* which is discussed as follow:

Deterministic radio wave propagation models are mainly based on geometric behaviour and theoretical principles of the wave propagation phenomenon. These models have a high level of accuracy and their accuracy can only be

achieved when the simulated scenario databases are firstly accurate. The parameters of these databases have a relation with the properties of obstacles in the environment and are applied the boundary conditions on material interfaces e-g reflections, refractions and diffractions which is also called the physical phenomenon of radio waves. These propagation models are usually associated with indoor and outdoor propagation environments, so insufficient details and inaccurate databases can initiate a major disadvantage of deterministic models [53, 58]. Ray launching model, ray tracing models and Finite-difference time-domain (FDTD) are the main types of deterministic model which is briefly explained as follow:

i. Ray launching model:

The type of deterministic model based on physical and ray launched a phenomenon from the transmitter (Tx) at a distinct angle to simulate the radio wave propagation, such as reflections, refractions and diffractions over obstacles. The rays arriving at the receiver (Rx) at a significant power level at last discovered. The propagation ray can be terminated when the power level falls down a pre-defined threshold. The disadvantage of ray launching model is that if the angle between rays is very small at the transmitter point, may be missed by the distant objects as shown in Fig 3.1. Ray launching model may only be implemented for both transmitter (TX) and receiver (Rx) to increase the accuracy [59].

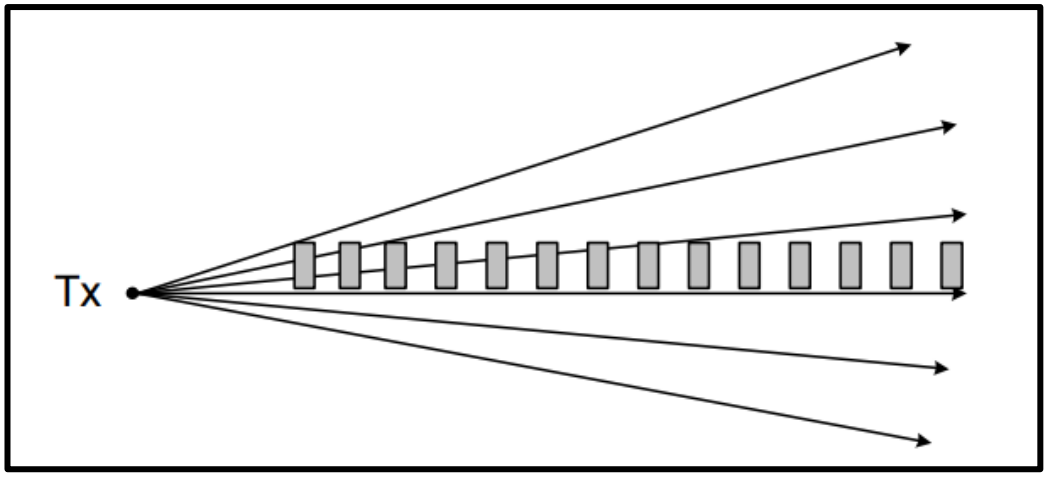

Figure 3.1: Distant objects missed by rays

ii. Ray tracing model:

When the ray is traced from the source to the destination directly or it may be reflected and diffracted many times before the destination point. In an urban scenario of propagation is to determine that if the ray hits an object, a reflected and diffracted ray will be released. The model using geometrical optics theory for the treatment of reflection and transmission for surfaces are based on ray estimations. Rays from transmitter located within the building scenario using reflection and transmission to states that all the paths from source to destination, satisfy the boundary conditions after reflections through walls or objects. Ray tracing method for radio propagation prediction is shown in Figure: 3.2.

In ray launching model as discussed above, the large number of rays launches form the transmitter but only a few rays reach to a specific receiver and the rest of rays may be wasted.

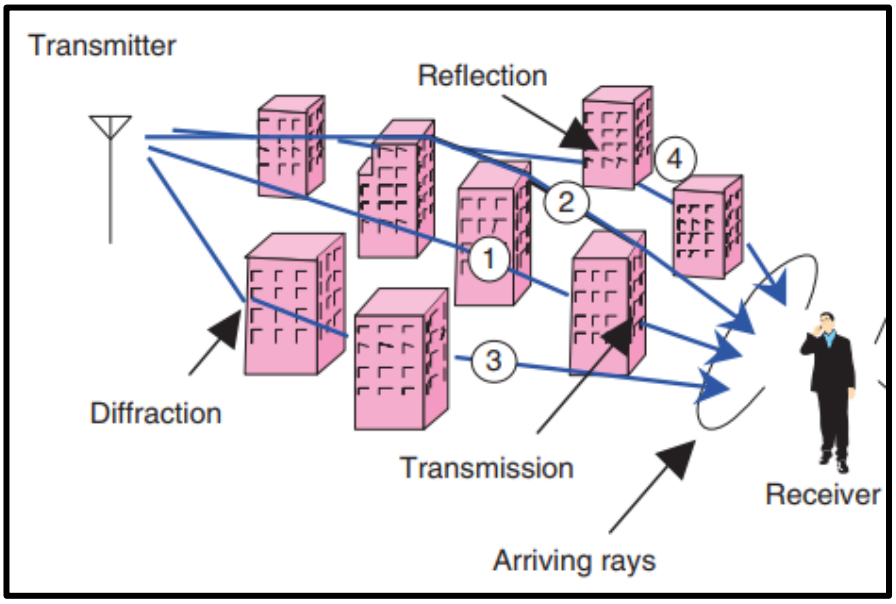

Figure 3.2: Ray tracing [4]

In addition, the main advantage of ray tracing model is that it examines only the paths that really exists between the transmitter and receivers and needs low-level computation time than the ray launching model. The disadvantage of a ray tracing model is the growing of computational time with the order of calculated reflections and their computational load because of more obstacles with a large number of reflections and diffractions.

iii. Finite-Difference Time-Domain Method (FDTD):

The finite-difference-time-domain (FDTD) method is possibly the simplest, in terms of concept and implementation, to solve the electromagnetic response of a number of walls in a building. The Maxwell's equations were considered as the most accurate description of how magnetic field and electric field interact with each other and how electromagnetic waves propagate. It is very hard to solve the

partial differential equations of Maxwell's equations. The FDTD method is a time domain solution of Maxwell's equations explained in a different form and is used in circuit analysis of its simplicity. It provides simple programming and data structure and the FDTD method can solve complicated problems, but generally computational is very expensive. Solutions for its problems may require a large amount of memory and computation time. The weakness of FDTD method is, there is no way to regulate unique values for permeability and permittivity at a material interface [58, 60].

Therefore, deterministic approach (theoretical) has become the preferred technique for channel propagation models and its simulation that can be performed with the application of Maxwell's equation or by ray tracing technique as briefly described in section 3.2. If there is a high number of multipath interactions in the calculations then 3D simulation provide sufficient computational accuracy for any scenario [61].

Ray tracing models simulate propagation mechanisms and can predict channel impulse response. The technique is very useful and attractive for MIMO modelling because the channel space-time properties are directly acquired during the simulation.

3.3 Propagation channel characteristics:

A channel model is a simplified representation of reality that identifies those aspects of channel behaviour that affect the performance of a particular class of wireless technologies. Channel behaviour is characterized by many parameters,

in which the most important are shown below with expressions for the proposed research work.

3.3.1 Path loss model:

Path loss is the most fundamental measure of channel quality that can be defined for the large-scale effects of the propagation channel on the signal received. Path loss is the reduction in the power density of an electromagnetic wave when it propagates from transmitter to receiver [62].

Wireless channel propagation characteristics have investigated, based on the deterministic path loss models. In decibels, the path loss is defined as:

$$L_{path}(dB) = P_T(dBm) - P_R(dBm) + G_{T,Max}(dBi) + G_{R,Max}(dBi) - L_s(dB) \quad (3.6)$$

Here $G_{T,Max}$ and $G_{R,Max}$ are the maximum gain of transmitter and receivers respectively. While L_s is the sum of all other losses in dB including the overlap factor of bandwidths.

Due to differences in environments, it's difficult to make a general propagation model with detailed parameters; thus it's widely accepted to adopt a model that covers the main propagation aspects with reasonable results, this model the most simple and general path loss (PL) is the n^{th} power law [63]:

$$PL(d)[dB] = PL(d_0) + 10n\, log_{10}(d/d_0) + X\sigma \quad (3.7)$$

Where n is the path loss exponent which has different values as shown in table 3.2, d is the distance between the transmitter and the receiver, $X\sigma$ is Gaussian-distributed random variable with standard deviation σ dB for shadowing and $PL(d_0)$ is the reference path loss, In order to exclude the near field effect of the measurements, power is measured in the far field region of the antenna at d_0 (usually at 1 m) by applying Free space Friis formula or by empirical measurements [7]. reference path loss is given by [64]:

$$PL(d_0) = 20\log_{10}\left(\frac{4\pi f}{c}\right) + 20\log_{10}(d_0) - G_T - G_R \qquad (3.8)$$

Where f, c, G_T and G_R are respectively: operating frequency, speed of light, transmitter gain and receiver gain.

Table 3.1: Path Loss exponent values for different environments for (0.9 GHz and 1.9 GHz) [6] [7].

Environment	n
Free space	2
Urban macrocells	3.7-6.5
Urban microcells	2.7-3.5
Shaded urban microcells	3-5
Suburban	3-5
Indoor (single floor)	1.6-3.5
Indoor (Multiple floors)	2-6
Store	1.8-2.2
Factory	1.6-3.3
House	3

Alpha, beta and gamma (ABG) is called a multi-frequency three-parameter model can be used to investigate the frequency dependent and distance-dependent in terms to explain path loss at specific various frequencies. The model equation is given by:

$$PL_{\alpha\beta\gamma} = 10\alpha log_{10}\left(\frac{d}{d0}\right) + \beta + 10\Upsilon log_{10}\left(\frac{f}{c}\right) + X_{\sigma}^{\alpha\beta\gamma} \qquad (3.9)$$

do = 1m

Where β is the slope of the line and can expressed as:

$$10.log_{10}(d)$$

Where the coefficient α describes the distance dependant factor of path loss, Υ is the coefficient describes the frequency dependence on path loss and β is the offset parameter that is lacking physical mean. f Represents the frequency in Ghz and $X_{\sigma}^{\alpha\beta\gamma}$ is a variable presents the large scale signal about the mean path loss against the distance [65].

3.3.2 Received Power:

The total received power can be obtained from the combination of the power for each ray path and the time average received power is given by:

$$\mathrm{P_R} = \sum_{\mathrm{i=1}}^{\mathrm{N_P}} \mathrm{P_i} \qquad (3.10)$$

Where in equation (3.10) N_P is the number of paths and $\mathrm{P_i}$ is the time average power for the i^{th} path, other methods including the effect of each path phase as [66]:

$$P_R = \left|\sum_{i=1}^{N_P} \sqrt{P_i} e^{-j\varphi_i}\right|^2 \qquad (3.11)$$

Where φ_i is i^{th} ray phase in radian.

While other models consider the paths coming from the same path to be combined with phase [67].

$$\mathrm{P_i} = \frac{\lambda^2 \beta}{8\pi n_0} [E_{\theta,i} g_\theta(\theta_i, \emptyset_i) + E_{\emptyset,i} g_\emptyset(\theta_i, \emptyset_i)]^2 \qquad (3.12)$$

λ is the wavelength

n_0 is the impedance of free space (377Ω)

$E_{\theta,i}$ and $E_{\emptyset,i}$ represents the theta and phi elements of the electric field of the receiver point at i^{th} path.

Similarly, g_θ and $g_\emptyset$ are the theta and phi elements of the direction of arrival at receiver point.

The electric field components θ_i (theta) and $\emptyset_i$ (phi) give the arrival direction expressed in equation (3.18) and (3.19).

By combining equation (3.10) and (3.12) the total received power is:

$$\mathrm{P_R} = \frac{\lambda^2 \beta}{8\pi n_0} \left|\sum_{\mathrm{i}=1}^{\mathrm{N_P}} \left[E_{\theta,i} g_\theta(\theta_i, \emptyset_i) + E_{\emptyset,i} g_\emptyset(\theta_i, \emptyset_i)\right]\right|^2 \qquad (3.13)$$

Equation (3.13) is the received power in watts, the power in dBm is determined from:

$$P_R(dBm) = 10log_{10}[P_R(W)] + 30dB - L_S(dB) \qquad (3.14)$$

Where L_S show the additional loss in the system.

3.3.3 Delay Spread (σ_t):

Delay spread σ_τ is defined as the square root of the second central moment which describes how the delays are spread with respect to the mean, although in many cases delay spread is similar to mean delay (first moment where each path contributes proportional to its power), however in cases where NLOS propagation is dominant with large delay, the mean delay will provide a misleading indicator compared to the RMS delay. That is why σ_τ is widely used as a delay spread metric [68]. σ_τ calculates the energy of power for each ray path reached in time and defined as a delay spread [69].[70].

Delay spread is another important parameter used to measure a variety of multipath related impacts. It calculates the energy of power for each ray path reached in time and defined as a delay spread.

$$\sigma_t = \sqrt{\frac{\sum_{t=1}^{Np}(t_i - \bar{t})^2 P_i}{P_R}} \qquad (3.15)$$

Where t_i is the arrival time while $\bar{t}$ is the mean time of arrival as defined in equation (3.16) and (3.17). N_p is the number of paths, P_i is the average power of i^{th} path and P_R is the received power.

Where t_i is the arrival time while $\bar{t}$ is the mean time of arrival. Table 3.2 presents typical Median RMS delay spread in different indoor environments.

Table 3.2: Median RMS delay spread in different environments [8]

Frequency	Environment	Median RMS delay spread (ns)
1.9 GHz	House	70
	Office	100
	Commercial	150
2.625 GHz	Office	11
	Corridor	18.53
	Air cabin	11.89
	Factory	69.2
3.7 GHz	House	22
	Office	38
	Commercial	145
5.2 GHz	House	23
	Office	60
	Commercial	190
60 GHz	Office	1.77

3.3.4 Mean Time of Arrival ($\bar{t}$):

Mean time of arrival (MTOA) is the average time of arrival of a signal from transmitter to a receiver of every path and is given by the following expression.

$$\bar{t} = \frac{\sum_{i=1}^{N_P} P_i t_i}{P_R} \qquad (3.16)$$

Where P_i and P_R is expressed in section (3.3.2), t_i represents the time of arrival (TOA) for each propagation path given by equation (3.11).

$$t_i \ \frac{L_i}{c} \qquad (3.17)$$

L_i = total path length

c = speed of light

3.3.5 Mean direction of arrival:

In terms of spectral-based techniques, AOA estimation methods can be classified to beamforming techniques and Subspace techniques [71]. The idea behind beamforming is to let the array pattern to steer (using the weighting vector) to scan all possible angles, the angle which has the maximum corresponding power is considered as the AOA [72], two major algorithms are using beamforming concept in localization, Bartlett Beamformer and Capon minimum variance method [72]. Subspace techniques consider the effectiveness of the signal space and noise space, compared to beamforming techniques, subspace techniques show better performance and higher resolution estimation even with low SNR [71]. Antenna arrays can be used to detect the angel of arrivals, the direction of arrival is used for many application including beamforming, localization and detection [73], DOA requires the use of antenna arrays which makes the technique more expensive and more power consumption compared to time of arrival (TOA) and received signal strength (RSS) [74]; however it requires less equipment's as only two Access Points are required to give a localization [75]. DOA is suitable in mediums with heterogeneous mediums (like water) where the velocity of waves will be different compared to those in free space, TOA and RSS will give an error in location estimation while DOA is less affected, that is why is used in biomedical localization especially in the human body [73].

The direction of arrival can have expressed as:

$$\bar{\theta}_A = \tan^{-1}\left(\frac{\sqrt{A^2{}_x + A^2{}_y}}{A_z}\right) \quad (3.18)$$

$$\overline{\emptyset}_A = \tan^{-1}\left(\frac{A_y}{A_x}\right) \quad (3.19)$$

Where A is:

$$A = \sum_{i=1}^{N_P} P_i \, \hat{a}_i$$

$\hat{a}_i$ is the unit vector in the direction through the *ith* path arrives at the receiver points, so equation (3.19) is given by:

$$\overline{\emptyset}_{\sum_{i=1}^{N_P} P_i \hat{a}_i} = \tan^{-1}\left(\frac{A_y}{A_x}\right) \quad (3.20)$$

3.4 Conclusions:

In this chapter, we categorized propagation channel models into two groups; Experimental approach and Theoretical approach. The empirical model is a common model for the experimental approach and famous for computational efficiency and simplicity. The models are optimized according to measured data, but the disadvantage of this model is the low accuracy for a specific scenario. While the theoretical approach is associated with a deterministic model which

simulate radio wave propagation based on Maxwell's equation and take the specific environment for radio propagation to possess a high level of accuracy.

Finally, we have explained the important characteristics of channel behaviour of propagation models, for example, path loss, received signal power, delay spread, mean arrival time and mean direction of arrival respectively with mathematics following by research work.

4. INDOOR SIMULATION OF DIFFERENT CHANNEL PROPAGATION MODEL

4.1 Introduction:

A number of changes planned for 5G are the extension into high frequencies in the wave spectrum, the increasing demands of high-speed data and multimedia services, need to accurately predict the multipath effects of indoor environments.

In mobile radio propagation studies, the qualitative description of the environment is usually using terms rural, urban, dense urban and suburban. Dense urban is the area defined tall buildings, commercial building areas and multi-storey office blocks, while suburban is the area contains residential houses, flats, gardens and parks. Rural areas are generally defined as with scattered buildings and agricultural fields and forests. The average signal level in suburban and rural areas is better because of the environmental effect, so the signal variation in urban areas have been discussed so far. In urban areas, there is no direct line of sight (LOS) between the user equipment and base station (BS) antenna. There is a number of different paths because of reflection from tall buildings, for which signal arrives at a mobile station (MS) through many paths and the received signal over each path has a random phase and amplitude [76].

In this chapter, multi-storey office environment is presented to evaluate the propagation channels for indoor-indoor including a line of sight (LOS), non-line of

sight (NLOS) and indoor to outdoor scenarios which provide the comparisons of these metrics at 5.8, 26, 28 and 60GHz in an office building. The model includes the full description of buildings in terms of materials used where the signal strength, angle of arrival, delay spread, and path loss evaluated.

Propagation models are designed by using a deterministic approach and have become a preferred technique for channel propagation simulations. Deterministic is the model that can be performed through Maxwell's equation and by ray tracing techniques (SBR).

4.2 Indoor multi-storey scenario:

Indoor scenarios tend to be complex and needs an accurate description of the walls and objects inside the building. The radio wave counting these objects and walls in front of it could raise multiple reflections, penetrations and diffractions. There is a number of telecommunication users in any tall buildings, need to provide high-quality radio communication services. The distance between transmitter and receivers are very small but the occurrence of obstruction like floors, walls, objects etc. means that the path loss may be high and difficult to predict. Figure 4.1 shows a brief model for ground, first, second and third floors of an office building and Table 4.1 explained the frequency dependent electrical properties of building for each material given in the Recommendation ITU-R P.527 including permittivity and conductivity and defining the particular range.

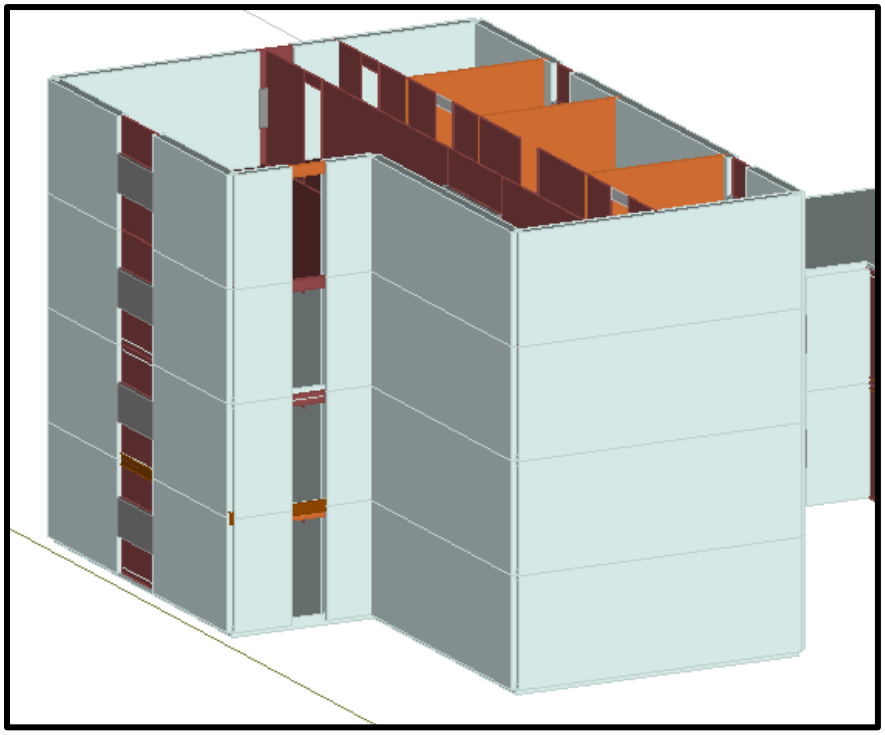

Figure 4.1: Ground, First, second and third floors of an office building

Table 4.1: Properties of materials Rec. ITU-R P.2040-1.

Material class	Real part of relative permittivity		Conductivity S/m		Frequency range
	a	*b*	*c*	*d*	GHz
Vacuum (≈ air)	1	0	0	0	0.001-100
Concrete	5.31	0	0.0326	0.8095	1-100
Brick	3.75	0	0.038	0	1-10
Plasterboard	2.94	0	0.0116	0.7076	1-100
Wood	1.99	0	0.0047	1.0718	0.001-100
Glass	6.27	0	0.0043	1.1925	0.1-100
Ceiling board	1.50	0	0.0005	1.1634	1-100
Chipboard	2.58	0	0.0217	0.7800	1-100
Floorboard	3.66	0	0.0044	1.3515	50-100
Metal	1	0	10^7	0	1-100
Very dry ground	3	0	0.00015	2.52	1-10 only
Medium dry ground	15	−0.1	0.035	1.63	1-10 only
Wet ground	30	−0.4	0.15	1.30	1-10 only

Different materials used in the building have very diverse penetration loss characteristics. Materials such as concrete or brick have losses that increase rapidly with frequency. Figure 4.2 summarizes some recent measurements of material losses.

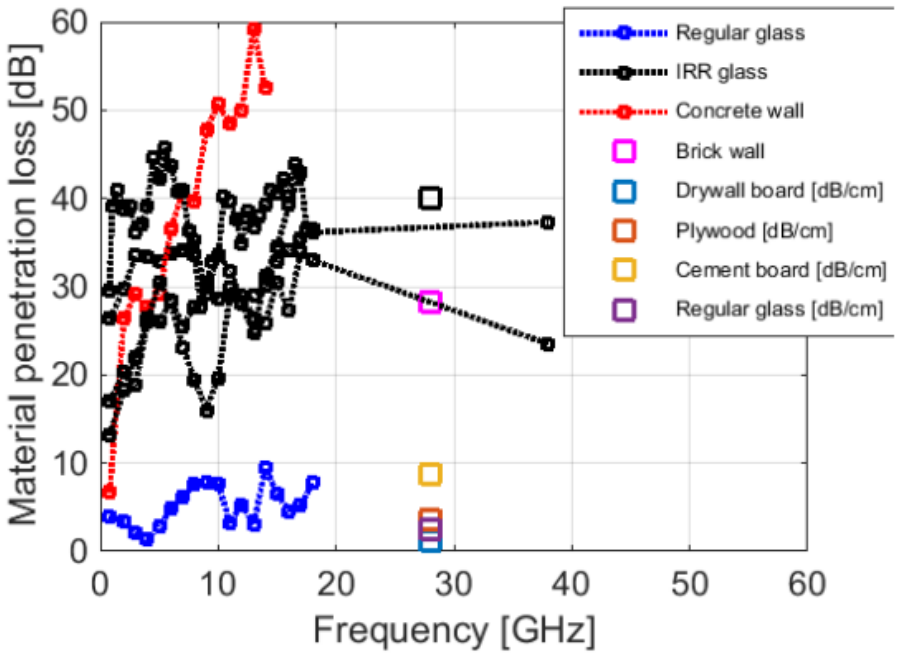

Figure 4.2: Materials penetration losses. Source: [11], Measurements by Samsung and Nokia

4.3 Model structure:

The scenario and the analysis of the system is the corridor, main entrance and outdoor ground environment of the third floor of the office building as shown in Figure 4.1. The ceiling was set to invisible so that the walls, doors, windows and floors can be seen clearly. The materials of the doors, walls, ground and floors have an estimation of the width of each element. The simulation performed by 3D shoot and bouncing Ray also called 3D SBR technique with ray spacing,

reflection, transmission and diffraction for the evaluation of paths launching from the transmitter as discussed in propagation mechanisms in section 2.4. The configuration of particular parameters is allowed in the Wireless InSite models to complete simulations such as a transmitter, receiver, waveform, antennas, model, materials and outputs.

4.4 Simulation Setup:

One transmitter and three receiver's routes used with a separation in different locations. The type of waveform used for the simulation is a sinusoid waveform with 5.8GHz, 26GHz, 28GHz and 60GHz frequencies having the 100MHz bandwidth.

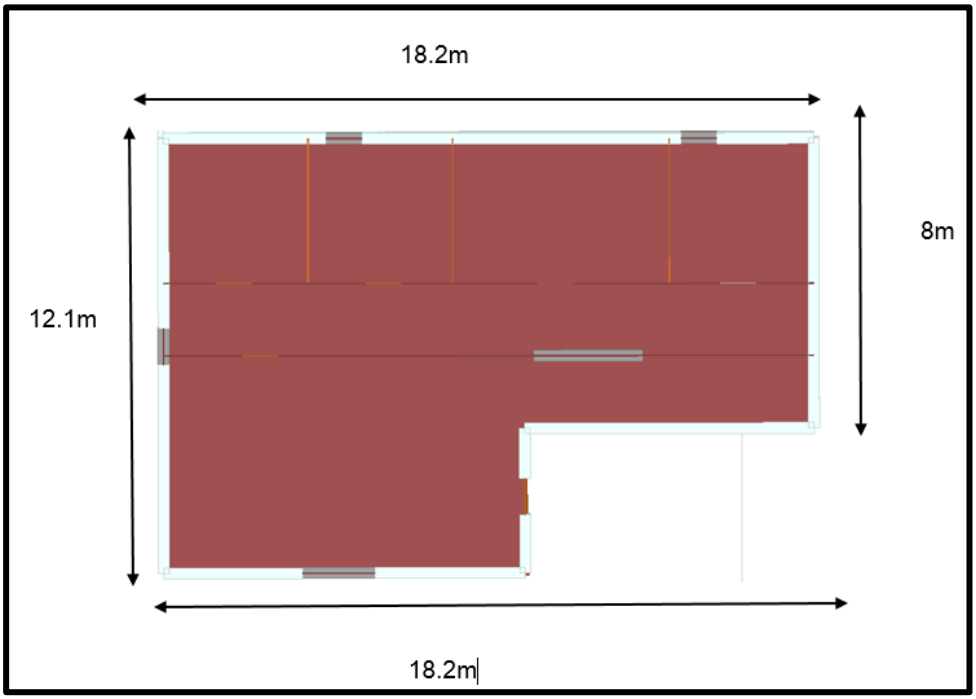

Figure 4.3: Floor Plan for Simulation

The antenna type used for Transmitter is directional and omnidirectional with vertical polarization and Receivers threshold is of up to -160 dBm. The antenna

using at the receiver side is Isotropic vertically polarized with the Sinusoid waveform. The model, therefore, has the dimensions of the building corresponding to 18 x 12 x 8 x 3 meters as shown in figure 4.3.

The model structure followed the indoor corridors of the third floor of the office building and the outdoor ground layout. The model completed by a detailed modelling using three types of walls: 30cm concrete wall, 12cm thick layered dry-wall and wooden wall, according to the layout of the floor as shown in figure 4.3.

Two types of door used which includes a wooden door (office doors) and, glass door and the type of window used, glass made window. The glass material used in office window is 3 cm in width. The floor and ceiling are 3m above the floor and the second ceiling is simulated 2.5m above the floor with 3cm thick made of dielectric material.

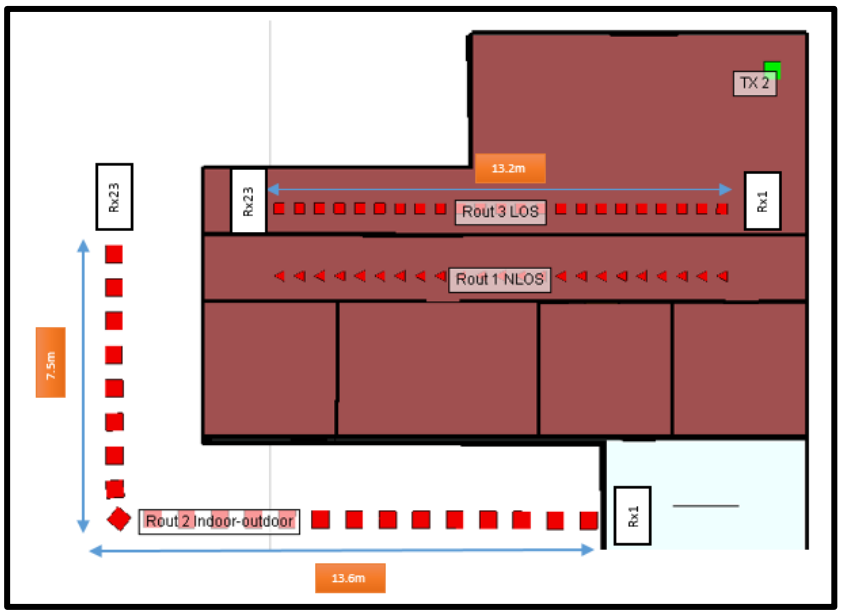

Figure 4.4: Floor layout with simulation routes and its dimensions.

Two routes named route 1 and route 3 having 23 receivers points with 0.6 m Separation from each other with 1.5 m height from the floor have distributed in the corridor; each receiver with the same characteristics. It is to be noted that the receivers in the triangular shape of Route 1 as shown in fig: 4.4 is moving with an average velocity of 0.5 m/s. Route 2 is located on the ground floor outside of the building with 23 receiver points as same as of route 1 and route 3 but the height of this route is just 2 m high from the city floor. One transmitter (Tx2) is implemented at 2m height on the same floor, 10 m high from the ground and the model was evaluated for three scenarios such as the same floor LOS 'Route 3', same floor NLOS 'Route 1' and indoor-outdoor 'Route 2' .as shown in Figure: 4.4. The properties of the transmitter and receivers are described in table 4.2.

Table 4.2: Properties of the Transmitter and receiver antenna

Properties	Transmitter antenna		Receiver Antenna
	Directional	**Omnidirectional**	**Isotropic**
Gain (dBi)	7.8	1.8	
Polarization	Vertical	Vertical	Vertical
Waveform	Sinusoid	Sinusoid	Sinusoid
Input Power (dBm)	23.0	23.0	-
E-Plane Half power bandwidth	90	90	
Temperature (K)	293.00	293.00	293.00
VSWR	1.00	1.00	1.00
Receiver Threshold	-160.00	-160.00	-160.00

- Line of sight (LOS) is the type of propagation, which transmits and receive data when transmitter and receivers are in view of each other with no objects or obstacles between them.
- While on the other hand non-line of sight (NLOS) is the path of propagation of radio frequency (RF) used when the transmitter and receiver are not in the direct visual line of sight and the radio transmission across a path is partially or completely obstructed, by a physical object. Some of the obstruction or objects reflect radio frequencies and some simply absorb the signals which lowers the effective received power [77].

The main medium between the Line of sight (LOS) named route 3 and non-line of sight (NLOS) named route 1 is a layered dry-wall having one door and one window built with a glass material which separated them as a line of sight (LOS) and non-line of sight (NLOS) from each other. In addition, the Route 3 which has two parts; partly LOS and partly NLOS receivers as shown clearly in figure 4.4. 13 receiver points out of 23 receiver points have a clear view between the transmitter Tx2 represents LOS scenario while the rest of 10 receiver points have NLOS scenario between the transmitter.

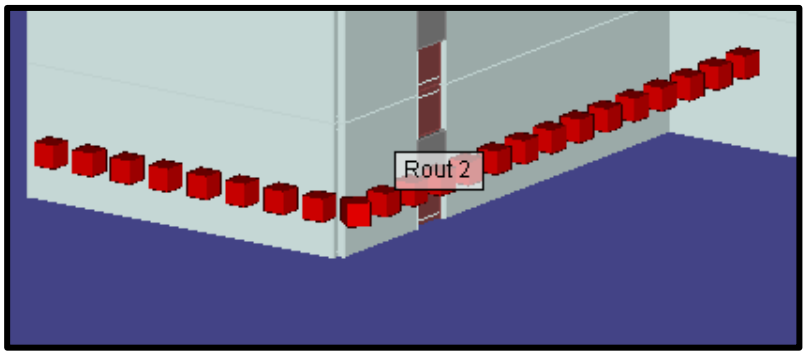

Figure 4.5: Route 2 Indoor-outdoor scenario

As Route 2 is also the main part of the scenario is located on the ground just 2m high from the city floor outside of the office building for the proposed scenario. It has 23 receiving points separated by 1m from each other and is bended after the receiver point 15, around the building as shown in figure 4.5.

4.5 Radiation Pattern:

Performing propagation calculations using transmitters and receivers, each of them with related antennas and waveform. When an antenna is added to a project and its parameters are set, it can be used in multiple instances by associating it with any number of transmitters and/or receivers.

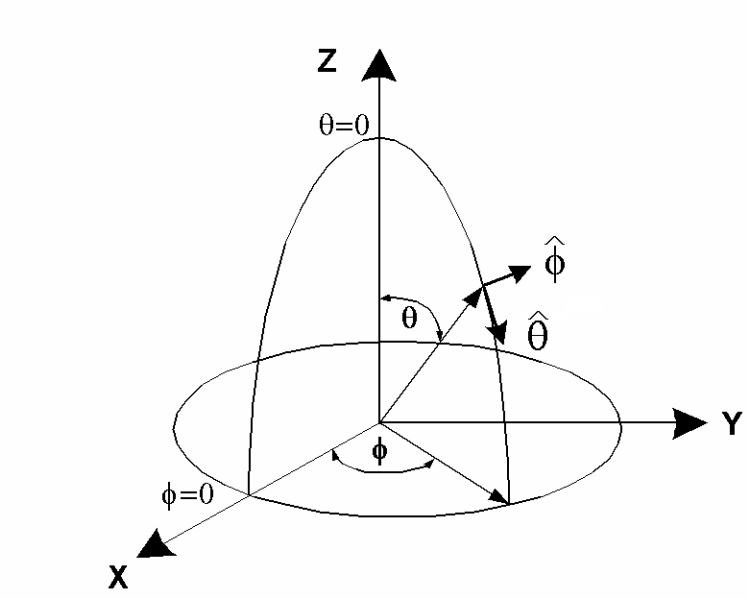

Figure 4.6: Spherical coordinate system

The location, orientation, and polarization of the antenna are set by the location of the associated transmitter or receiver. The rotation angles are determined based on the global x, y, and z axes for each association of the antenna with a transmitter or receiver. The coordinate system for these rotations is shown in

Figure 4.6.

There are two type of transmitter antenna used; directional transmitter antenna and an omnidirectional transmitter antenna, the receiver antenna is isotropic as shown in figure 4.7.

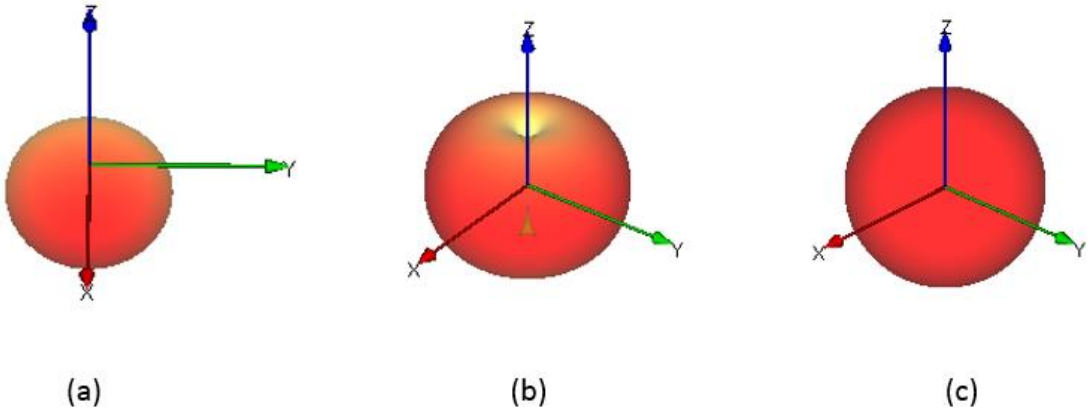

Figure 4.7: The radiation pattern for (a) Directional transmitter antenna (b) Omnidirectional transmitter antenna (c) Isotropic receiver antenna.

Directional antenna radiates or receives greater power in a direction allowing for increased performance, while omnidirectional antenna radiates radio wave uniformly in all directions and oriented vertically to radiate in all horizontal directions. The isotropic antenna radiates in all direction over a sphere centre. The radiation pattern for these types of transmitter and receiver antenna with a rotation angle of x, y, z-axes is described above as shown in Figure 4.6.

The properties of transmitter and receiver antennas as per simulation are described by Table 4.2. There are three types of antennas used; directional, omnidirectional and isotropic for transmitter and receiver with the vertical

polarization of sinusoid waveform for which the gain is assigned in dBi. The input power for both of transmitter is 23 dBm.

4.6 Results and Discussion:

Figure 4.8 illustrates the rays radiating from the transmitter to many different receiver's positions over the geometrical scenario. The simulator calculated the number of rays. Some rays fall below a certain level was ignored because of the sensitivity level of the receivers.

It is clear from the ray tracing that different materials dominate the scattering of rays differently. Some materials have signal reflection and diffraction with no effect on power and less attenuation. The highest ratio of ray penetration is from glass and layered dry-wall. Comparatively for concrete walls, ray penetration decreases, depends on the thickness of the wall and incident angle. The walls and doors made of wood material have a minor penetration of signals with increasing level of attenuation and scattering. Therefore, it is cleared that for the proposed scenario, NLOS and indoor-outdoor signals greatly assumed where wooden and concrete walls/doors exist as compared to the glass and layered drywall with minor effect.

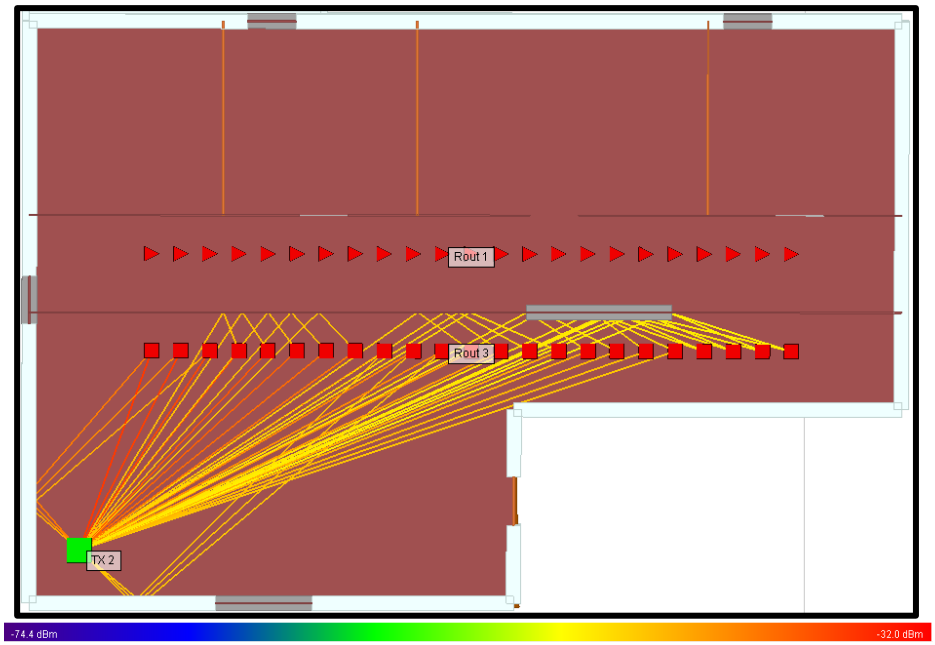

Route 3(LOS) 3D SBR Propagation Model

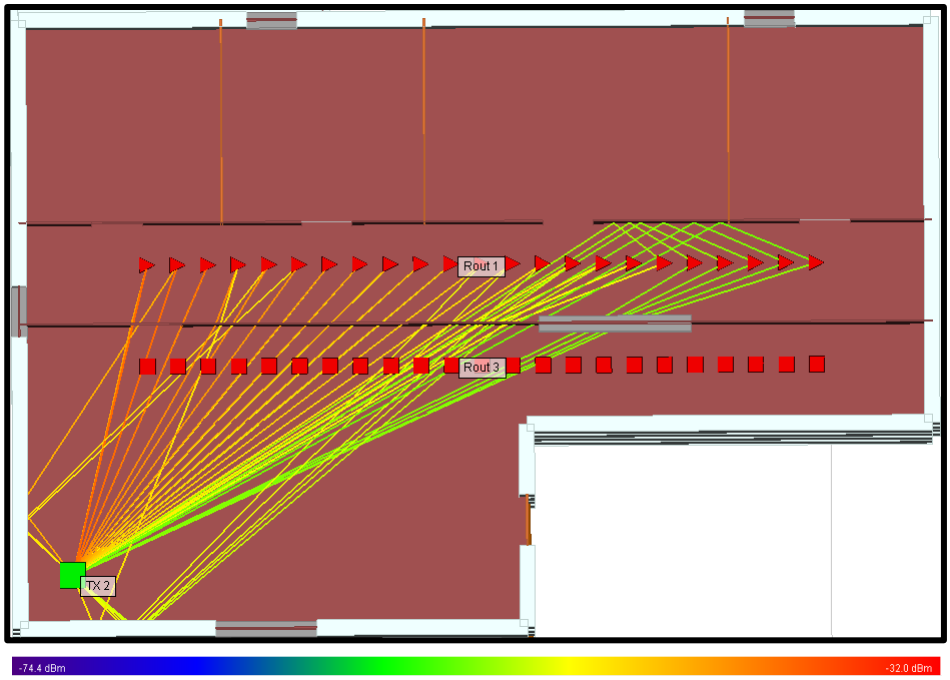

Route 1(NLOS) 3D SBR Propagation model

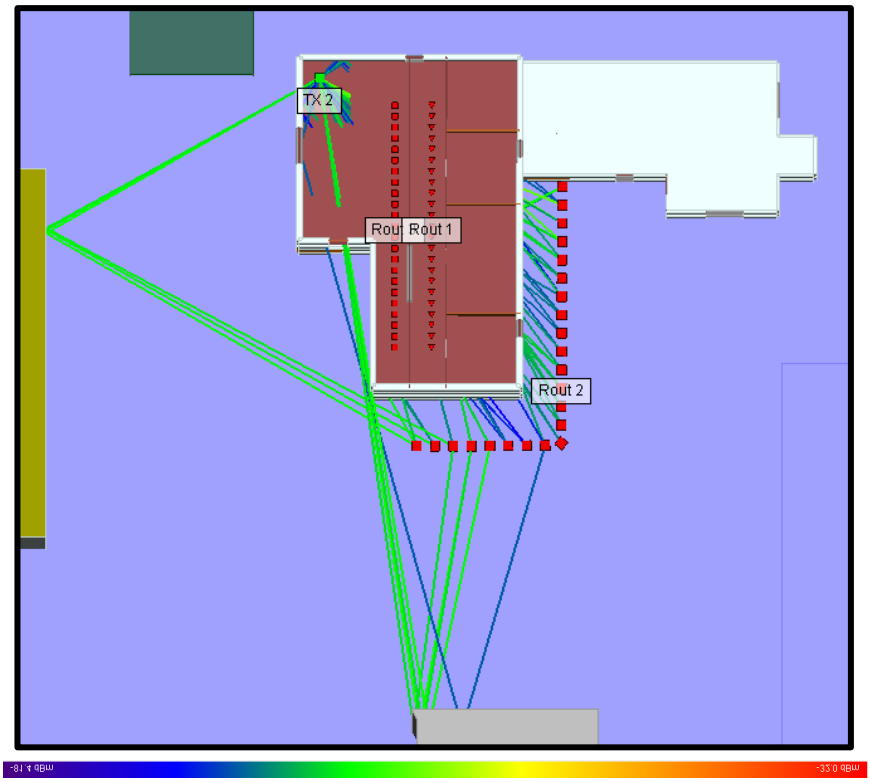

Route 2(Indoor to outdoor) 3D SBR Propagation model

Figure 4.8: 3D Ray Tracing Indoor-indoor and indoor-outdoor for Rout 3 (LOS), Rout 1 (NLOS) and Rout 2 (Indoor-outdoor).

Figure 4.9 represents the path loss (dB) simulation scenario verses Tx-Rx Separation distance in meters for LOS (receivers Route3), NLOS (receivers Route1) and indoor to outdoor (receivers Route 2) at four different frequencies that is 5.8GHz, 26GHz, 28GHz and 60GHz with directional antenna pattern at transmitter side and isotropic at receivers side for the dimensions of the office building layout and the indoor structure described in section (4.3). Figure (a), (b), (c), and (d) has a clear path loss comparison for each frequency.

The path loss model for the expected path loss (EPL) is derived using a linear polynomial fit of the PL vs. distance (d) between transmitter and receiver. We proposed the formula for polynomial fit is:

$$Pl = B + Alog_{10}(d) = B + 10_n log_{10}(d)$$

Where B is the path loss intercept and n is the path loss exponent.

As a result, the path loss increasing when the distance increases, therefore there is no continuous relationship between the results in three different routes. A simple slope channel model was plotted to summarize the results as shown in Figure 4.9.

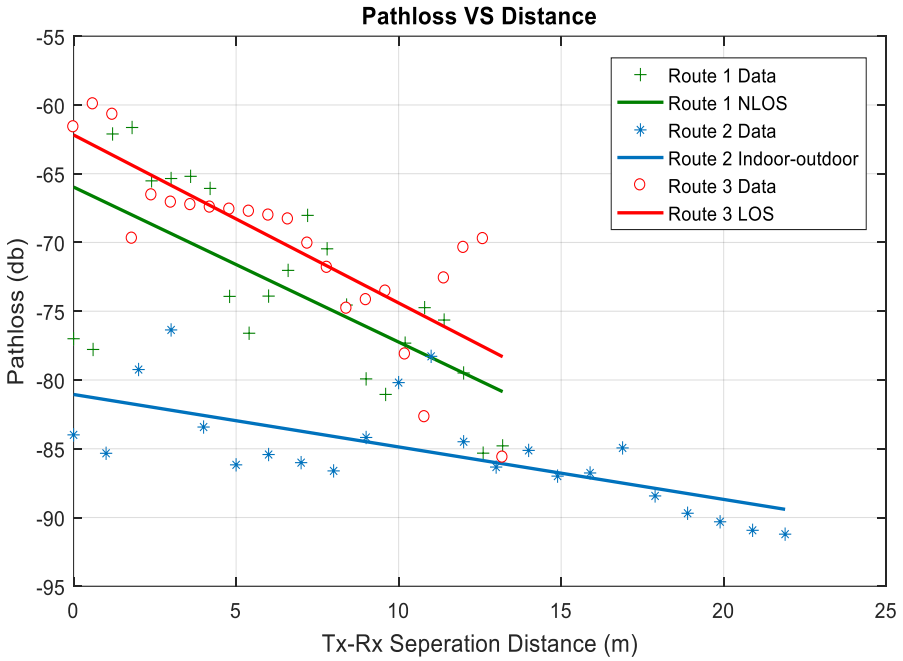

(a)

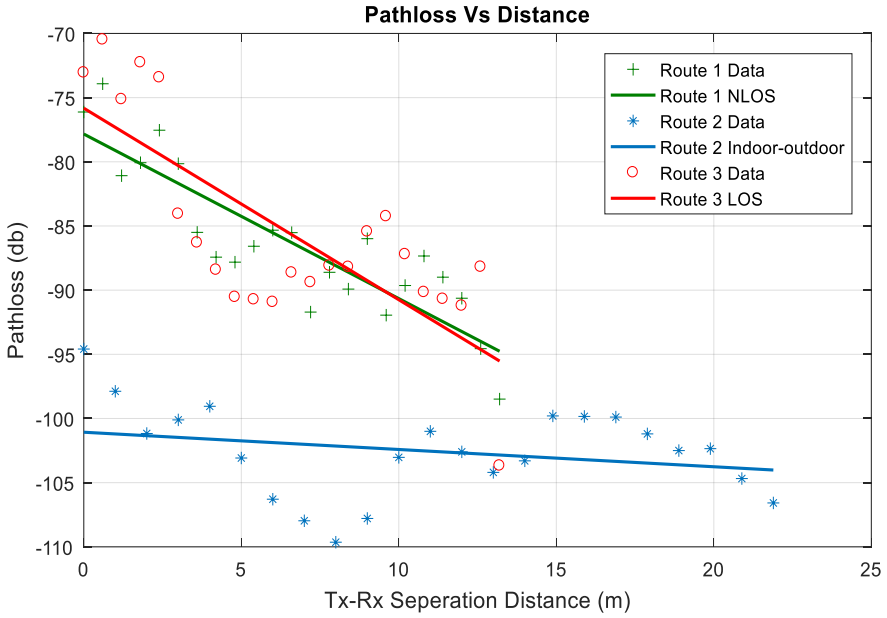
Pathloss Vs Distance
Route 1 Data
Route 1 NLOS
Route 2 Data
Route 2 Indoor-outdoor
Route 3 Data
Route 3 LOS
Pathloss (db)
Tx-Rx Seperation Distance (m)
-70
-75
-80
-85
-90
-95
-100
-105
-110
0
5
10
15
20
25

(b)

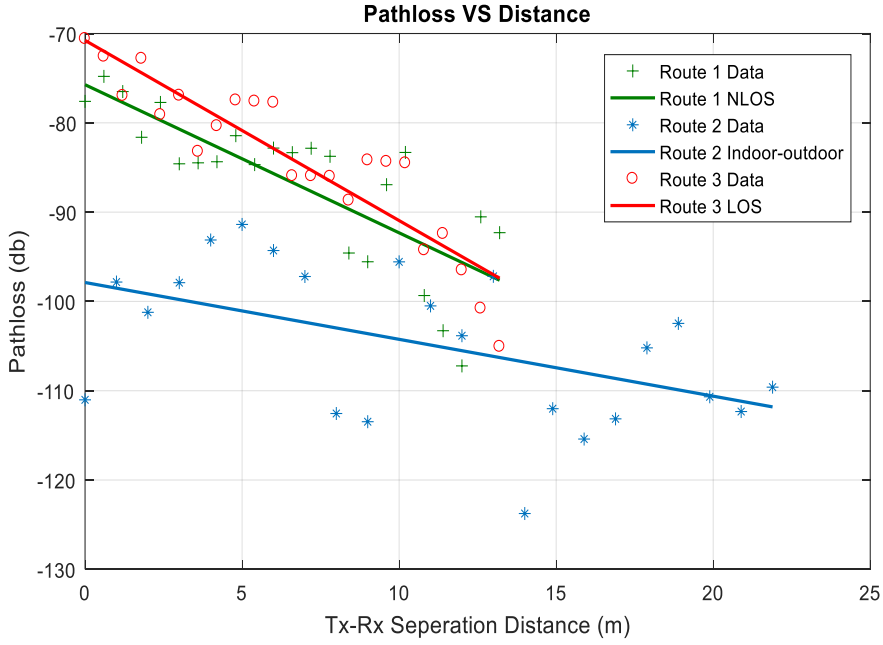
Pathloss VS Distance
Route 1 Data
Route 1 NLOS
Route 2 Data
Route 2 Indoor-outdoor
Route 3 Data
Route 3 LOS
Pathloss (db)
Tx-Rx Seperation Distance (m)
-70
-80
-90
-100
-110
-120
-130
0
5
10
15
20
25

(c)

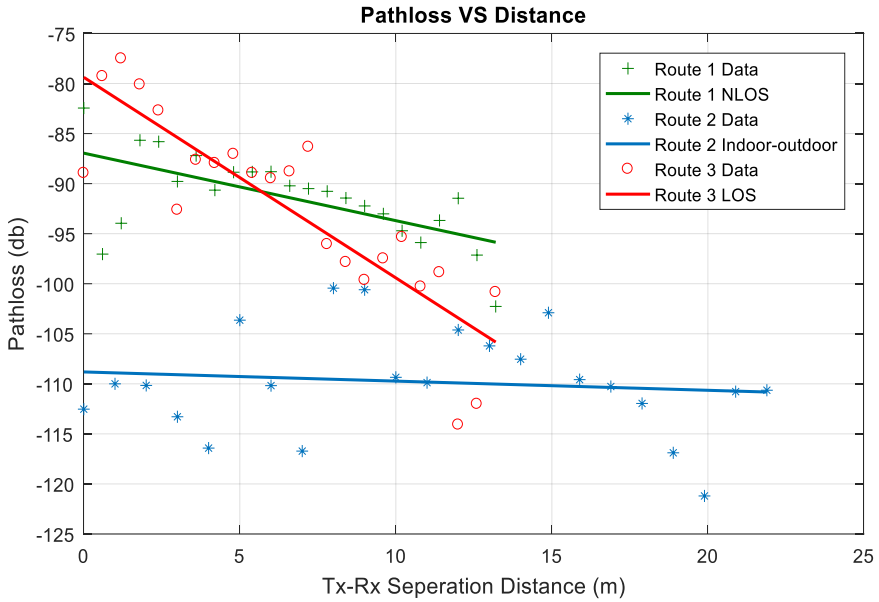

(d)

Figure 4.9: Indoor directional Path loss vs Tx-Rx separation distance for LOS, NLOS, Indoor-outdoor with linear fitting and at frequencies (a) 5.8GHz, (b) 26GHz, (c) 28GHz and (d) 60GHz.

The maximum variations of path loss at 5.8GHz found approximately between ±5dBs, ±7dBs and ±9dBs respectively to route 3, route 1 and route 2. Similarly, the max variations of path loss at 26GHz were computed ±4.5dBs, ±6.5 and ±7.5dBs respectively to rout 3, rout 1 and rout 2. Following the same tone of changes, results have also computed for path loss at 28GHz and 60GHz.

Figure 4.10 illustrates the path loss against the Tx-Rx separation distance, where the vertical polarised omnidirectional antenna was used for the transmitter. The average result with curve fitting for Route 3, the path loss data in Fig: 4.10 (a-d) is between -53db to -85db, NLOS route 1 -67db to -87db and indoor-outdoor is -

80db to -100db. The path loss here is increases as compared to Figure 4.9(a-d) because of the class of antenna that radiates radio wave uniformly in all directions.

A simple slop (solid lines) channel model was adopted to summarise the results in Figure 5.10(a-d). It is shown in the simulated results that the maximum variation for path loss at 5.8 GHz using the omnidirectional antenna is found approximately between ±5, ±7 and ±9; at 26GHz ±4, ±5 and ±8; at 28 GHz ±4, ±3 and ±6; 60 GHz ±6, ±7 and ±8 respectively to route 3, route 1 and route 2.

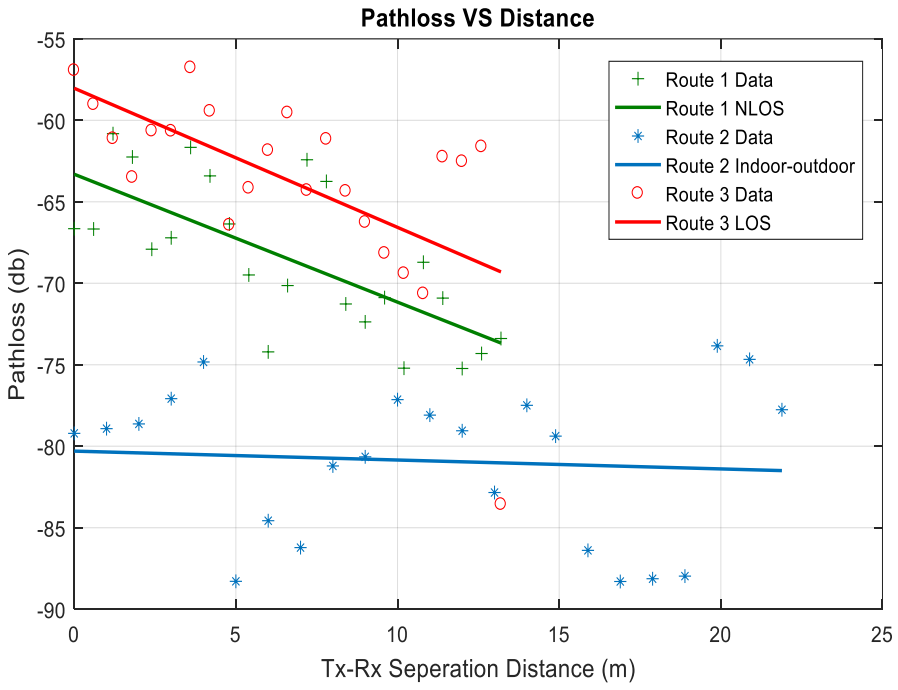

(a)

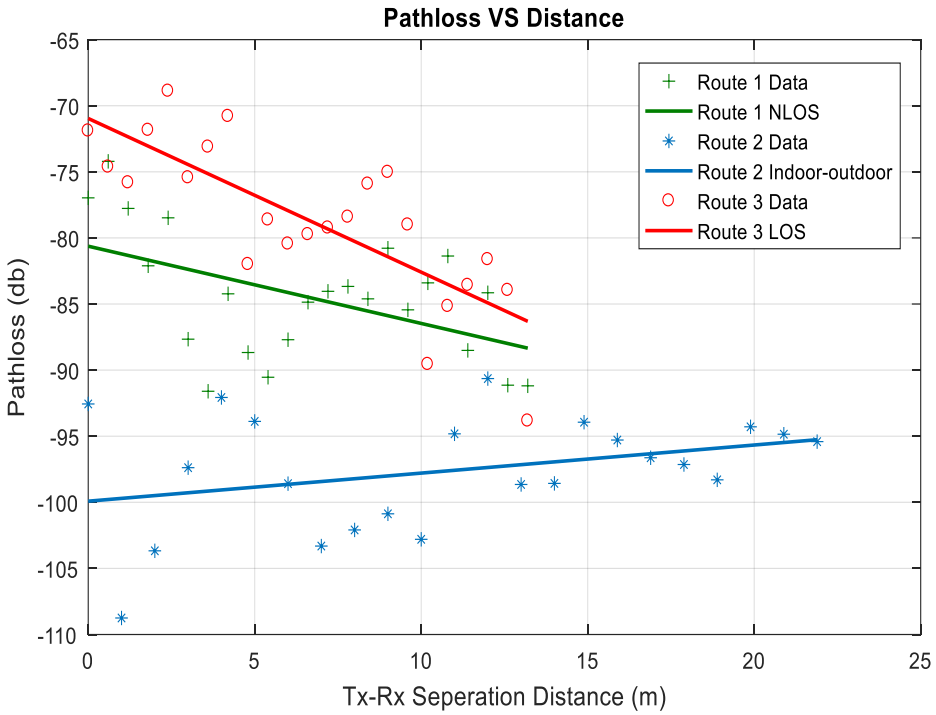
Pathloss VS Distance
Route 1 Data
Route 1 NLOS
Route 2 Data
Route 2 Indoor-outdoor
Route 3 Data
Route 3 LOS
Pathloss (db)
Tx-Rx Seperation Distance (m)
-65
-70
-75
-80
-85
-90
-95
-100
-105
-110
0
5
10
15
20
25

(b)

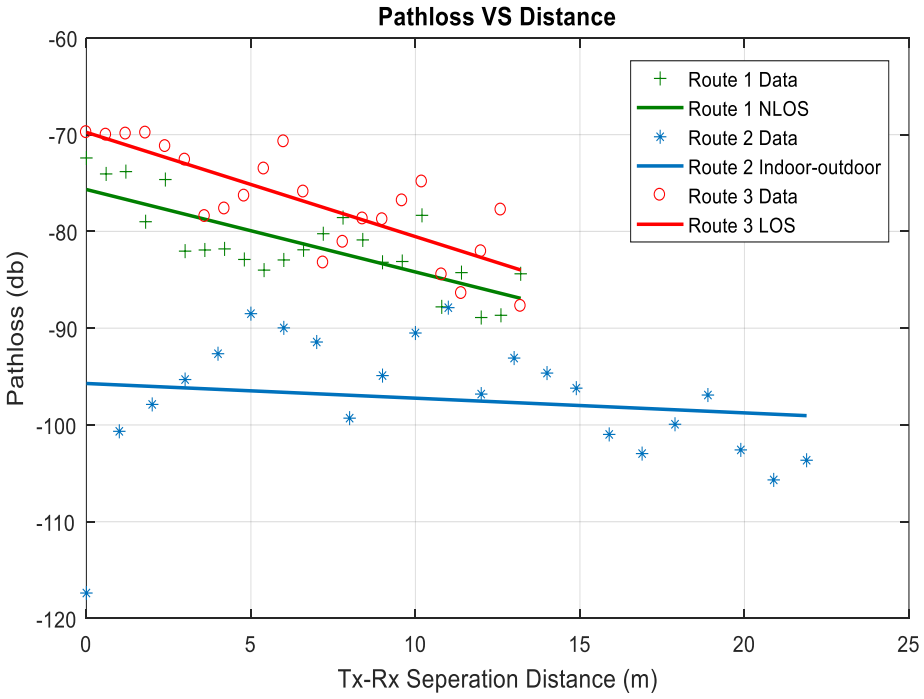
Pathloss VS Distance
Route 1 Data
Route 1 NLOS
Route 2 Data
Route 2 Indoor-outdoor
Route 3 Data
Route 3 LOS
Pathloss (db)
Tx-Rx Seperation Distance (m)
-60
-70
-80
-90
-100
-110
-120
0
5
10
15
20
25

(c)

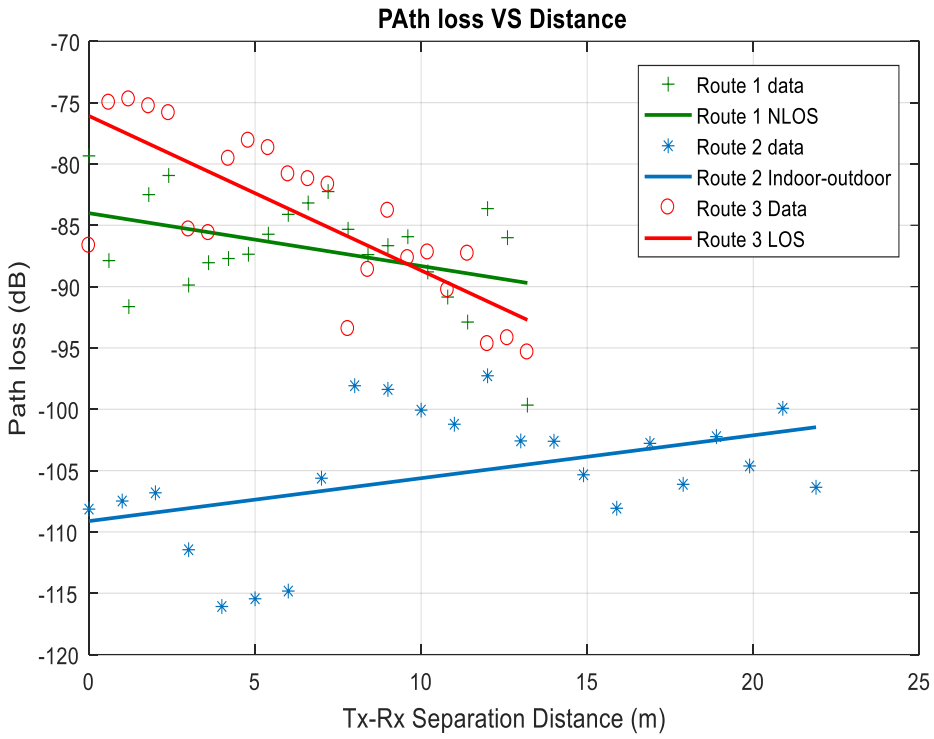

(d)

Figure 4.10: Indoor omnidirectional Path loss vs Tx-Rx separation distance for LOS, NLOS, Indoor-outdoor with linear fitting and at frequencies (a) 5.8GHz, (b) 26GHz, (c) 28GHz and (d) 60GHz.

Figure 4.11 have investigated for the received power in dBm versus Tx- Rx separation distance in meter for LOS, NLOS and outdoor receiver rout with directed radiation antenna pattern.

The computed result shows that the worst case is for route 3 partly NLOS at 60GHz, where the received power is limited between -55dBm and -70dBm for a short distance because of the losses due to attenuations. While for route 1 the power is constant between -55dBm and -65dBm because of the most multipath are added constructively and vice versa.

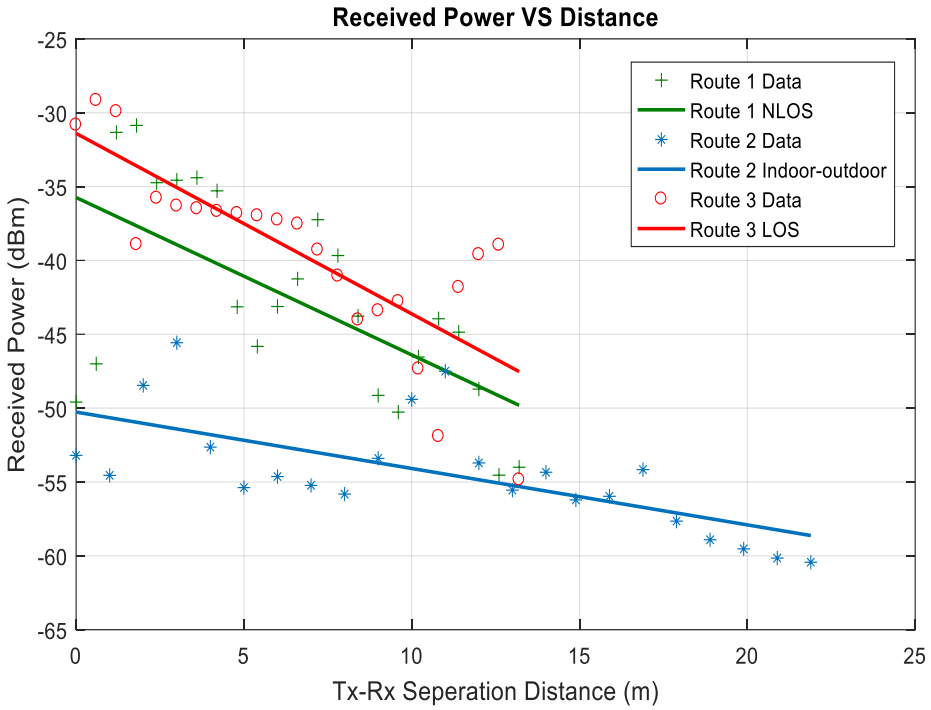
Received Power VS Distance
Route 1 Data
Route 1 NLOS
Route 2 Data
Route 2 Indoor-outdoor
Route 3 Data
Route 3 LOS
Received Power (dBm)
Tx-Rx Seperation Distance (m)
-25
-30
-35
-40
-45
-50
-55
-60
-65
0
5
10
15
20
25

(a)

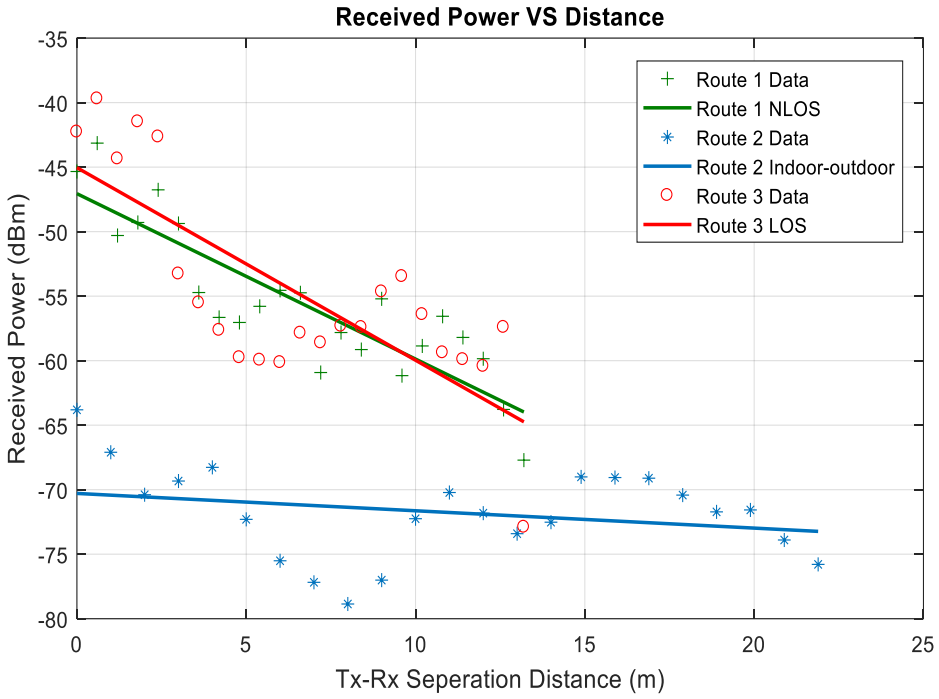
Received Power VS Distance
Route 1 Data
Route 1 NLOS
Route 2 Data
Route 2 Indoor-outdoor
Route 3 Data
Route 3 LOS
Received Power (dBm)
Tx-Rx Seperation Distance (m)
-35
-40
-45
-50
-55
-60
-65
-70
-75
-80
0
5
10
15
20
25

(b)

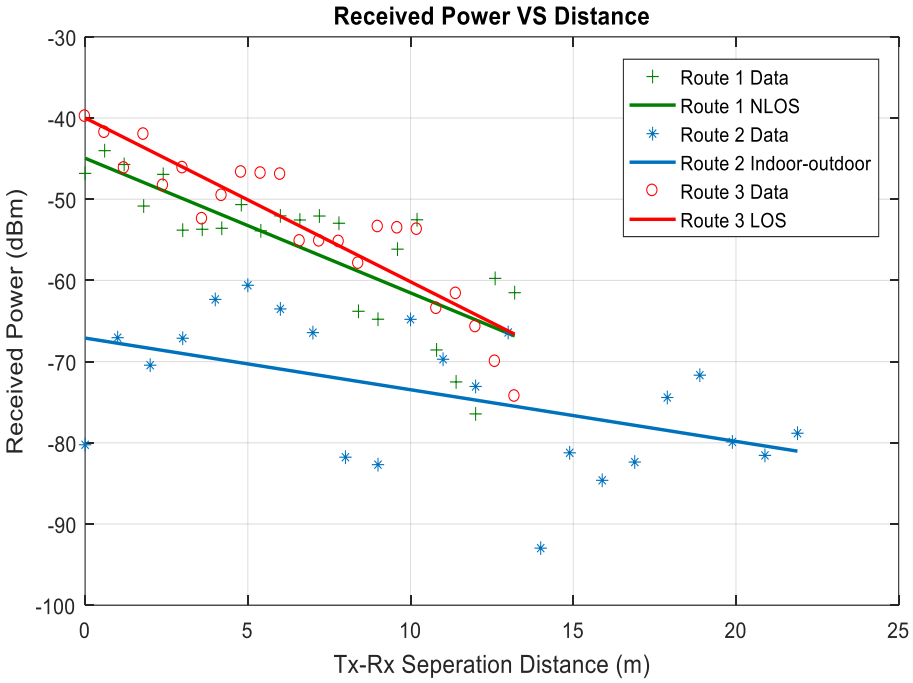

(c)

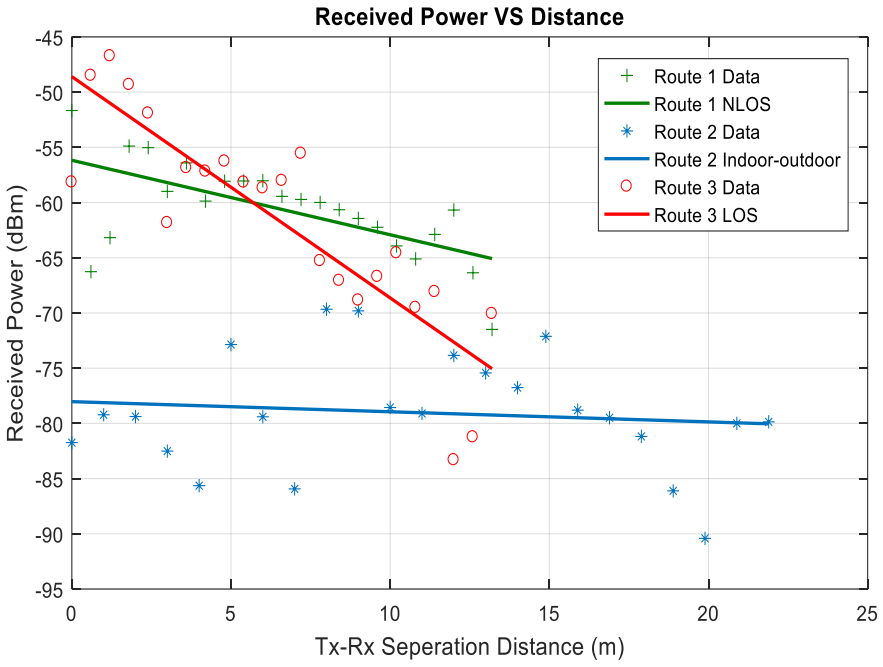

(d)

Figure 4.11: directional Received power vs TX-Rx separation distance for LOS, NLOS, Indoor-outdoor with linear fitting and at frequencies (a) 5.8GHz, (b) 26GHz, (c) 28GHz and (d) 60GHz

Figure 4.12 shows the received power at each receiver point against the Tx-Rx separation distance, where omnidirectional antenna was used for transmitter antenna. The average result with curve fitting for Route 3 LOS, the received power data in Figure: 4.12 (a-d) is between -30dBm to -70dBm, NLOS route 1 -35dBm to -65dBm and indoor-outdoor is -50dBm to -85dBm. The result here at each receiver point is increased as compared to the Figure 4.11(a-d) because of the class of antenna that radiates radio wave uniformly in all directions. The received power with omnidirectional radiation pattern increases for a short distance especially when the building materials is the main interruption for transmitted rays and the receiver receives its signal strength in all direction as compared to the directional antenna.

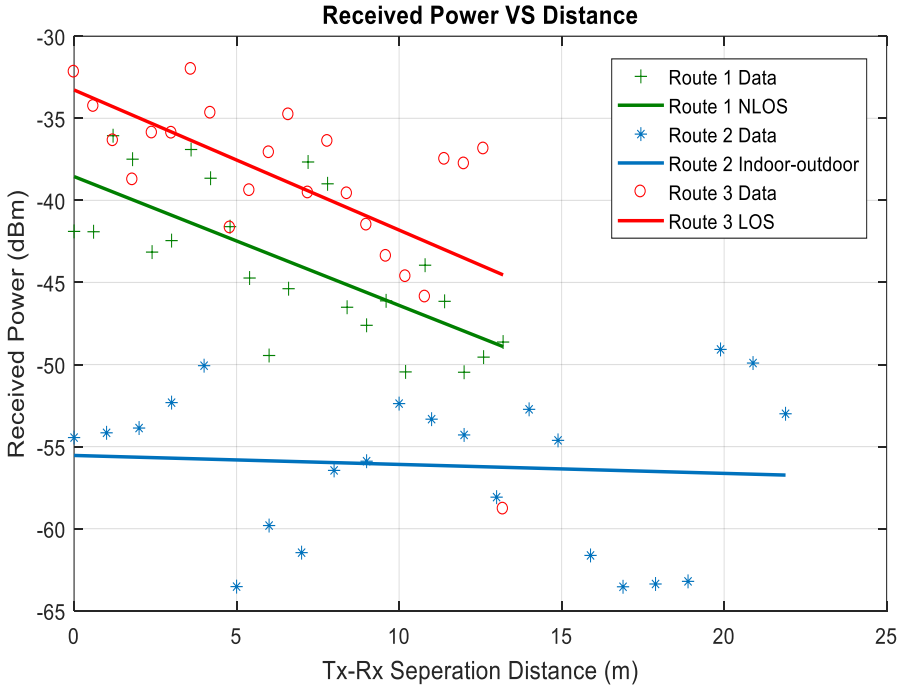

(a)

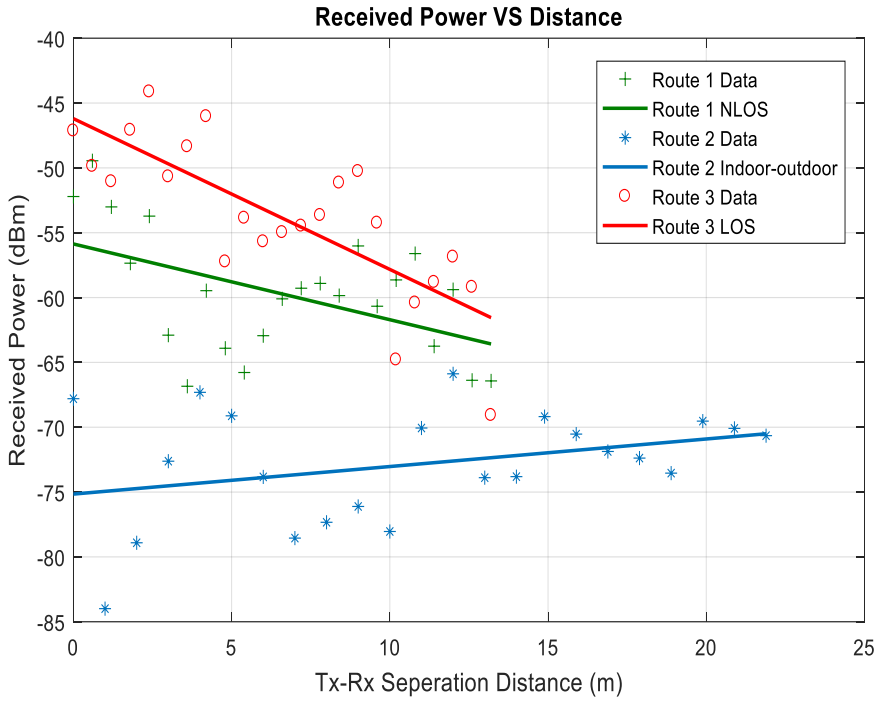
Received Power VS Distance
Route 1 Data
Route 1 NLOS
Route 2 Data
Route 2 Indoor-outdoor
Route 3 Data
Route 3 LOS
Received Power (dBm)
Tx-Rx Seperation Distance (m)
-40
-45
-50
-55
-60
-65
-70
-75
-80
-85
0
5
10
15
20
25

(b)

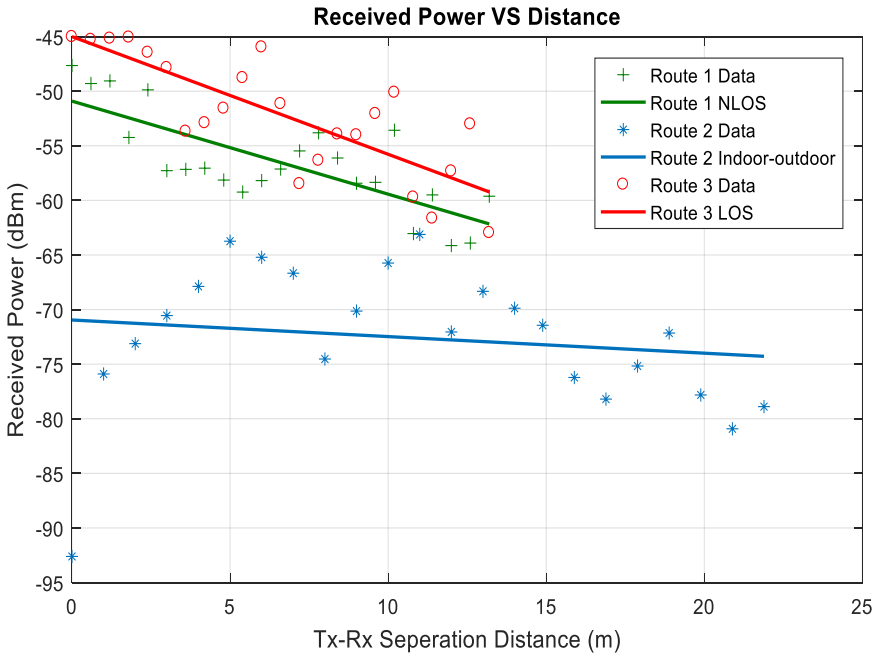
Received Power VS Distance
Route 1 Data
Route 1 NLOS
Route 2 Data
Route 2 Indoor-outdoor
Route 3 Data
Route 3 LOS
Received Power (dBm)
Tx-Rx Seperation Distance (m)
-45
-50
-55
-60
-65
-70
-75
-80
-85
-90
-95
0
5
10
15
20
25

(c)

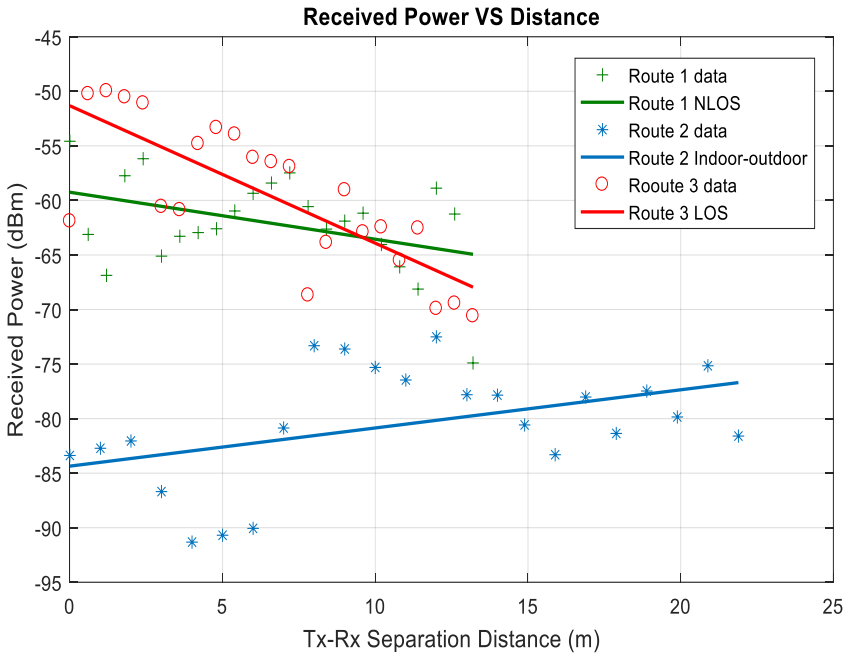

(d)

Figure 4.12: Omnidirectional Received power vs Tx-Rx separation distance for LOS, NLOS, Indoor-outdoor with linear fitting and at frequencies (a) 5.8GHz, (b) 26GHz, (c) 28GHz and (d) 60GHz

With the reference of figure 4.8, the received power in figure 4.12(d) for route 2 is increasing with the distance because of the receiver points at a higher distance is located from the transmitted rays with less multipath effects as compared to the receiver points with lower distance.

As we have concluded from the overall results of path loss and received power that omnidirectional radiation pattern, gives better receive signal strength as compared to the directional antenna. In terms of frequencies, it has been observed that 60GHz transmitter has less coverage compared to the 26 and

28GHz.

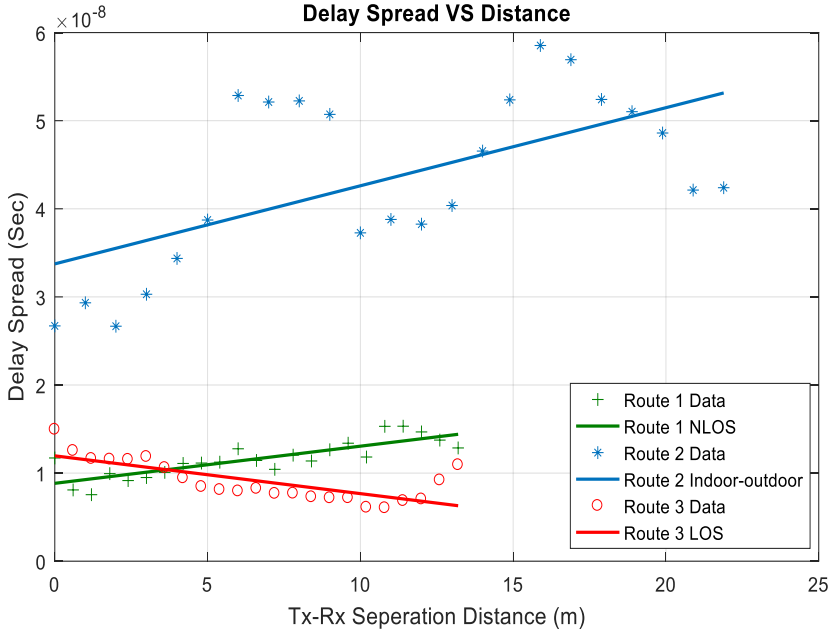
Delay Spread VS Distance
×10^-8
Delay Spread (Sec)
Tx-Rx Seperation Distance (m)
Route 1 Data
Route 1 NLOS
Route 2 Data
Route 2 Indoor-outdoor
Route 3 Data
Route 3 LOS

(a)

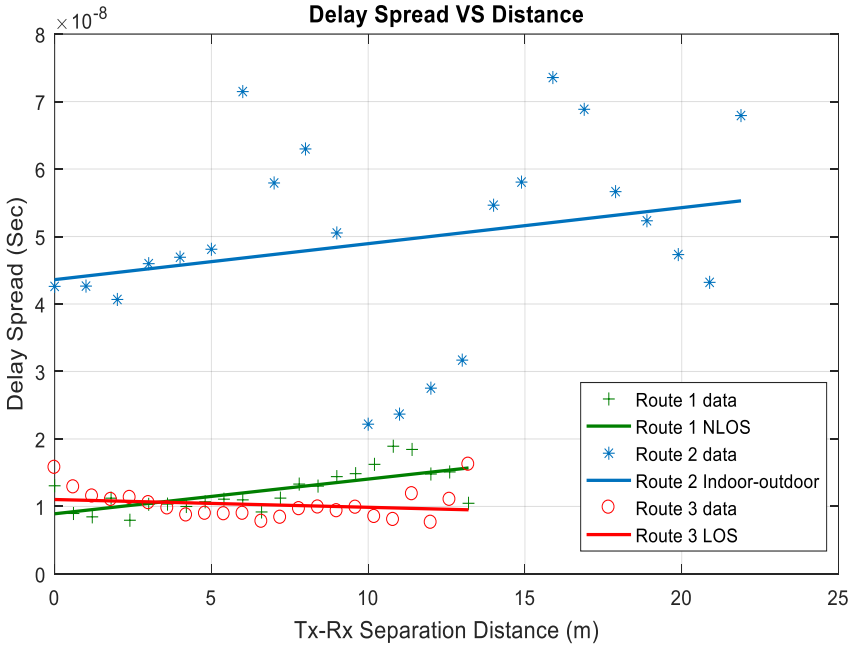
Delay Spread VS Distance
×10^-8
Delay Spread (Sec)
Tx-Rx Separation Distance (m)
Route 1 data
Route 1 NLOS
Route 2 data
Route 2 Indoor-outdoor
Route 3 data
Route 3 LOS

(b)

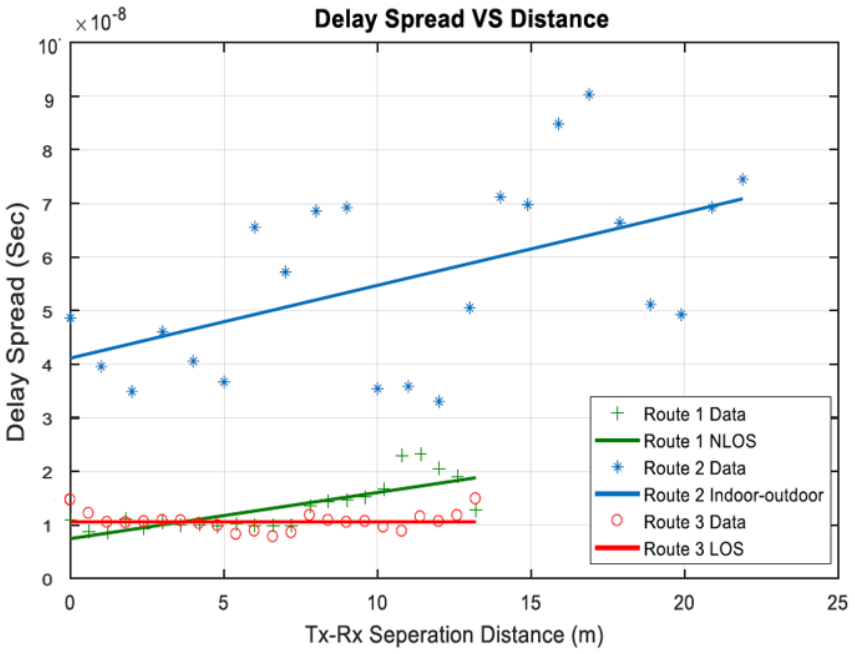

(c)

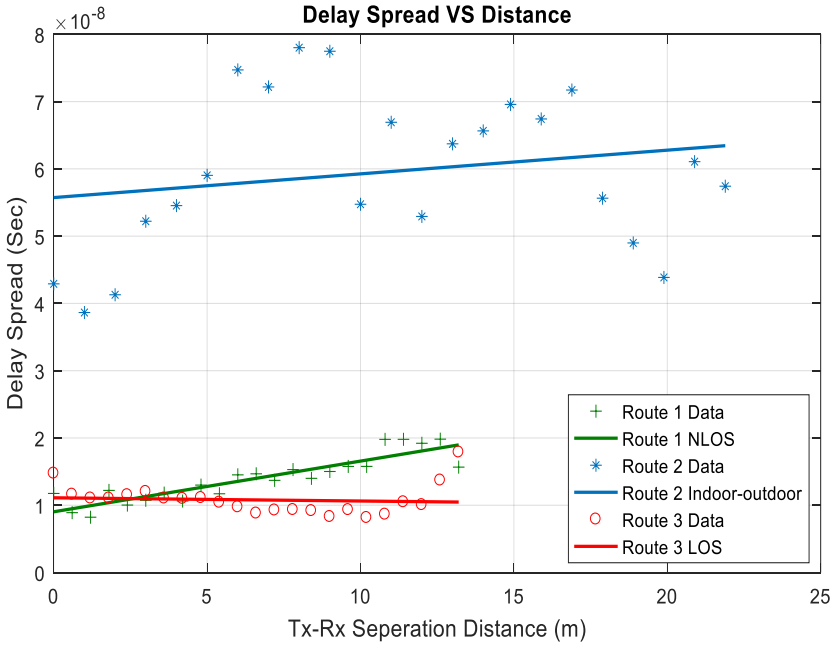

(d)

Figure 4.13: Omnidirectional Delay Spread vs Tx-Rx separation distance for LOS, NLOS, Indoor-outdoor with linear fitting and at frequencies (a) 5.8GHz, (b) 26GHz, (c) 28GHz and (d) 60GHz

So, the channel behaviour is characterised by some other important parameters including delay spread and mean direction of arrival for a system using an omnidirectional antenna at the same four frequencies for the same scenario. The results are investigated for Line of sight (LOS), Non-line of sight (NLOS) and indoor-outdoor (NLOS).

Figure 4.13 shows a comparison between the performance of the four different frequencies using an omnidirectional antenna for LOS, NLOS and NLOS indoor-outdoor. It can be observed that at 5.8GHz and 26GHz the delay spread is higher than at 28 GHz and 60GHz especially for NLOS indoor-outdoor as shown in Figure 4.13(c,d).

The delay spread for NLOS indoor-outdoor receivers route 2 is much higher as compared to the same floor LOS and NLOS because of the height of the transmitter and a large number of materials assumptions used between them. The initial rise is due to the position of the receivers with respect to the transmitter antenna. For line of sight (LOS) at higher separation distance the travel time of all multipath components are mostly the same, resulting much smaller delay spread.

Figure 4.14 shows the mean direction of arrival where the rays arrive at each receiver point in a particular direction at four different spectrums against the Tx-Rx separation distance (m).

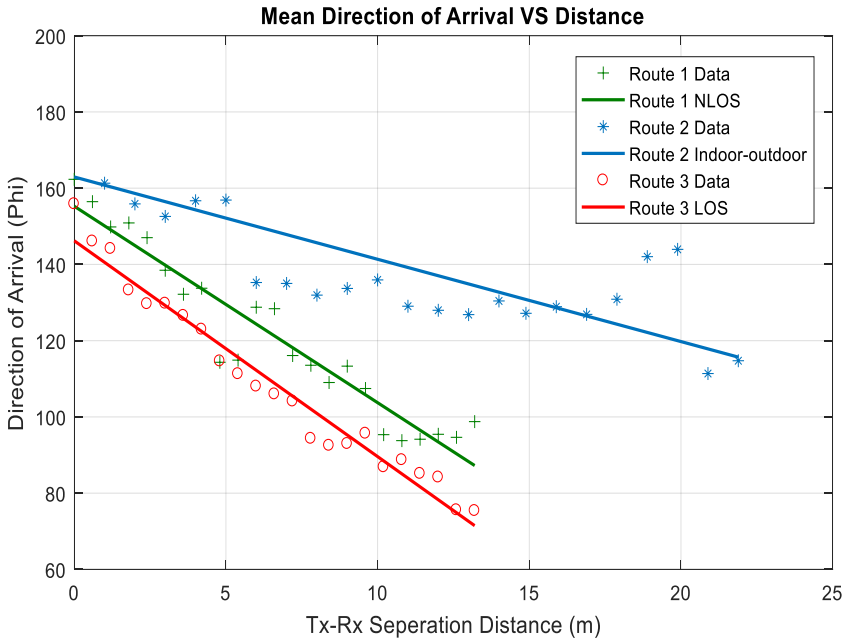
Mean Direction of Arrival VS Distance
Direction of Arrival (Phi)
Tx-Rx Seperation Distance (m)
Route 1 Data
Route 1 NLOS
Route 2 Data
Route 2 Indoor-outdoor
Route 3 Data
Route 3 LOS

(a)

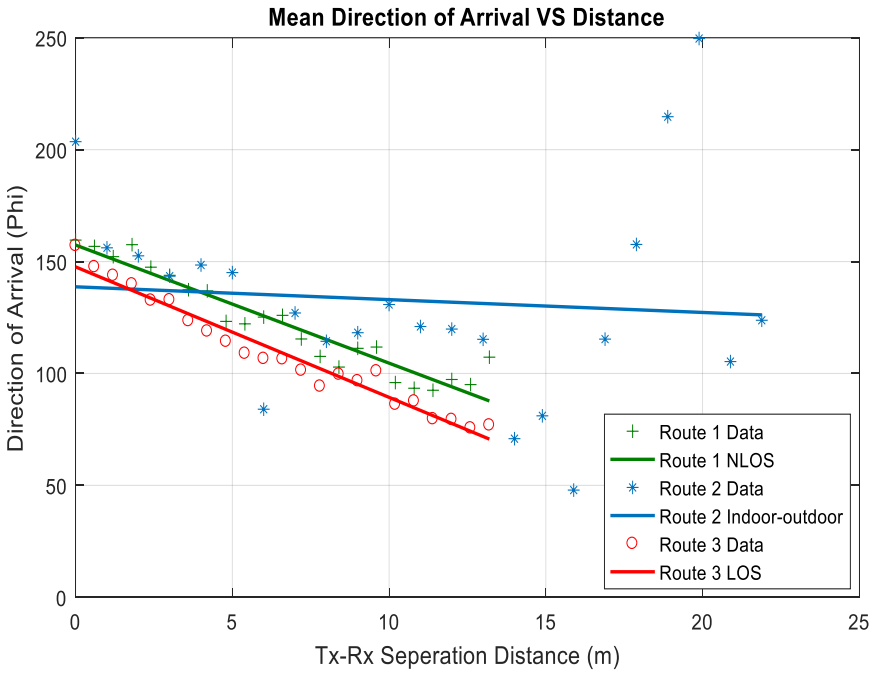
Mean Direction of Arrival VS Distance
Direction of Arrival (Phi)
Tx-Rx Seperation Distance (m)
Route 1 Data
Route 1 NLOS
Route 2 Data
Route 2 Indoor-outdoor
Route 3 Data
Route 3 LOS

(b)

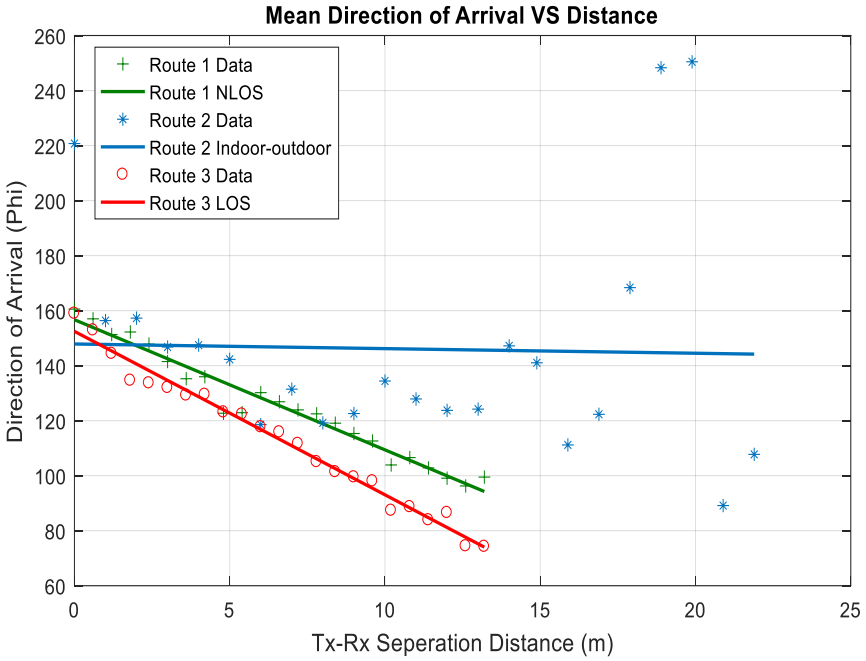

(c)

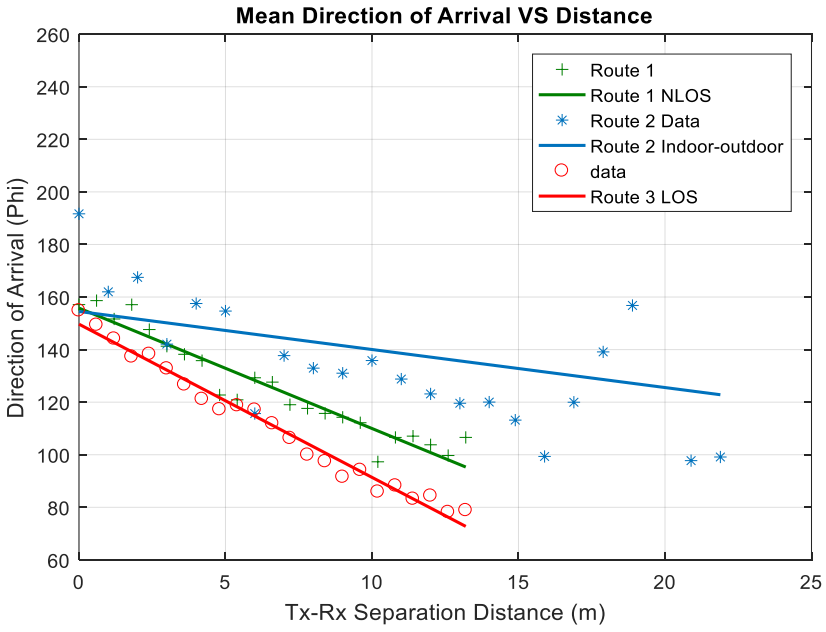

(d)

Figure 4.14: Mean Direction of Arrival vs TX-Rx Separation distance (m) for LOS, NLOS, Indoor-outdoor with linear fitting and at frequencies (a) 5.8GHz, (b) 26GHz, (c) 28GHz and (d) 60GHz.

Figure: 4.14(a) is the direction of arrival at 5.8 GHz frequency for LOS, NLOS and Indoor-outdoor (NLOS) in which the true angle found where the ray arrives at the receiver point in simulation is 70-150 degrees, 90-160 degrees and 110-160 degrees for route 3, route 1 and route 2. Similarly, Figure 4.14(b) represents the arrival direction at 26 GHz followed the similar tone for same scenario is 70-150 degrees, 90-160 degrees and 50-250 degrees respectively. Followed the same procedure the direction of arrival for 28GHz and 60 GHz is found in Figure 4.14(c) and Figure 4.14(d).

4.7 Conclusions:

An indoor office environment was simulated using Wireless Insite for indoor-indoor (LOS, NLOS) and indoor-outdoor (NLOS) propagation channels under four different frequencies; 5.8GHz, 26GHz, 28GHz and 60GHz. Channel parameters characteristics such as path loss model, received power, delay spread, mean direction of arrival and mean arrival time for multi-frequencies were presented and modelled.

The effect of building materials, multipath effect and changes in antenna radiation has been presented. It has been observed that signal is much more effected by concrete and wood and reacting differently for LOS and NLOS at each particularized frequency. The results shown that path loss behaves at higher frequency and due to the number of obstructions, while the received power and delay spread decreases by increasing frequency.

5. MEASUREMENT RESULTS OF THE INDOOR MULTIPATH CHANNEL PROPAGATION FOR 5G MM-WAVE

5.1 Introduction:

After simulation of ray tracing for the indoor multipath channel propagation of mm-wave as shown in chapter 4, it is necessary to test the performance of the system for practical analysis to get a good agreement between the simulated results and the measurements results. In this chapter, we have also briefly discussed the procedure of our real environments measurements to understand the hardware architecture and the software system for which the channel sounder can be deployed to make a useful measurement.

5.2 60GHz Channel Sounder Communication process:

Channel sounder is used to measure the propagation channel at new frequencies and bandwidth between transmitter (TX) and receiver (RX) for new use cases, generating information for characteristics of the wireless channel. The important factor of channel sounders is their multi-purpose functionality to also assume in creating statistical and site-specific models and for learning fundamentals about channel behaviour at new frequencies, bandwidths, and operating environments[78].

Figure 5.1 represents the channel sounder behaviour and beamforming with multipath channel effects received by the receiver (Rx) from the transmitter (Tx).

MATLAB is the most powerful tool to setup up and controls the channel sounder that involves setup and control of the SiversIMA Transceiver via the CO2201A Evaluation Board as well as control of the DSO-X3014A Oscilloscope as shown in figure 5.3 and figure 5.4.

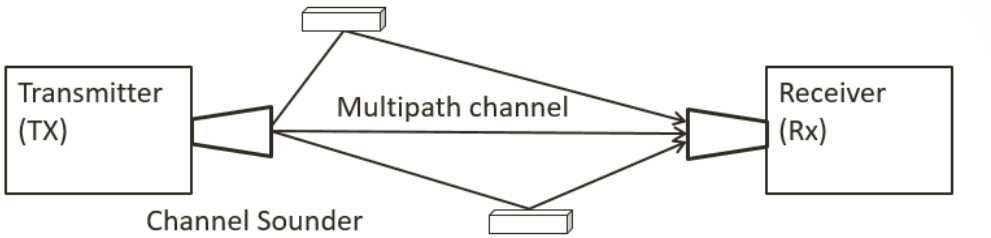

Figure 5.1: Channel Sounder behaviour.

A channel sounder is used to measure the impulse response h(τ), or equivalently, the frequency response H(f) of a radio channel (τ delay, t time, f frequency) and these are Fourier Transform pairs h (τ) $\leftrightarrow$ H(f).

Several techniques can be used for channel sounding, based on the type of signal transmitted. The simplest, conceptually, is a pulse signal, however, pulse sounders require a large peak to mean power and are susceptible to interference. The pattern of received pulses in time gives the impulse response directly. A network Analyser connected between transmitter and receiver can provide a frequency swept signal to measure the frequency response of the channel directly.

The methods include chirp sounders and sliding correlators involves transmission of a pseudo-random binary sequence, PSK modulated onto the

carrier. This approach has a low peak-to-mean power ratio and is insensitive to interference. We choose an m-sequence length $M = 2^m-1$, m is an integer and M-sequence has autocorrelation (ACF) function comprising an impulse of height M at delay $\tau = 0$ and -1 elsewhere. The cross-correlation of the m-sequence with the received signal gives the impulse response.

The transmitted signal be:

$$s(t) \leftrightarrow S(f)$$

Transmit and receiver filter response be:

$$F_{TX}(f), F_{RX}(f)$$

Channel response be:

$$h(\tau) \leftrightarrow H(f)$$

Receiver noise be

$$n(t) \leftrightarrow N(f)$$

It is to be noted that the transmit sequence is repeated continuously then the received signal is:

$$r(t)+n(t) \leftrightarrow R(f)+N(f) = F_{TX}.H.F_{RX}.S + N$$

An estimate of H can thus be obtained from

$$H \approx (R(f)+N)/ (F_{TX}.F_{RX}.S) = H + N/ (F_{TX}.F_{RX}.S)$$

The channel sounder architecture can be simply defined from figure 5.2.

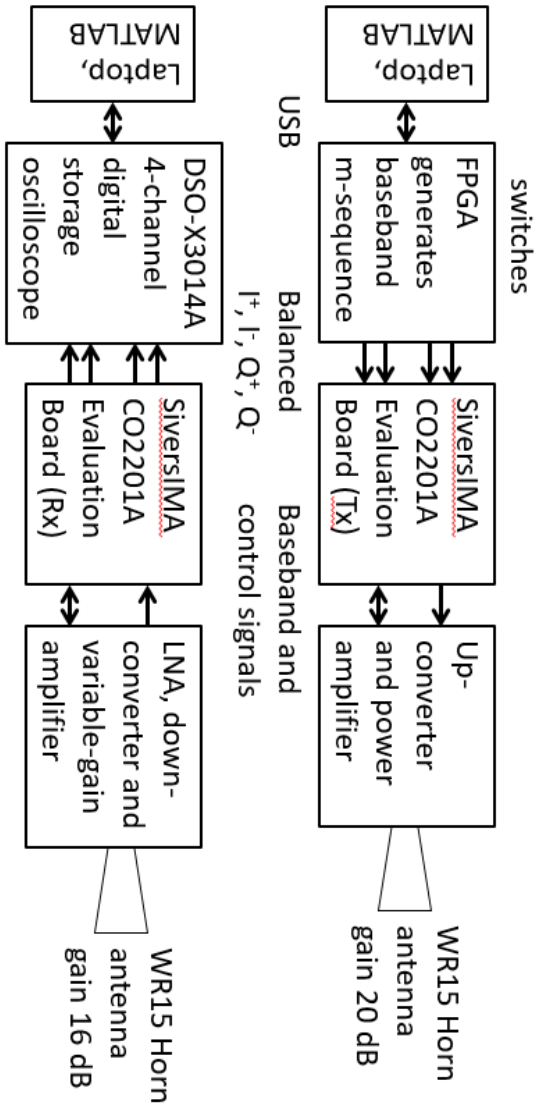

Figure 5.2: Channel Sounder Architecture

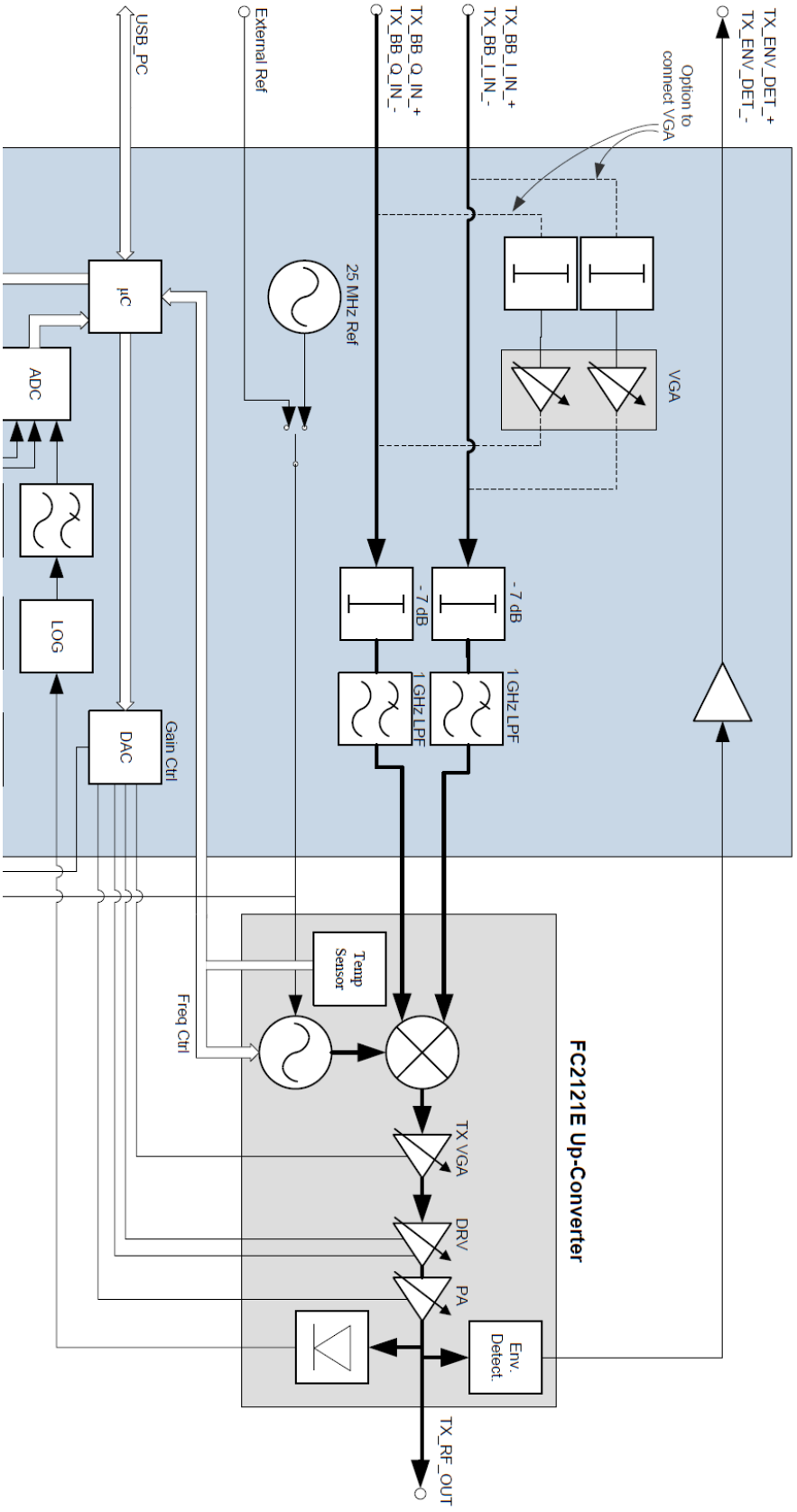

Figure 5.3: CO2021A Transmitter section

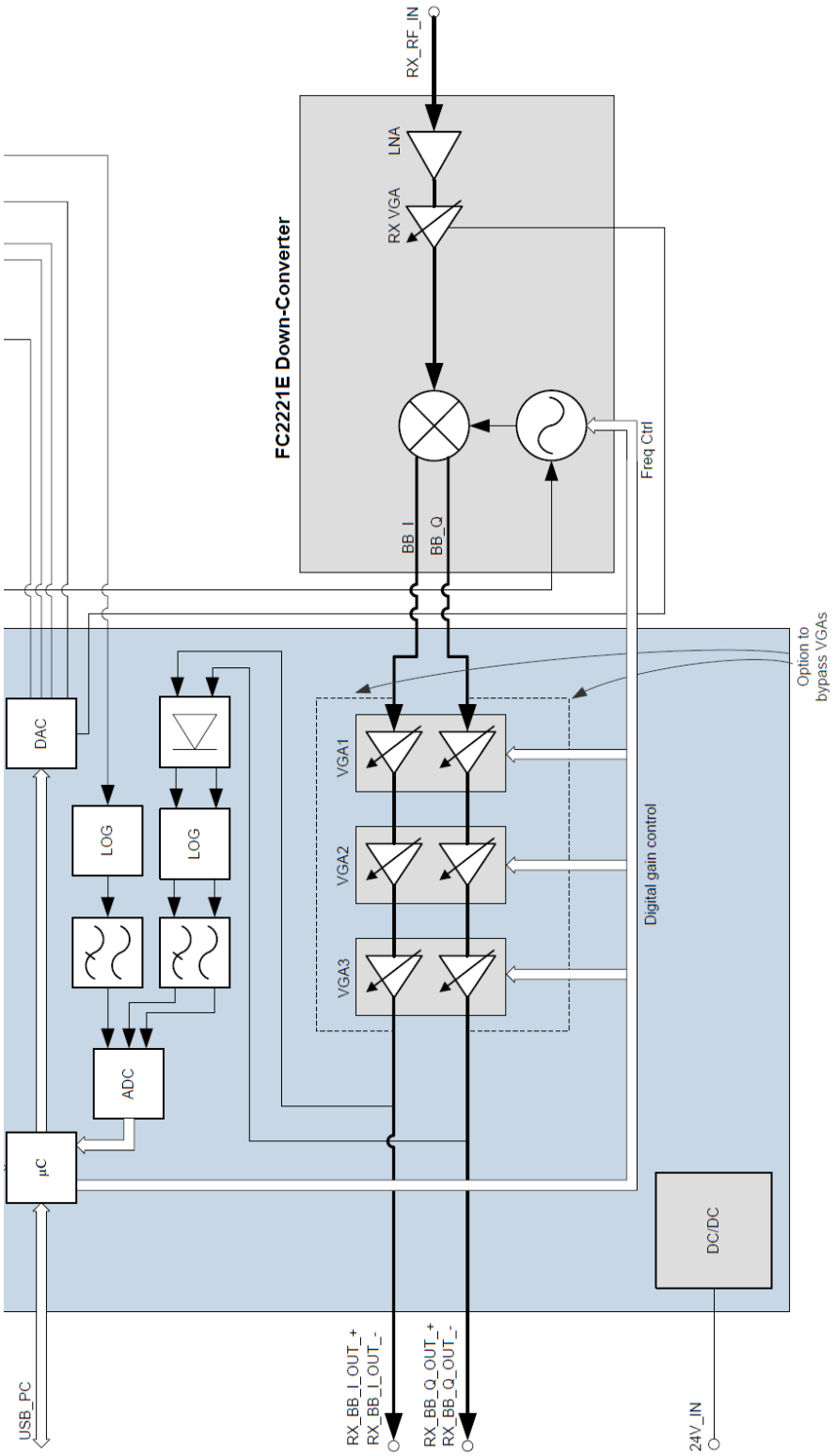

Figure 5.4: CO2201A Receiver Section

SiversIMA provides a graphical user interface (GUI) program to connect to a PC over USB and it can be replaced this with direct commands from MATLAB. The MATLAB script for transmitter (Tx) initialises the transmitter section of the board, sets the carrier frequency and the transmitter power amplifier gain. The script for receiver (Rx) initialises the receiver side and sets the receiver carrier frequency, range of system parameters, automatically sets up the system and captures an impulse measurement.

The Altera FPGA board is programmed to provide a balanced baseband m-sequence at a range of clock frequencies for which the sequence length is 2^m-1, and m can be from 6 to 10. The choice of data rates is 100, 125, 150, 200 and 250 MHz.

Ray-tracers like Wireless InSite provide powerful tools to explore the channel and investigate spatial diversity strategies. Indoor paths have many obstacles, walls, windows, corridors and multi-path channel has many rays. Focus for channel sounder is to validate ray-tracing predictions and determine values of electrical property to give the best match.

5.3 LOS Simulation setup and Measurement Campaign:

The actual environment for the simulations and measurements was the lab B3.26 of the 3rd floor of the Chesham building at the University of Bradford. The dimensions were obtained from the layout of the building and then compared with the physical dimension of the measurements for the accuracy of geometry. A transmitter Tx with the vertically polarized antenna was placed in the lab room at

height of 1.5 m and the horn receiver point Rx were placed at a different position in the line of sight (LOS) at 1.5 m height as shown in figure 5.5. A separation distance between Tx-Rx is 5 m.

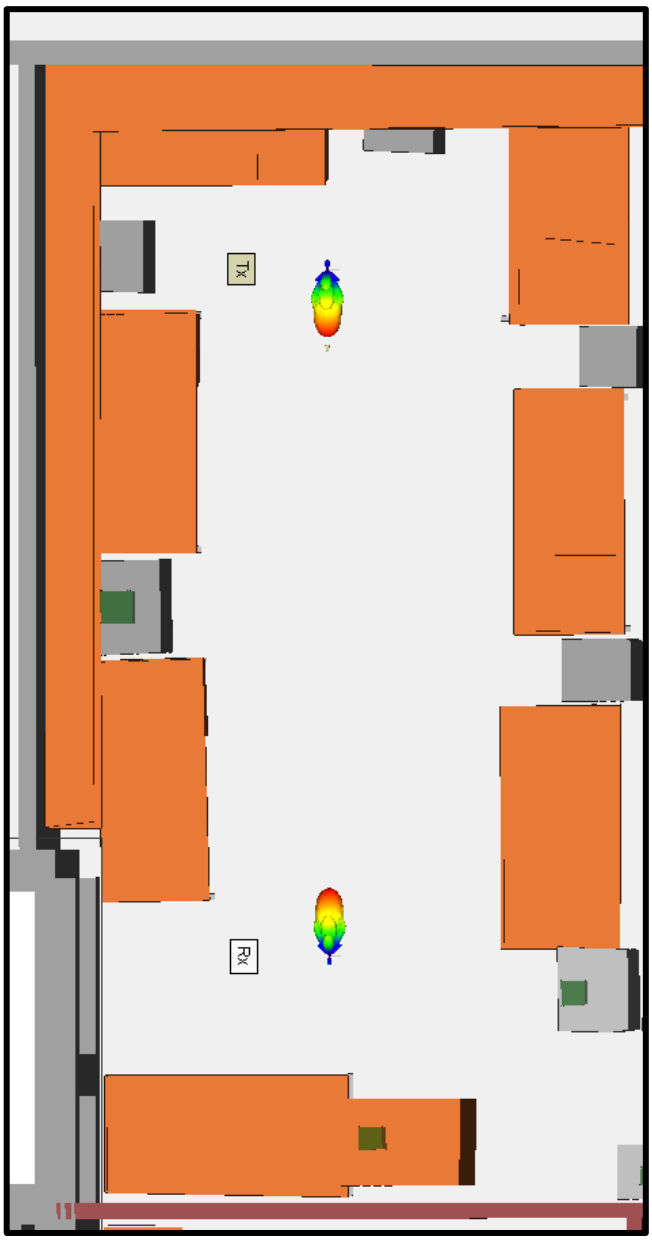

Figure 5.5: LOS Scenario with Transmitter Tx and Receiver Rx location

The simulation was performed through 3D shooting and bouncing ray (SBR) technique. Wireless Insite (Software package) allows specific parameters configurations for its complete simulation: electrical properties of the materials, waveform, transmitter, receivers, antenna and output. The sinusoid waveform is used for the simulation at 60 GHz frequency with an input power of 30 dBm. A maximum of 7 ray paths with greatest received power was obtained from transmitter Tx to the receiver Rx of ray tracer as shown in Figure 5.6.

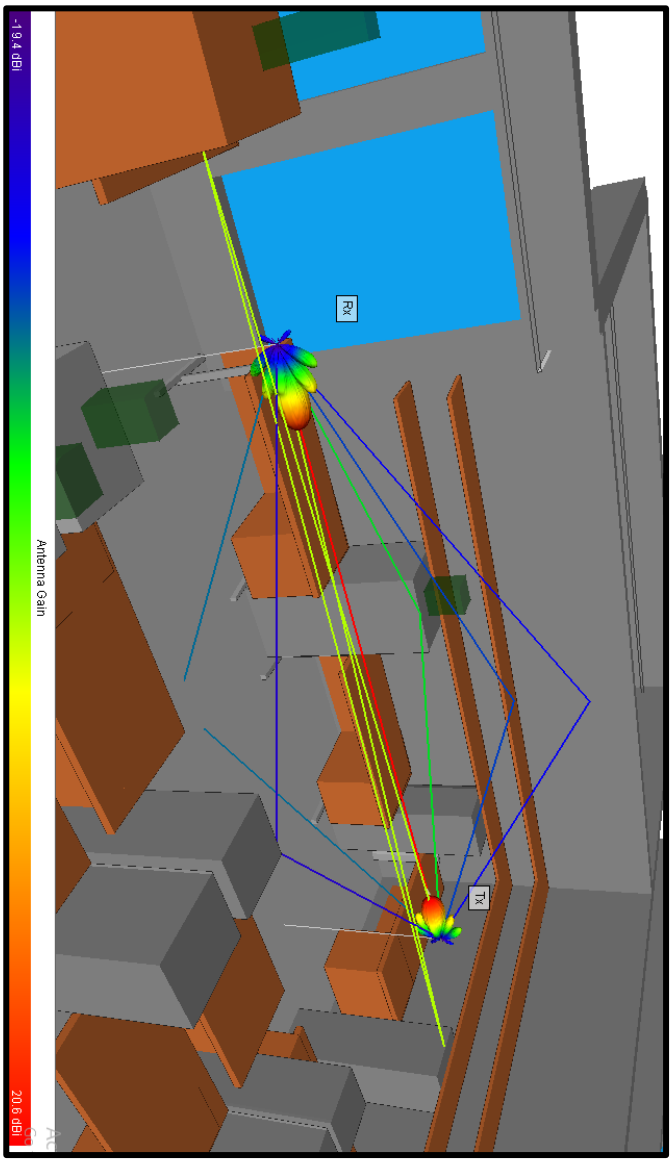

Figure 5.6: LOS 3D Shooting and bouncing ray

It can be clearly seen in the ray tracing figure that only one ray with red colour is the direct path from the transmitter to receiver without any obstruction such as reflection, transmission, diffraction and penetration, represents the LOS path with highest received power in the multipath propagation.

The measurements were performed using the 60 GHz channel sounder in a lab B3.26. In the measurements, the Tx and Rx were fixed at a certain position in a Lab as same as of the simulation with the same dimensions. The real measurement campaign images are shown in Figure 5.7

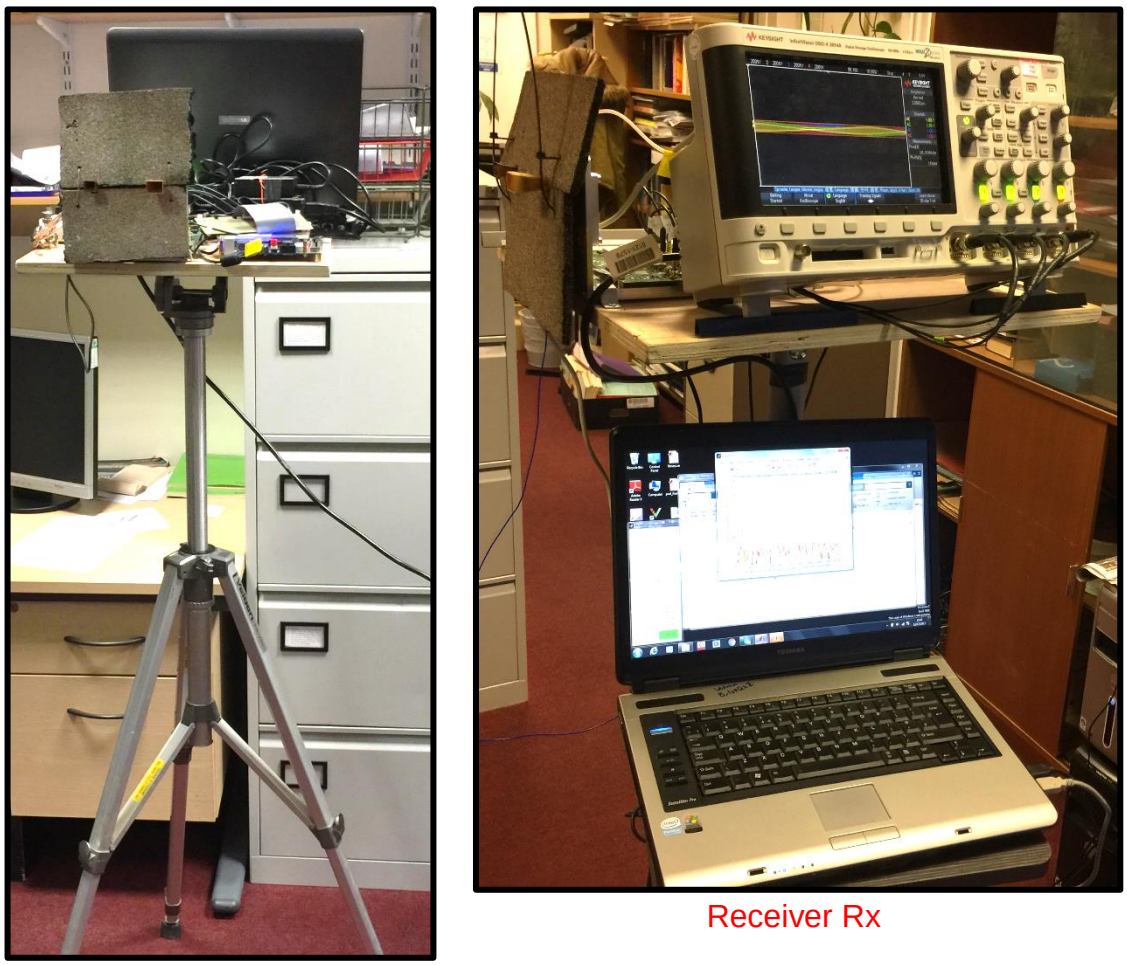

Figure 5.7: LOS Measurement images for transmitter and receiver in Lab B3.26

5.4 NLOS Simulation setup and Measurement Campaign:

The real environment for the simulations and measurements was the same landscape explained in (section 5.3) and the printer corridor of the 3rd floor of the building B3 was selected for the NLOS scenario. A horn transmitter Tx1 was placed in the printer room of the corridor at height of 2m and the receiver route 3 having 22 receiver points were placed in the printer corridor at 1.5m height.

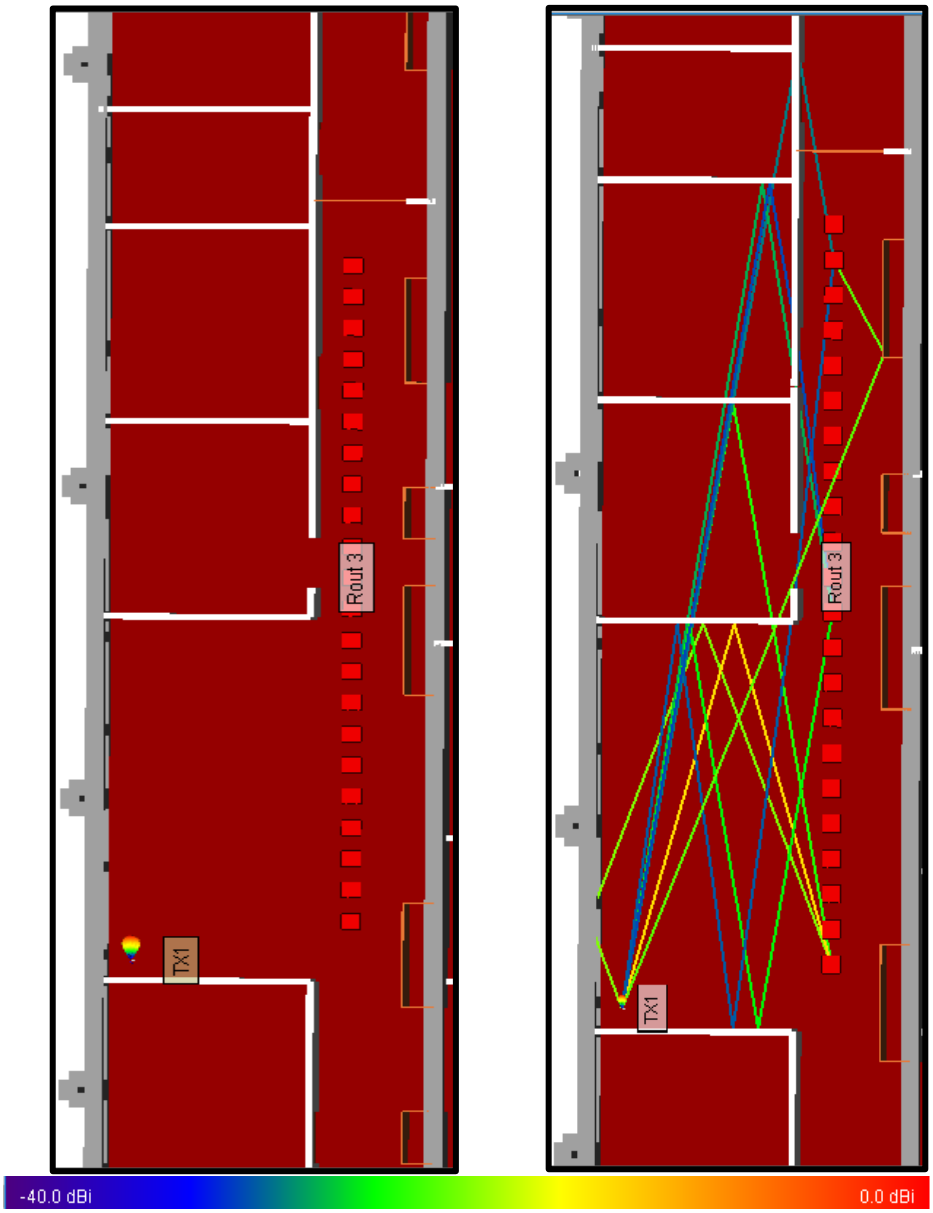

Figure 5.8: NLOS 3D simulated result scenario

The sinusoid waveform is used for the simulation at 60 GHz frequency with a vertically polarized horn antenna. A maximum of 10 ray paths was obtained for each receiver from ray tracer. The location of the transmitter Tx 1 and receiver route 3 for NLOS with ray tracing is as shown in Figure 5.8.

An anechoic chamber is a room that is designed to absorb the reflections of electromagnetic radiation and reduces the interfering energy disturbances from any external source. This has been conducted back to back and direct including corner reflections calibration for frequencies scan in a chamber to measure the performance of the antenna under test as shown in Figure 5.9.

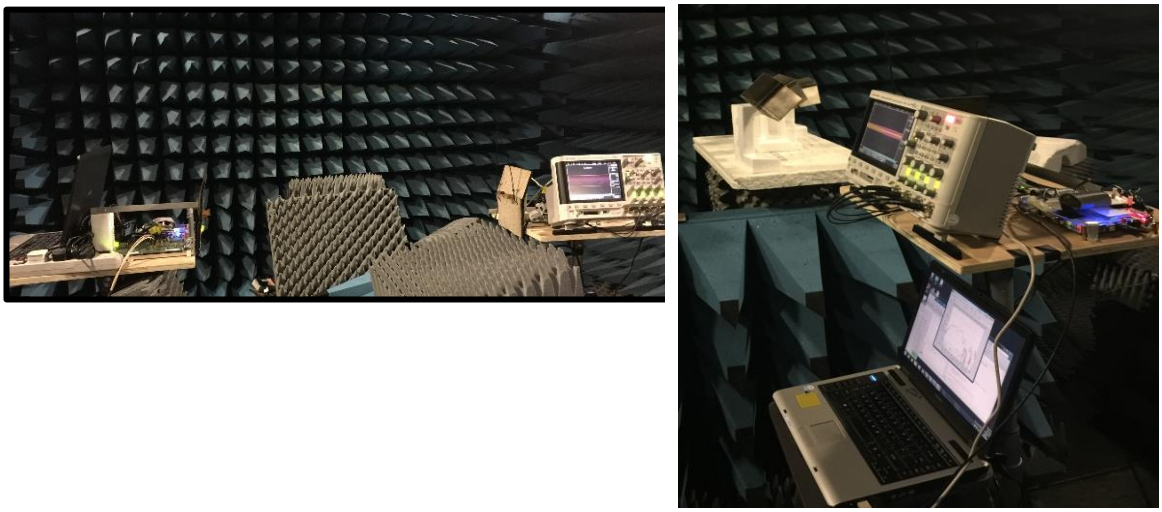

Figure 5.9: Back-back and reflection calibration in an Anechoic chamber

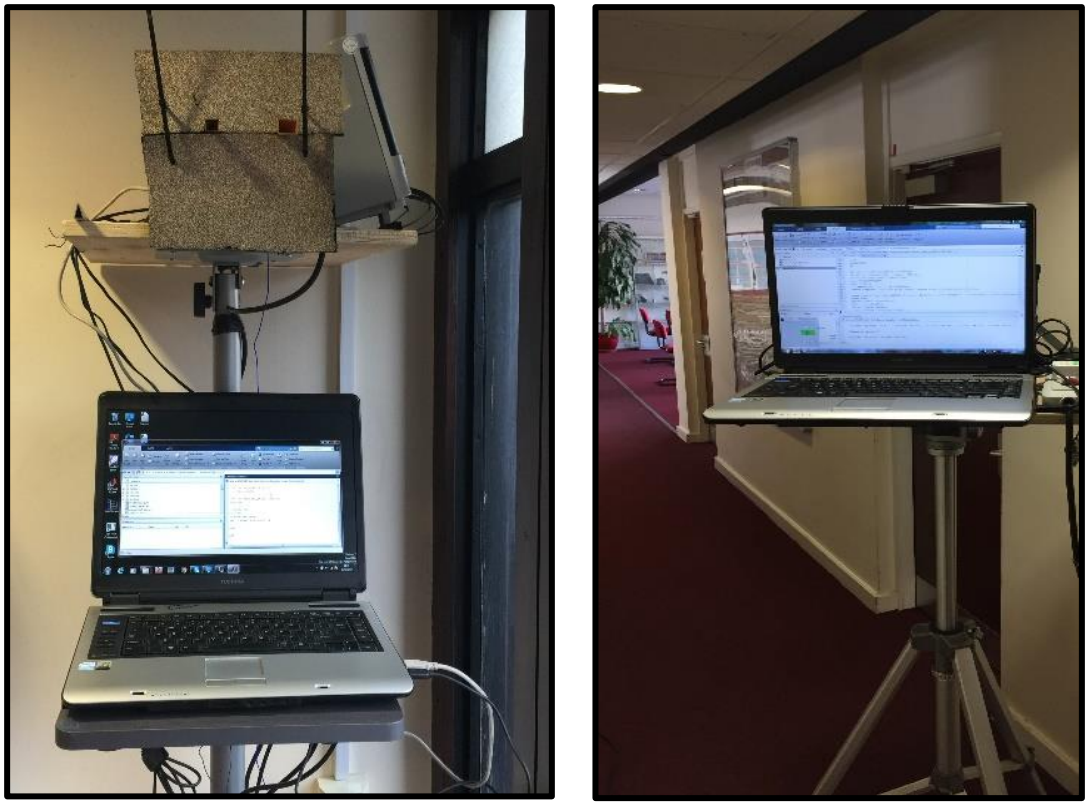

Figure 5.10: Measurement images for the transmitter and receiver in the corridor NLOS

After frequencies scan calibration in the chamber, the measurement movement was developed to evaluate the complex impulse response against the delay using transmitter at 60GHz and the interested three receiver points (Rx 1, Rx 11 and Rx 21) of route 3 using receiver antenna along the printer corridor of the third floor of the Chesham building at the University of Bradford as shown in the figure 5.10 images. The measurement setup is summarised for the ray paths and its behaviour, obtained from ray tracer in Table 5.1.

Table 5.1: Ray paths and interactions

Paths No.	Interactions at Rx 1	Interactions at Rx 2	Interactions at Rx 3
Path 1	Tx-R-Rx	Tx-R-R-Rx	Tx-T-R-Rx
Path 2	Tx-R-R-Rx	Tx-T-T-R-T-Rx	Tx-T-T-T-R-T-Rx
Path 3	Tx-T-R-T-Rx	Tx-T-T-R-T-Rx	Tx-R-R-T-Rx
Path 4	Tx-R-T-R-T-Rx	Tx-T-T-R-T-T-Rx	Tx-T-T-T-Rx
Path 5	Tx-R-T-R-T-Rx	Tx-R-T-R-T-Rx	Tx-R-R-T-T-Rx
Path 6	Tx-R-T-T-R-T-T-Rx	Tx-T-R-T-R-Rx	Tx-T-R-R-T-Rx
Path 7	Tx-R-T-T-R-T-Rx	Tx-Rx	Tx-T-T-R-R-T-Rx
Path 8	Tx-T-T-R-T-T-Rx	Tx-R-T-T-R-T-Rx	Tx-T-R-R-T-T-Rx
Path 9	Tx-T-T-T-R-R-T-T-T-Rx	Tx-T-R-T-Rx	Tx-R-T-T-T-Rx
Path 10	Tx-T-T-R-T-R-T-T-T-Rx	Tx-R-T-T-T-R-T-T-Rx	Tx-R-T-R-T-Rx

As the pattern from Table 5.1 is described as:

Tx represents transmitter, Rx is a receiver and the interaction between transmitter and receiver is symbolised by T and R. T means transmission and R is a reflection from an object or wall. If we take one pattern from the above table such as Tx-R-T-R-T-Rx which describes the indirect ray interaction between transmitter and receiver as:

Tx-R = Transmitter – Reflection

R-T = Reflection – Transmission

T-R = Transmission – Reflection

R-T = Reflection – Transmission

T-Rx = Transmission – Receiver

The pattern for direct ray between transmitter and receiver with no obstruction is Tx-Rx.

5.5 Results and Discussions:

The simulation was performed for the scenario as explained in section 5.3 for LOS, using wireless insight ray tracer. The received power in dBm and delay were computed for each ray with the greatest power in which we have found only one direct ray from transmitter to receiver. The highest peak of received power found in the simulation is 19.93 dBm at 4 ns time of arrival. As shown in Figure 5.11.

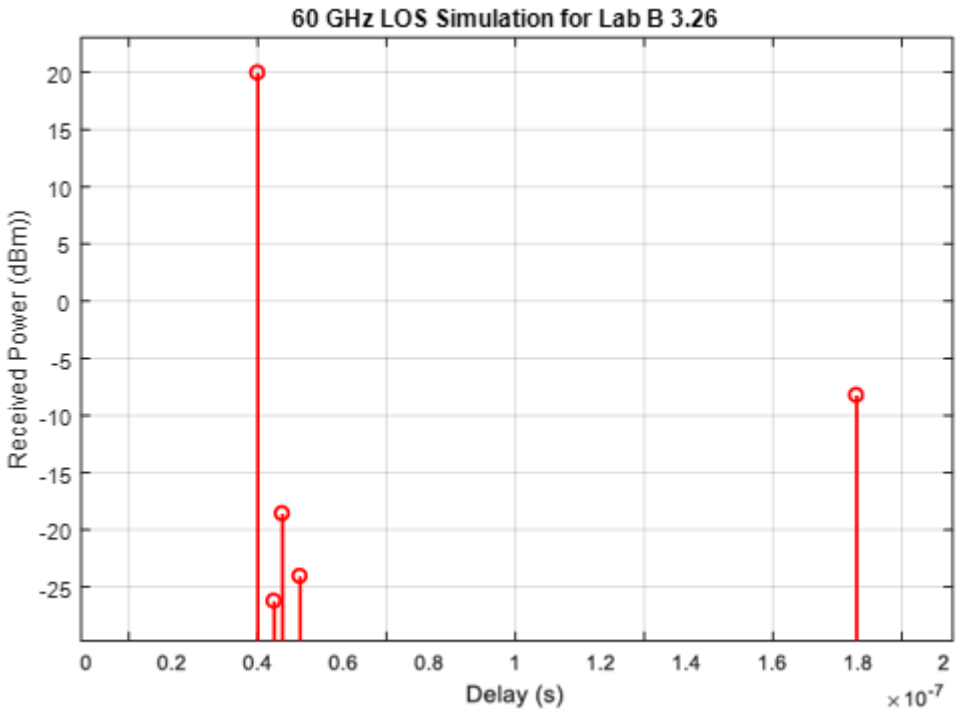

Figure 5.11: LOS Simulation result

Figure 5.12 illustrates the comparison between simulated and measured results at 60 GHz with horn antennas vertically polarized at both sides of power delay

profiles for a 5 m antenna separation. The first signal to reach the receiver, along with the direct ray, is depicted at about 20 dBm received power at the time of flight of 0.4 ns. The difference between the simulation and measurement thereafter are the relevant reflected rays distribution to take into the account for a short distance between transmitter and receiver. Some of the reflected rays have nearly the same time of flight to that of the first signal but the received power is much lower in which the highest peak is -18dBm.

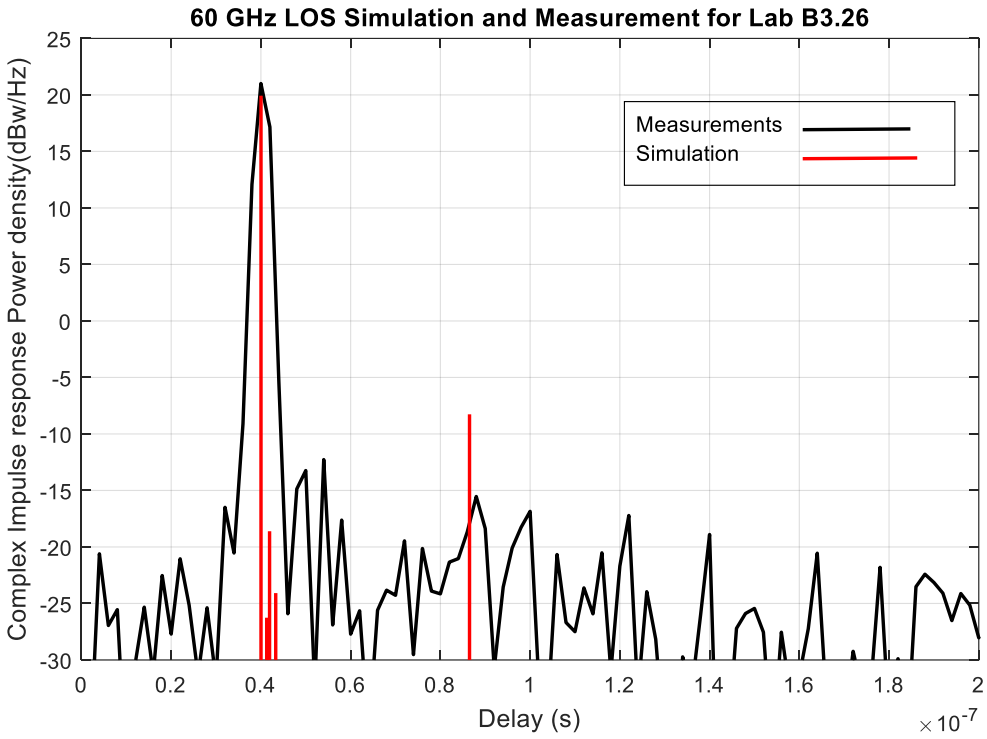

Figure 5.12: LOS Simulated and measured result.

The indoor radio propagation channel is complicated and diverse, as different structures cause different propagation phenomena, like reflection, refraction, diffraction, and scattering, which result in multipath propagation. So the direction of arrival (DOA) for NLOS were computed for simulation for each ray path.

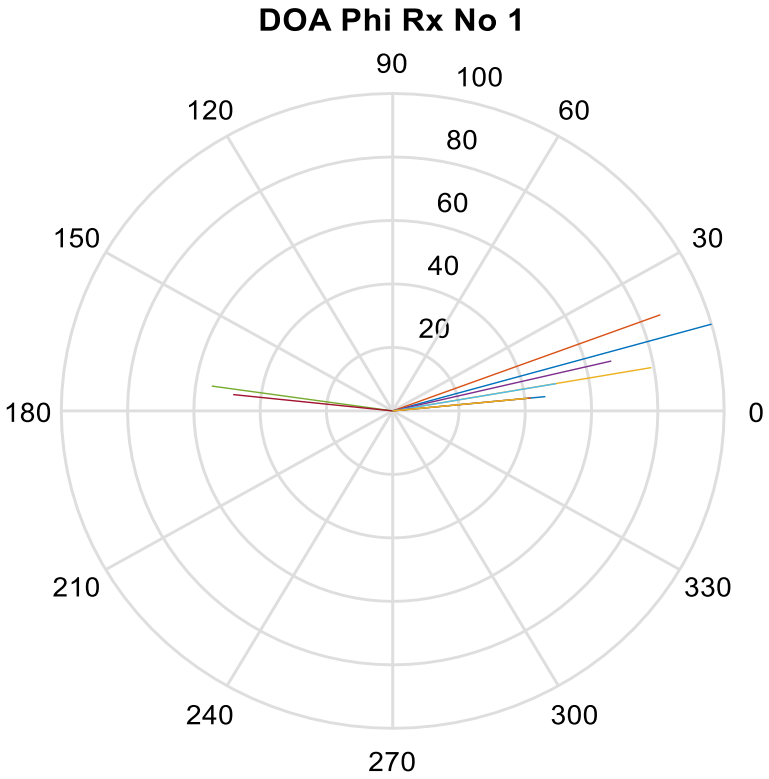

Figure 5.13: Direction of Arrival for 10 Rays at Rx 1(Degree Vs. dBi)

In the measurement campaign, the receiver point was rotated at 10-degree step size for the azimuth plane of 360 degrees and the results were investigated and processed. Figure 5.13 shows the angle estimation for the direction of arrival at first receiver for 10 rays in which the true angle found is ±20 degree.

Figure 5.14 shows the simulation and measurements results of each ray path for complex channel impulse response power density in dBw/Hz against the delay (s) for 10 paths of first receiver point in a route 3 NLOS. Pretty similar results are obtained from simulation and measurements which produces a fine peak of

channel impulse response and delay. The first ray arrived at the receiver after single reflection in simulation has an impulse response power of -43dB while the highest peak in measurement result is -37dBw/Hz. The maximum variation between the simulated result and measured result is approximately ±6dB.

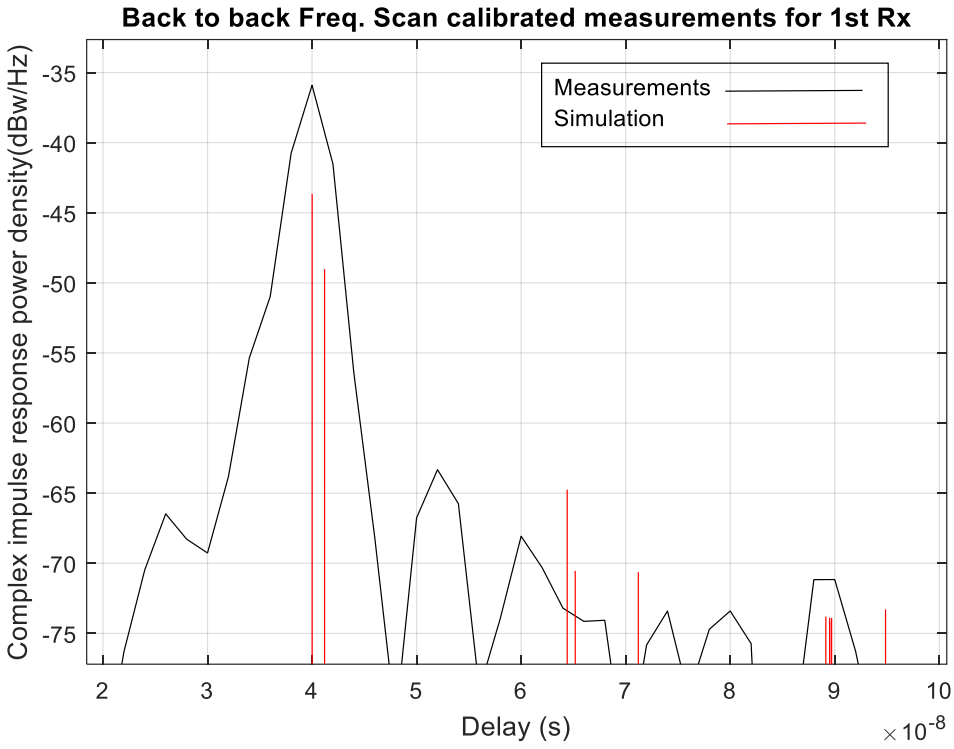

Figure 5.14: Performance of Measured and simulated paths for 1st Rx

The overall performance is quite similar except some of the ray paths from the simulation shows performance error and that is because of the interaction between the transmitter and receiver as shown in table 5.1.

The angle estimation for the second receiver (Rx 11) located at a different position in the corridor for which the true angle found is 10 and 170 degrees as shown in Figure 5.15.

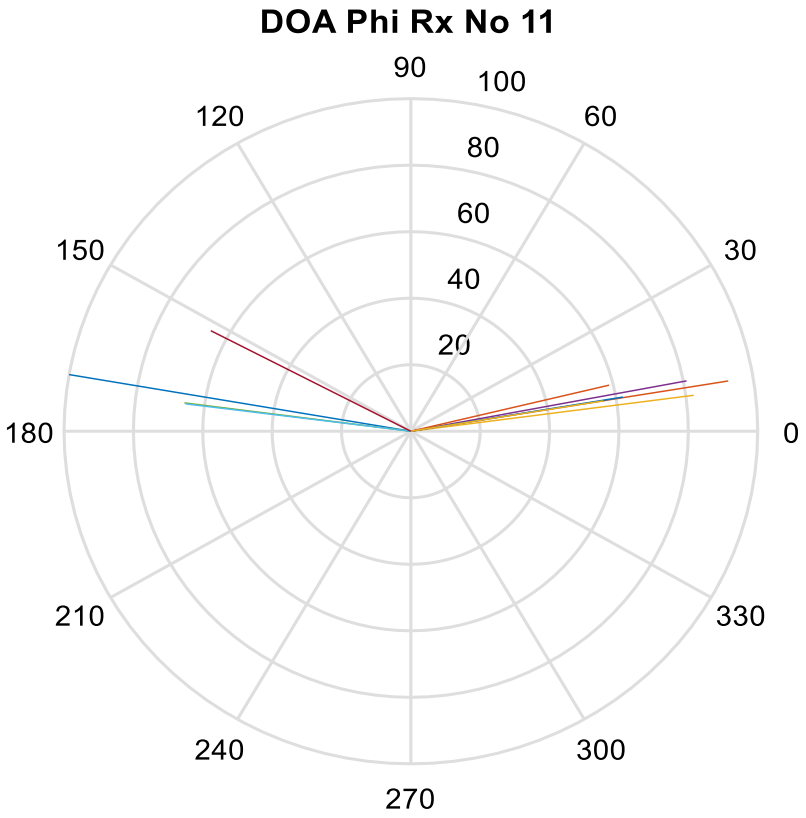

Figure 5.15: Direction of Arrival for 10 Rays at Rx 11(Degree Vs. dBi)

The performance comparison between the simulated results from the raytracer (Wireless Insite) and the measurements results are presented in figure 5.16. The results show that even though for more ray paths the peaks of simulations are little high than the peaks of measurements, but it is within the acceptable limits without any addition to the signal processing. It is clearly shown that the maximum variation of power density between the physical and simulation results are ±5dBs.

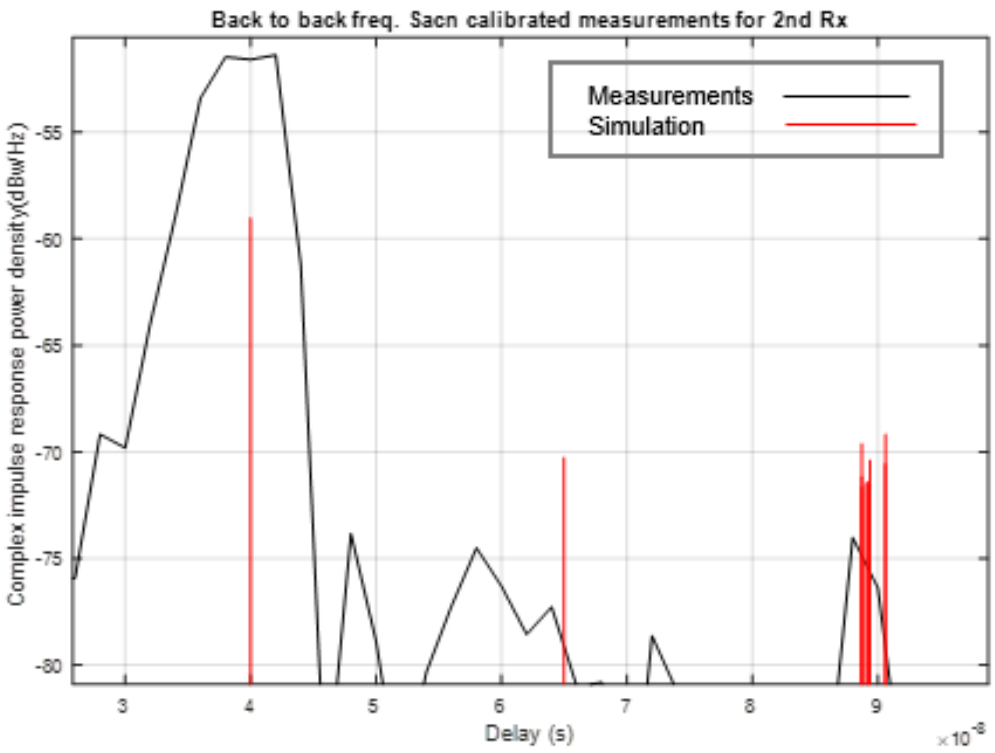

Figure 5.16: Performance of Measured and simulated paths for 2nd Rx

The direction of arrival (DOA) from the ray tracer for third receiver point (Rx 21) at a different location from the other two Rx points. The true angle of arrival is computed for most of the ray paths is approximately between 160-170 degrees. 10 and 210 degrees is also the promising angle of arrival for two ray paths as shown in figure 5.17.

Similarly, figure 5.18 shows the performance comparison between the simulated results and measurements results. Again, the peaks of some ray paths of the simulation are quite higher than the measurements by approximately ±7dBs but still, it is under the acceptable limits. The performance is quite similar except for some of the ray paths.

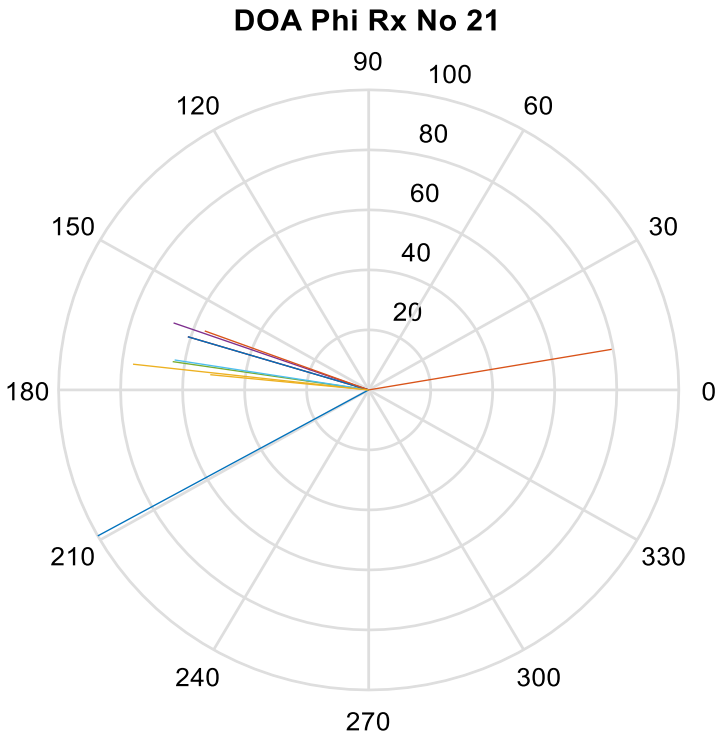

Figure 5.17: Direction of Arrival for 10 Rays at Rx 21(Degree Vs. dBi)

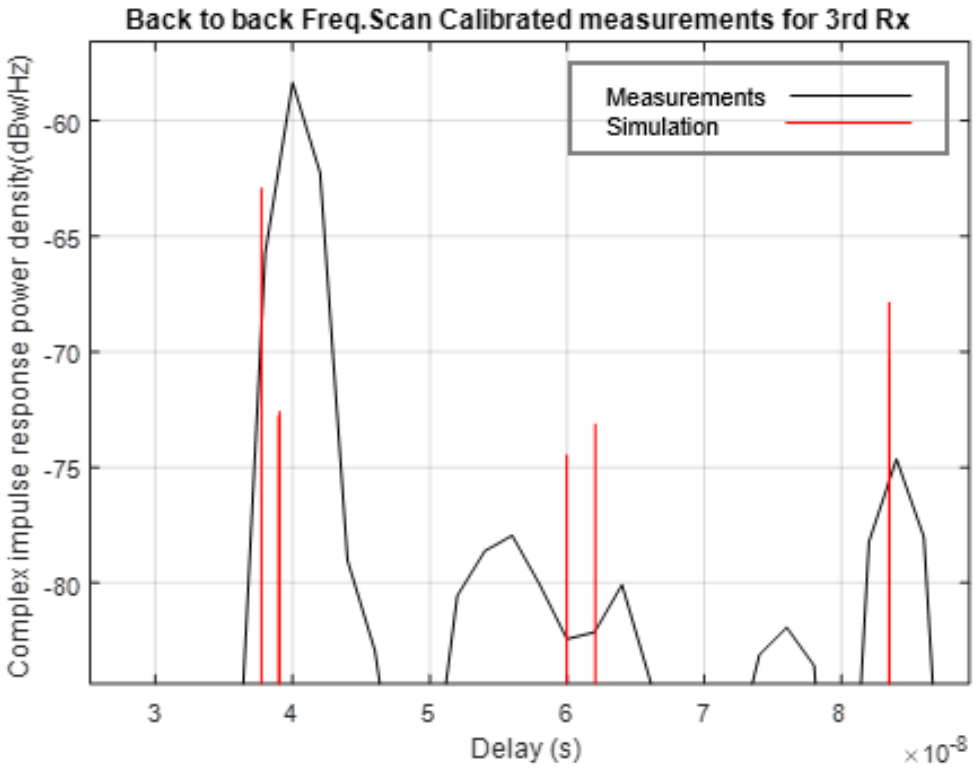

Figure 5.18: Performance of Measured and simulated paths for 3rd Rx

It is to be noted that some of the ray paths show variations between the simulation and the measurements. This is because of the simulation results carried out from the ray tracer without any furniture (Tables, chairs), plants and any other objects in the corridor of the third floor of the Chesham building B3 wing. While we have obtained the measurements results in the presence of these obstructions.

5.6 Conclusions:

An indoor multipath channel propagation for 60GHz was simulated using Wireless Insite and the results have been compared with the real environment measurements using 60GHz channel sounder for which the complex channel impulse response power and delay(s) were investigated for both line of sight (LOS) and non-line of sight (NLOS). The results recorded showed a good degree of similarity for simulated and measured results and provide a useful estimation of the propagation channel. The results have also shown that the proposed direction of arrival estimations was accurate in simulation and measurements.

6. OUTDOOR SIMULATION OF MM-WAVE CHANNEL PROPAGATION MODEL

6.1 Introduction:

The next generation wireless communication system is expected to offer high radio access to meet the increasing demand for high-speed data and multimedia services. Millimetre-wave channel propagation is one of the key technologies for the evolution of fifth generation mobile networks (5G). Especially the propagation of radio access in built-up areas are strongly influenced by the nature of the environment, size, location and solidity of the building. For the development of new 5G systems to operate in millimetre bands, there is a need for accurate propagation modelling at these bands [79].

In this chapter dense urban area dominated by tall buildings like office blocks and other commercial buildings, each with different heights and structures are presented to evaluate the channel propagation for the outdoor-outdoor scenario. The model presents the multipath components for LOS and NLOS scenario at three mm-wave frequencies: 26, 28 and 60GHz to evaluate signal strength and delay spread.

6.2 Outdoor-outdoor Scenario:

Outdoor scenario for urban city model is developed to evaluate the channel propagation for the outdoor-outdoor scenario at three different mm-wave frequency

bands. The model includes many buildings with different structures and dimensions as shown in figure 6.1.

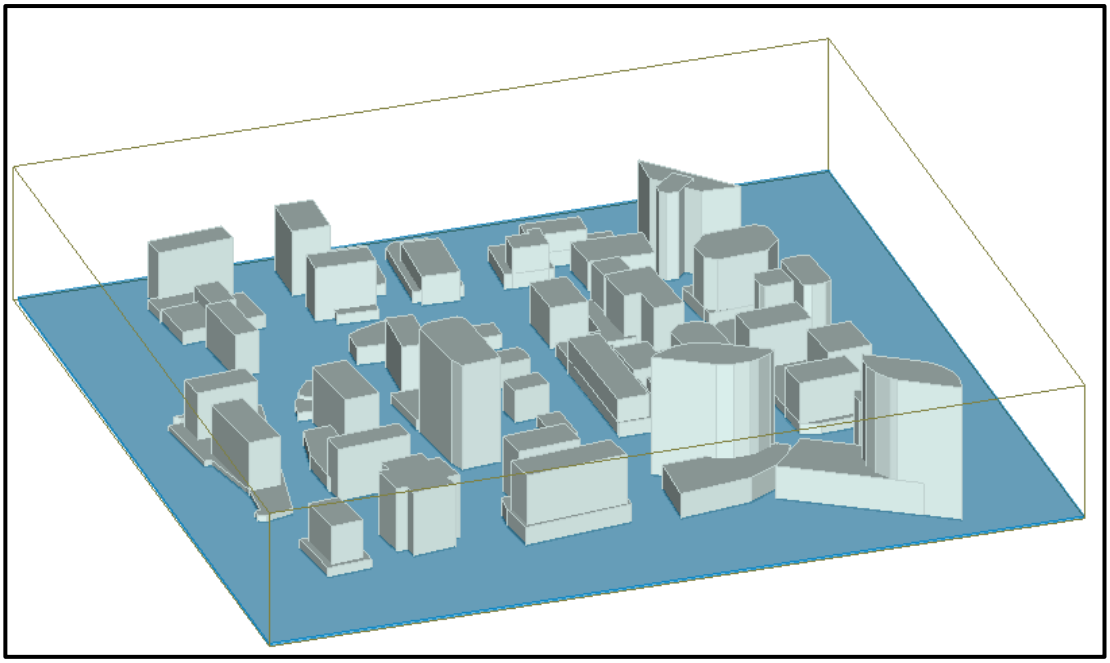

Figure 6.1: Outdoor Simulation environment for city model

The city model contains a total of 29 structure, 67 sub-structures and 445 faces. The buildings are assigned concrete material properties with a conductivity of 0.326 s/m and permittivity of 5.31 as shown in materials properties Table 4.1 *Rec. ITU-R P.2040-1.*

The analysis was carried out for the landscape shown in Figure 6.2. Three transmitters namely Tx1 (26GHz), Tx2 (28GHz) and Tx3 (60GHz) were placed on the top of three different buildings and locations at height of 40 m. The omnidirectional antennas are used at both sides of transmitters and receivers. There are three xy receiver's grids named Rx Grid 1, Rx Grid 2 and Rx Grid 3 implemented in a city model between the buildings at height of 2m above the ground. Each grid has 2500 receiver points with 1.5 m spacing from each other.

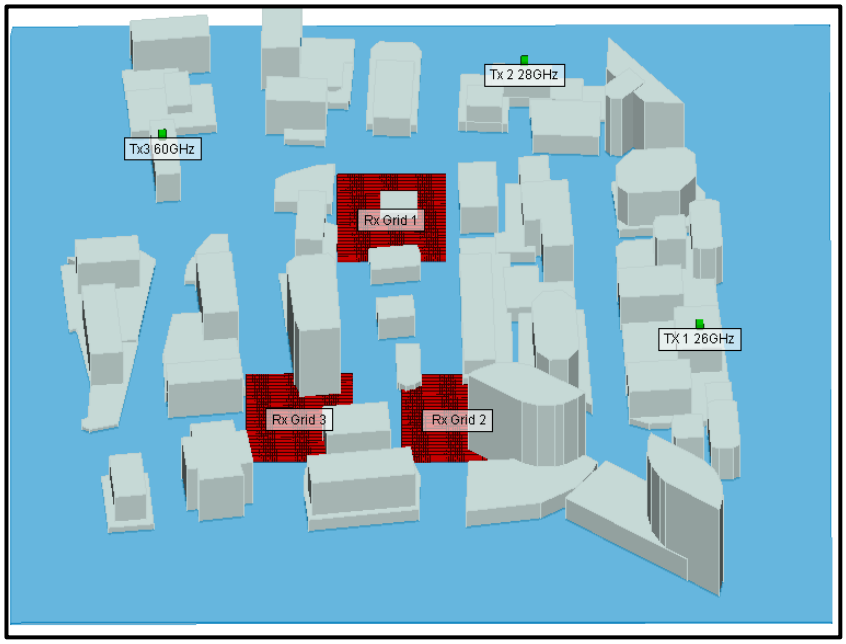

Figure 6.2: Location of Transmitters (Tx1, Tx2, Tx3) and Receivers Grids (Rx1, Rx 2, Rx3).

6.3 Simulation Results and discussion:

Simulation are performed for the landscape in section 6.2 under three mm-wave frequencies; 26GHz, 28GHz and 60GHz with omnidirectional antenna radiation

pattern for each receiver grids as shown in figure 6.2. The simulation parameters are shown in table 6.1.

According to the simulation results for the landscape shown in figure 6.2, the comparison among received signal power at 26GHz, 28GHz and 60GHz is shown in figure 6.3 for the three XY receiver grids in a different location from the transmitters.

There is a large number of receiver points and data involved, so it is hard to differentiate the received signal power for each categorically. By doing this we have applied the cumulative density function (CDF) to estimate the average received signal power for each case.

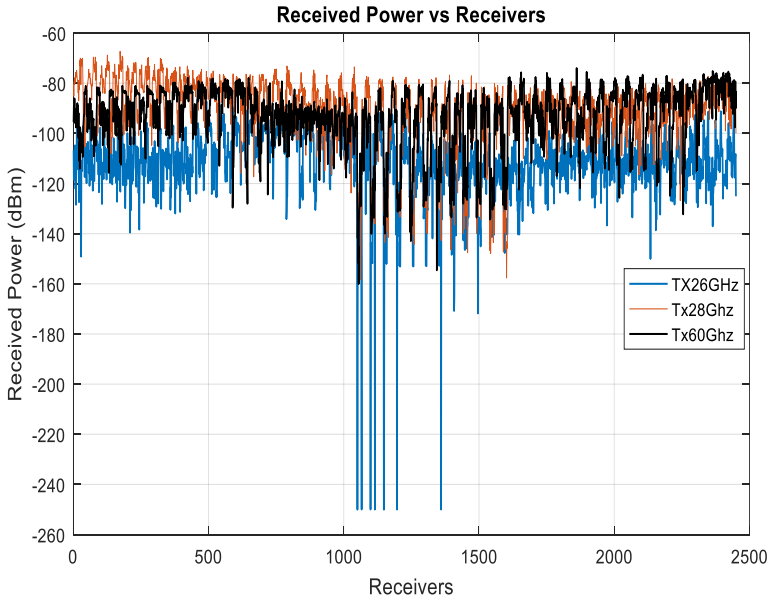

(a)

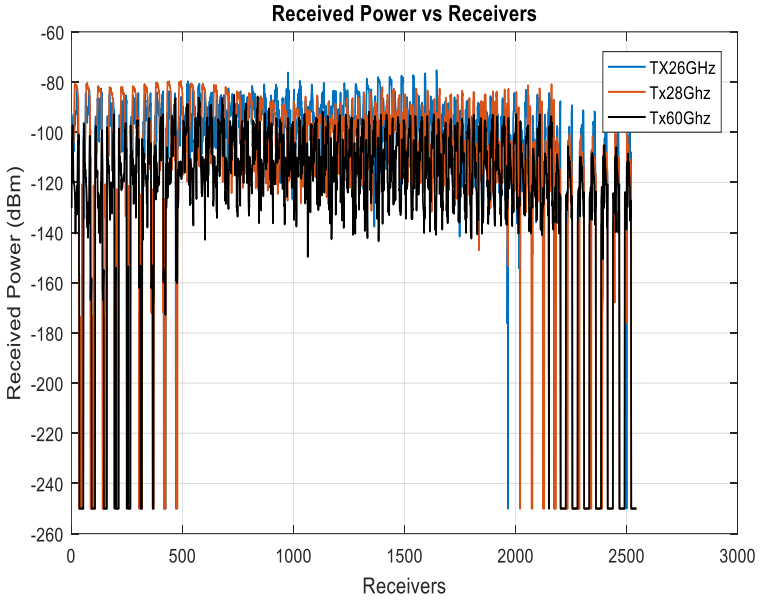

(b)

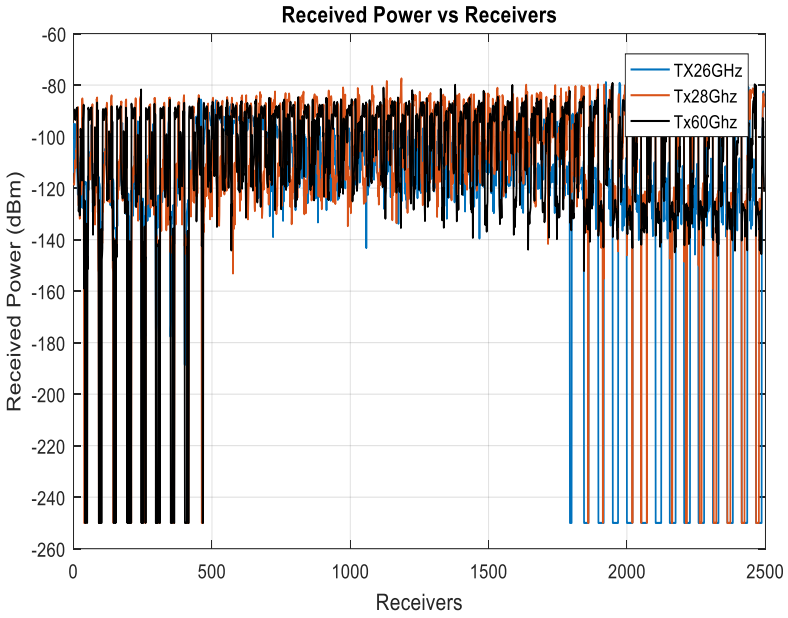

(c)

Figure 6.3: Received Power at 26, 28, 60GHz for a: RxGrid1, b: RxGrid2 and c: RxGrid3

Table 6.1: Simulation parameters

Simulation Environment	Parameters
Transmission Frequencies	26GHz, 28GHz, 60GHz
Transmission Power	30dBm
Transmitting Antenna height	40m
Receiving Antenna height	2m
Type of antenna	Omnidirectional antenna
Antenna polarization	Vertical
Waveform	Sinusoid
Receiver Threshold (dBm)	-160

Figure 6.4 shows the cumulative density function (CDF) of the received power for a: Rx-Grid 1, b: Rx-Grid 2 and c: Rx-Grid 3 at Transmitters Tx1 with 26GHz, Tx 2 with 28GHz and Tx 3 with 60GHz from which the probability of a particular value of power is received can be estimated.

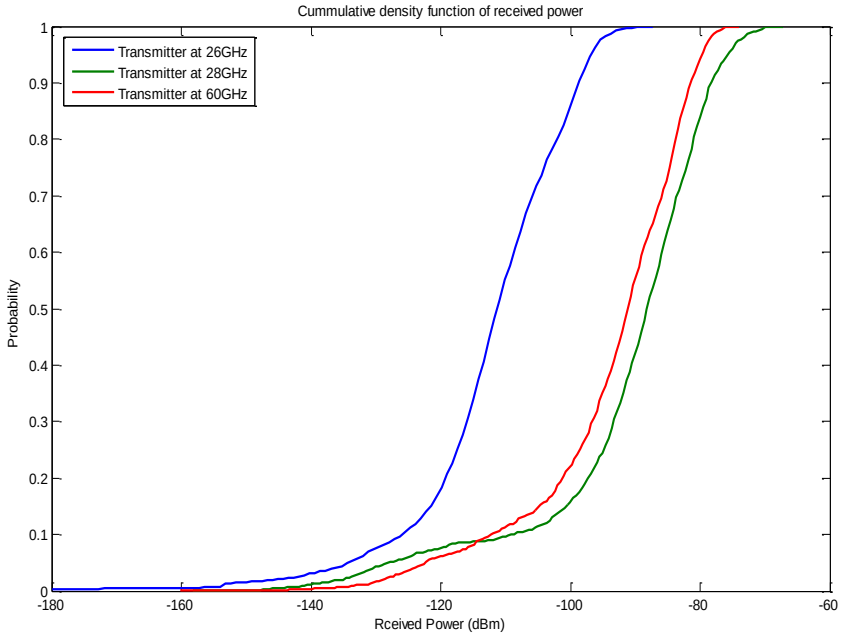

(a)

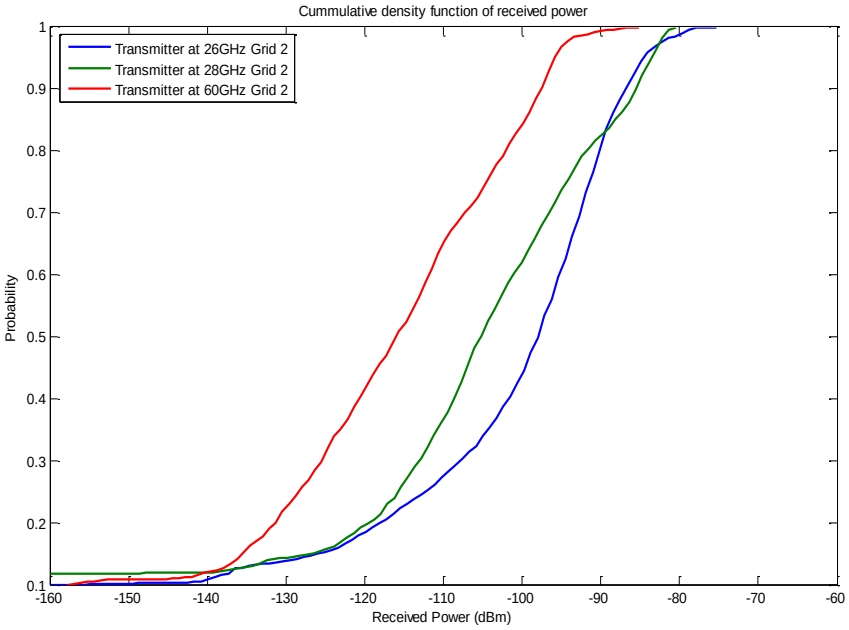

(b)

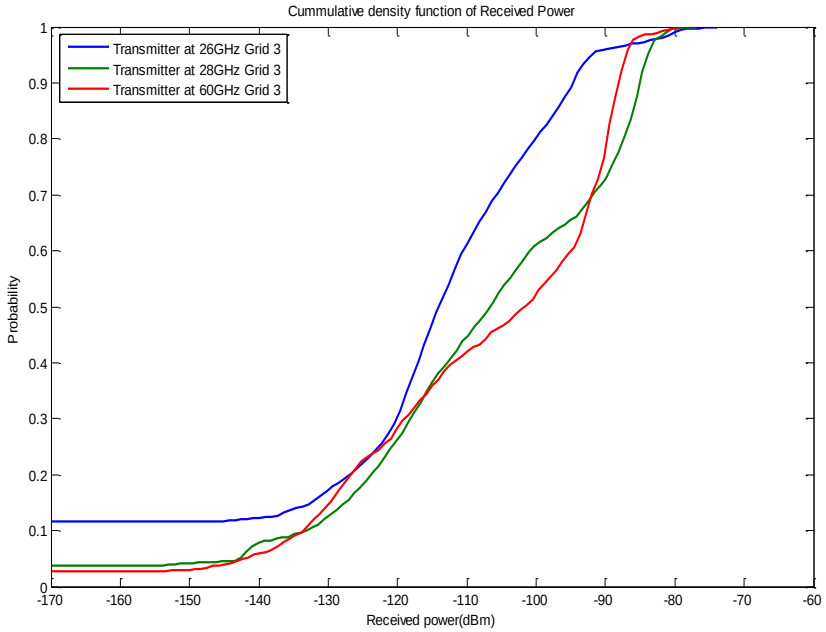

(c)

Figure 6.4: Cumulative density function of Received power at

a: RxGrid1, b: RxGrid2 and c: RxGrid3 with transmitter at different frequencies

It is clearly shown that for RxGrid1 in figure 6.4(a) the received power at 26GHz is approximately between -180dBm and -95dBm, this is because there are many reflections and diffraction paths caused by the buildings and the average received power is calculated -110dBm. Similarly, the average signal power at 28GHz is -85dBm and for 60GHz is approximately -90dBm. So, the transmitter at 28GHz is more line of sight (LOS) to the Rx-Grid 1 and less reflection paths caused as compared to the other two transmitters with 26 GHz and 60GHz.

Now for Rx Grid 2 in figure 6.4(b), the average received signal power was computed as -97dBm, -105dBm and -115dBm respectively for the transmitters at 26GHz, 28GHz and 60GHz. Similarly, the average received power for Rx Grid 3 shown in figure 6.4(c) is estimated as -115dBm, -105dBm and -100dBm for the transmitters at 26GHz, 28GHz and 60GHz. It can be seen that the received power is decreased by increasing the frequency. It is to be noted that if there are more reflections and diffraction paths caused, depending on the dimensions of the buildings for outdoor transmission, the results can be changed.

The delay spread is the second moment of the multipath signal power delay profile. The comparison among delay spread in 26GHz, 28GHz and 60GHz for the outdoor-outdoor scenario is shown in figure 6.5. According to the simulation results in the outdoor environment, about 2500 receiving points are selected for each receiver grid to complete the simulation.

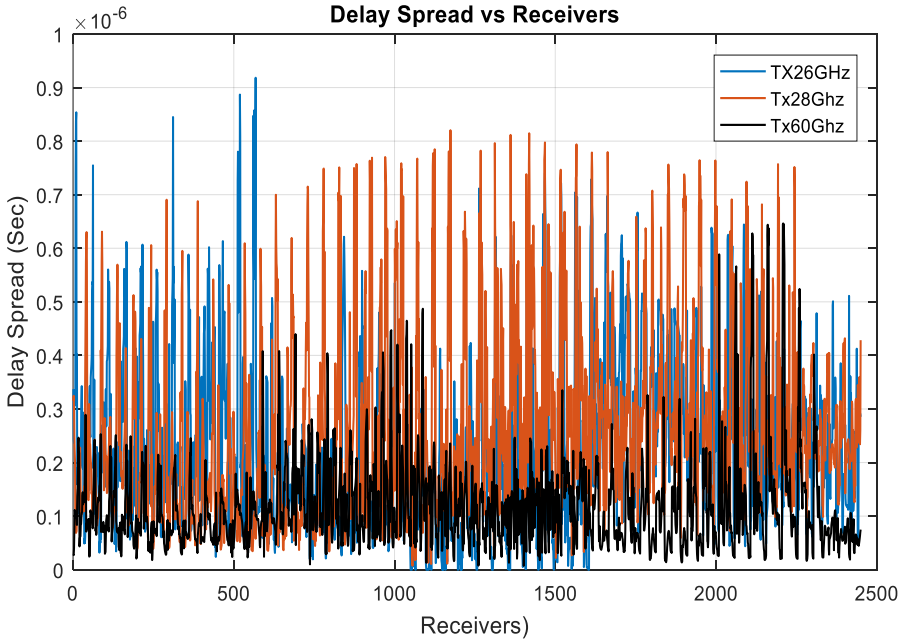
Delay Spread vs Receivers
×10^-6
Delay Spread (Sec)
Receivers)
TX26GHz
Tx28Ghz
Tx60Ghz
0
0.1
0.2
0.3
0.4
0.5
0.6
0.7
0.8
0.9
1
0
500
1000
1500
2000
2500

(a)

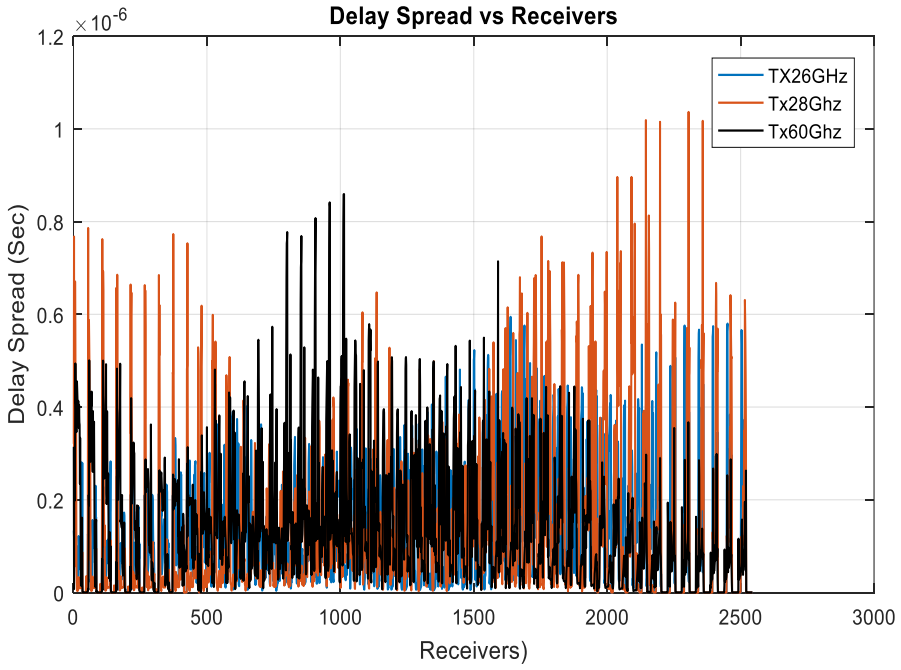
Delay Spread vs Receivers
×10^-6
Delay Spread (Sec)
Receivers)
TX26GHz
Tx28Ghz
Tx60Ghz
0
0.2
0.4
0.6
0.8
1
1.2
0
500
1000
1500
2000
2500
3000

(b)

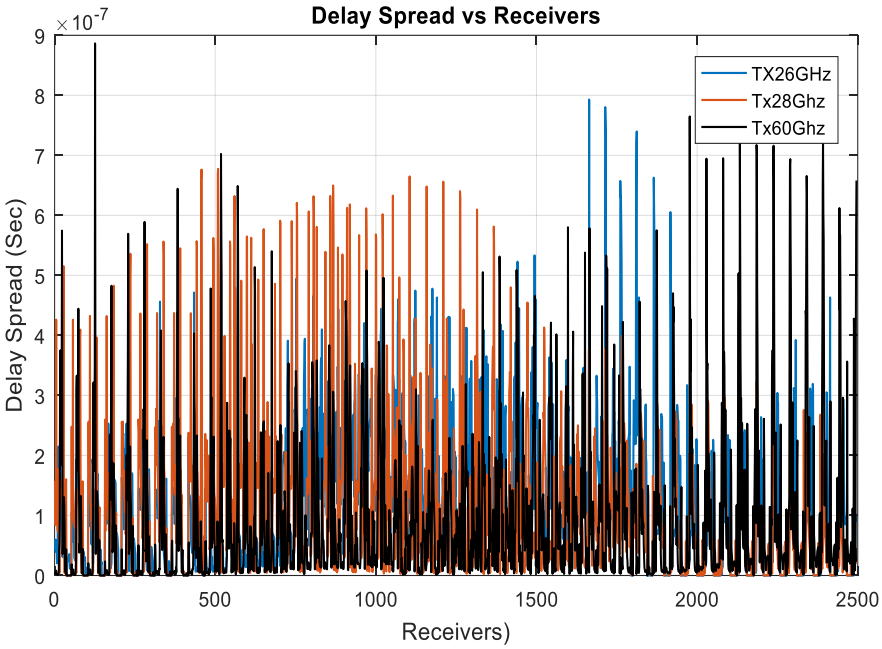

(c)

Figure 6.5: Delay Spread at 26, 28, 60GHz for a: RxGrid1, b: RxGrid2 and c: RxGrid3

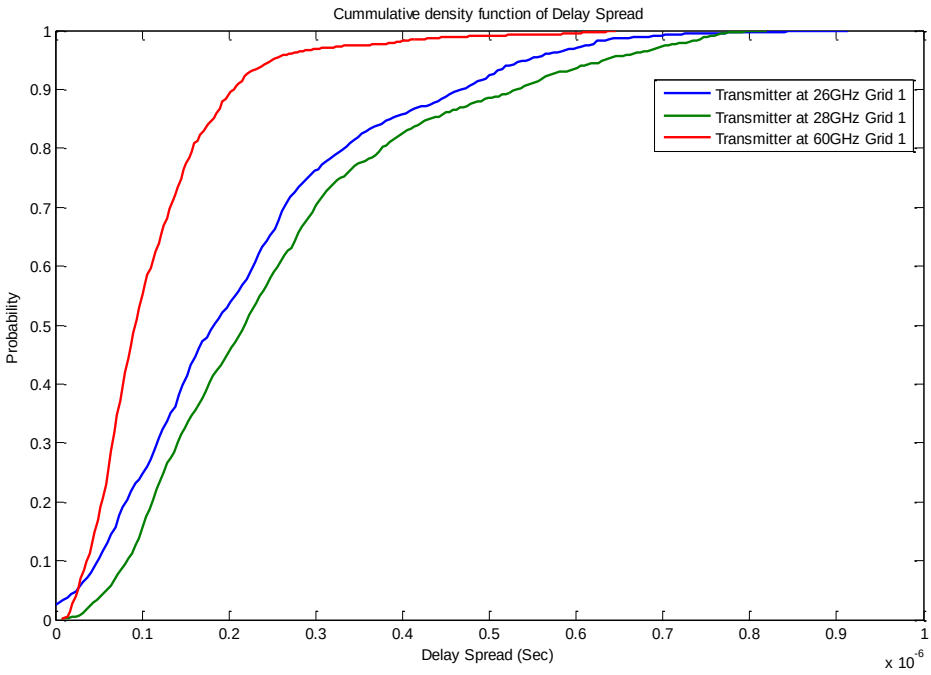

(a)

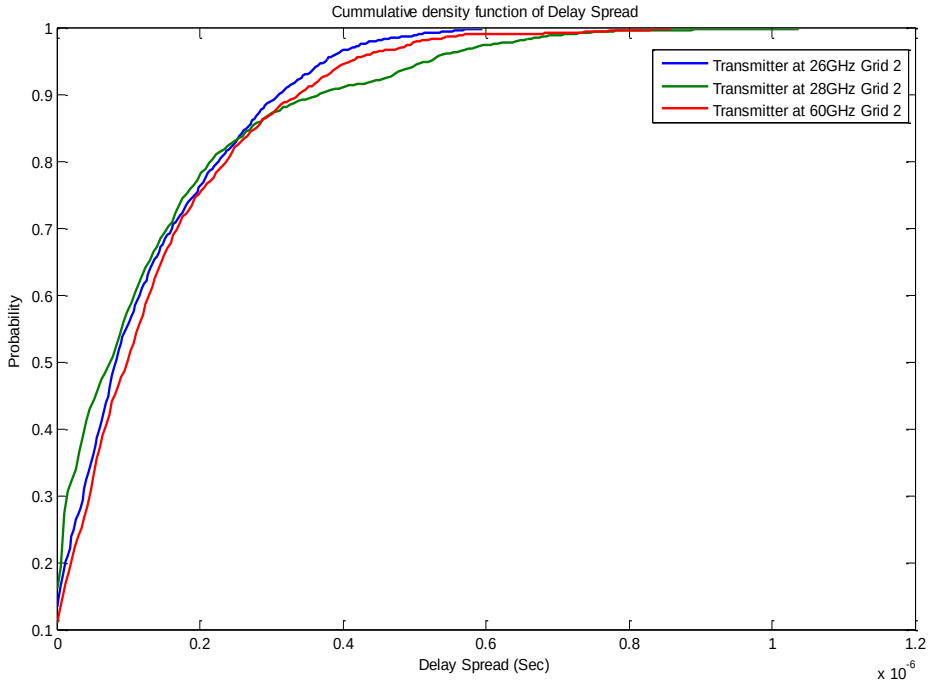

(b)

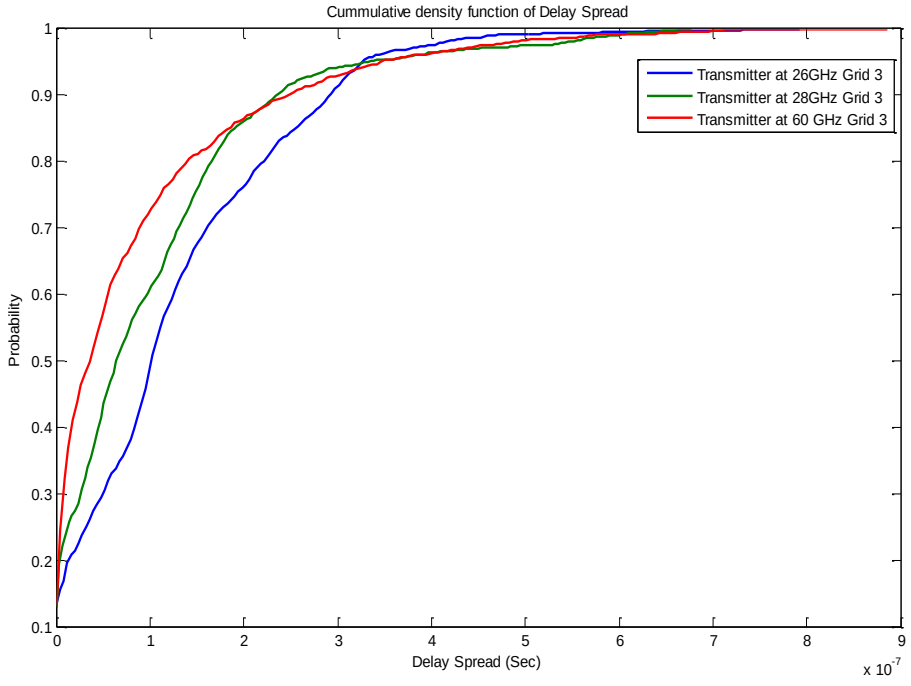

(c)

Figure 6.6: Cumulative density function of Delay Spread at a: RxGrid1, b: RxGrid2 and c: RxGrid3 with transmitter at different frequencies

Figure 6.6 shows the cumulative density function (CDF) of delay spread for receiver grids at different frequencies from which the probability of an average delay spread can be estimated. As from the Figure 6.6(a) at RxGrid 1, the average delay spread for 26 GHz, signal is 0.19 ns, the average delay spread in 28 GHz signal is 0.21 ns, and the average delay spread in 60 GHz signal is 0.1 ns, so it can be seen that the delay spread in 60 GHz signal is lower.

As can be seen from the Figure 6.6(b) at RxGrid 2, the delay spread trends in 26 GHz, 28 GHz and 60 GHz are in agreement, but there is a small difference in value, the average of delay spread in 26 GHz signal is 0.1 s, the average of delay spread in 28 GHz signal is 0.08 s, and the average of delay spread in 60 GHz signal is 0.12 s, so it can be seen that the delay spread in 60 GHz signal is higher here because there are many reflection paths caused by the tallest buildings faces.

The average delay spread also found to follow the similar tone of changes for 26GHz, 28GHz and 60GHz at RxGrid 3 is shown in figure 6.6(c). The average delay spread in 26 GHz signal is 1 ns, the average of delay spread in 28 GHz signal is 0.7 ns, and the average of delay spread in 60 GHz signal is 0.4 ns, so it can be seen from the overall average results that the delay spread in 60 GHz signal is lower.

6.4 Conclusions:

In this chapter, the 3-D shooting and bouncing ray (SBR) method is used to study the millimetre wave (mm-wave) channel propagation under outdoor-outdoor city

environment. Through the analysis of simulation results, the received power for mm-wave under the outdoor-outdoor complex propagation model was evaluated. The study has been investigated from the ray tracing and simulation results that if there are more obstructions with different dimensions between the transmitter and receiver which can cause more than one reflection and diffractions of a signal ray to be reached to the receiver will have a great impact on the received signal power and delay spread.

7. CONCLUSIONS AND FUTURE WORK

7.1 Conclusions:

As 5G will be the new technology that will be used to enable cellular networks and devices for better spectrum resources and it is expected to reach several Gbits/s data rates in supporting the mobile and wireless applications for which developing new propagation channel models is essential. The associated software tools for reliable propagation channel models are important for the successful implementation of the future wireless network system. It is common that transmission of the signal is not only in the direct path but also in a various number of propagation paths. The line of sight (LOS) is not available all the time so, in the case of Non-line of sight (NLOS), indirect paths are very important for efficient communication.

The research work has been studied for indoor and mixed propagation scenario, was simulated using Wireless Insite (Software) for indoor-indoor (LOS, NLOS) and indoor-outdoor (NLOS) propagation channels under four different frequencies with different radiation patterns. Channel parameters characteristics such as path loss, received power, delay spread, mean direction of arrival for multi-frequencies were presented and modelled under the directional and omnidirectional antenna.

The simulated data achieved from the ray tracer (Software Package) based on the effect of frequency dependent electrical properties of building materials which

includes reflections, penetrations and diffractions of walls and objects. It has been intensively investigated that signal is much more affected by the building materials and is responding differently for LOS and NLOS, due to the nature of the frequencies and the radiation pattern of antennas. In each resulted graph, a simple slope channel model was adopted to summarize the results.

The simulation results for indoor channel propagation of mm-wave were tested at the lab and the corridor of the third floor of the Chesham building, the University of Bradford for practical analysis. The simulation was carried out for each ray path with the greatest power from the transmitter to receiver using wireless insite ray tracer. The channel sounder communication process and its architecture have been briefly discussed in chapter 5. The 60GHz channel sounder used to measure the impulse response and frequency response of radio channel for the real environment measurement. The complex channel impulse response power and delay(s) were investigated for both line of sight (LOS) and non-line of sight (NLOS) and the simulated results and measured results are in a broad agreement. For NLOS, it was also concluded that the direction of arrival of each ray in the ray tracing simulation was also found a true angle in the measurements and found a useful angle estimation from 0 to 360 degrees.

The work also carried out for the 3-D shooting and bouncing ray (SBR) method that is used to study the millimetre wave channel propagation under three frequencies for an outdoor-outdoor city environment. The received signal power and delay spread were computed for outdoor-outdoor complex propagation channel model using ray tracing software package. The study has been

investigated from simulation results that if there are more obstructions with different dimensions between the transmitter and receiver which can cause more than one reflection and diffractions of a signal ray to be reached to the receiver will have a great impact on the received signal power and delay spread. It is also shown in the results that both the received signal power and delay spread decrease with increasing frequencies and the ray paths also increases due to reflections from buildings.

7.2 Future Work:

There are many aspects of this research work which can be further extended either to support the main system or to improve its performance.

The propagation channel model is enough flexible to support various numbers of channel models with a configurable number of paths per channel. The implementation needs further extensions to include more realistic and accurate radio propagation channel models.

The results in both chapter 4, 5 and 6 may be used to develop a new statistical propagation channel model for more practical indoor and outdoor environment, including the full support of the measurements results. One further study that might be considered by developing an indoor and outdoor system using huge data collection towards a technique such as a path loss, received signal strength, delay and mean direction of arrival. The use of accurate antenna and radiation pattern at both transmitter and receivers is needing to develop the system.

An extensive measurement campaign for accurate propagation channels should

be considered for the urban scenario of outdoor-outdoor simulation with a large data collection, especially the measurements under NLOS conditions. The identification and characterization of significant areas could lead us to the proposal of an empirical or statistical propagation model that accounts for more environmental variables with the aim of precise results.

REFERENCES

1. Katsuyuki Haneda , L.T., Yi Zheng , Henrik Asplund , Jian Li , Yi Wang , David Steer , Clara Li, *"5G 3GPP-like Channel Models for Outdoor Urban Microcellular and Macrocellular Environments"*, in *IEEE 83rd Vehicular Technology Conference*. 2016.

2. *" Reflection and Snell's Law"*. [cited 2017; Available from: http://em.geosci.xyz/content/maxwell1_fundamentals/reflection_and_refraction/Snells_law.html.

3. Jeffrey G, A., Arunabha Ghosh, *"Fundamentals of WiMAX understanding Broadband wireless networking"*. Prentice Hall Communications Engineering and Emerging Technologies Series. 2007.

4. Satvir Singh Sidhu , A.K.A.S., *"Implementation of 3-D Ray Tracing Propagation Model for Indoor Wireless Communication".* International Journal of Electronics Engineering, 2012.

5. GEORGE R. MACCARTNEY, J., THEODORE S. RAPPAPORT, MATHEW K. SAMIMI, AND SHU SUN, *"Millimeter-Wave Omnidirectional Path Loss Data for Small Cell 5G Channel Modeling".* SPECIAL SECTION ON ULTRA-DENSE CELLULAR NETWORKS, 2015. **3**.

6. Goldsmith, A., *Wireless communications*. 2005: Cambridge university press.

7. Rappaort, T.S., *Wireless communications: principles and practice*. 2 edition ed. 2002, Upper Saddle River, NJ, USA: Prentice Hall.

8. ITU, I.T.U., *Propagation data and prediction methods for the planning of indoor radiocommunication systems and radio local area networks in the frequency range 900 MHz to 100 GHz*, in *Recommendation ITU-R P.1238-7*. 2012, ITU: Geneva.

9. Amit Kumar, D.Y.L., Dr. Jyotsna Sengupta, Divya, *"Evolution of Mobile Wireless Communication Networks 1G to 4G".* International Journal of Electronics & Communication Technology, 2010.

10. Vergados, G., C, Vergados, D.J., *"The 3G wireless technology in tactical communication networks"*, in *Vehicular Technology Conference*. 2004 Greece p. 4883 - 4887.

11. Sharma, P., *"Evolution of Mobile Wireless Communication Networks-1G to 5G as well as Future Prospective of Next Generation Communication Network"* International Journal of Computer Science and Mobile Computing 2013. **2**.

12. André Mendes Cavalcante, M.J.d.S., *"A new computational parallel model applied in 3D ray-tracing techniques for radio-propagation prediction"*, in *Proceedings of Asia-Pacific Microwave Conference*. 2006 Yokohama, Japan.

13. Yahia Zakaria, J.H.a.J.M., *"Path Loss Measurements for Wireless Communication in Urban and Rural Environments".* American Journal of Engineering and Applied Sciences 2015.

14. Bonek, E., *"MIMO Propagation Channel Modeling"*, in *7th European Conference on Antennas and Propagation (EUCAP 2013) - Convened Sessions*. 2013, IEEE.

15. Andre Mendes Cavalcante, M.J.d.S., Joao Cristomo Weyl Albuquerque Costa, *"3D ray-tracing parallel model for radio-propagation prediction"*, in *Telecommunications Symposium, 2006 International*. 2006, IEEE: Fortaleza, Ceara, Brazil.

16. J. Medbo, K.B., K. Haneda , V. Hovinen, T. Imai, J. Järvelainen, T. Jämsä, *"Channel Modelling for the Fifth Generation Mobile Communications"*, in *Antennas and Propagation (EuCAP), 2014 8th European Conference on*. 2014, IEEE: The Hague, Netherlands.

17. Heejung Yu, H.L., Hongbeom Jeon, *"What is 5G? Emerging 5G Mobile Services and Network Requirements"*, in *5G Mobile Services and Scenarios: Challenges and Solutions*. 2017.

18. Vincent W. S. Wong, R.S., Derrick Wing Kwan Ng, Li-Chun Wang, *"Key Technologies for 5G Wireless Systems"*. 2017: Cambridge University Press, 2017.

19. Mamta Agiwal, A.R., and Navrati Saxena, *"Next Generation 5G Wireless Networks: A Comprehensive Survey"*, in *IEEE COMMUNICATIONS SURVEYS & TUTORIALS*. 2016, IEEE.

20. Shanzhi Chen, J.Z., *"The requirements, challenges, and technologies for 5G of terrestrial mobile telecommunication"*, in *IEEE Communications Magazine* 2014, IEEE.

21. Rodriguez, J., *"Fundamentals of 5G Mobile Networks"*, ed. J. Rodriguez. 2015: John Wiley & Sons, 2015.

22. Yoshihisa Kishiyama, A.B., Takehiro Nakamura, *"Future steps of LTE-A: evolution toward integration of local area and wide area systems".* IEEE Wireless Communications, 2013. **20**: p. 12 - 18.

23. Patrick Kwadwo Agyapong, M.I., Dirk Staehle, *"Design Considerations for a 5G Network Architecture"*, in *IEEE Communications Magazine*. IEEE.

24. Xi Zhang, W.C., Hailin Zhang, *"Heterogeneous statistical QoS provisioning over 5G mobile wireless networks"*, in *IEEE Network*. 2014, IEEE.

25. Chiosi, M., *"Network Functions Virtualisation ".* SDN and OpenFlow World Congress, – Introductory White Paper, http://portal.etsi.org/NFV/NFV_White_Paper.pdf 2012.

26. Cedric Dehos, J.L.G., Antonio De Domenico, Dimitri Kténas, and Laurent Dussopt, *"Millimeter-Wave Access and Backhauling: The Solution to the Exponential Data Traffic Increase in 5G Mobile Communications Systems"*, in *IEEE Communications Magazine*. 2014, IEEE.

27. Rappaport, T.S., *"Wideband Millimeter-Wave Propagation Measurements and Channel Models for Future Wireless Communication System Design".* IEEE TRANSACTIONS ON COMMUNICATIONS, 2015. **63**.

28. Jr., P.R.W.H. *"Analysis of Millimeter Wave Systems for 5G"*. Research in wireless communication and signal processing [cited 2017; Available from: http://www.profheath.org/analysis-of-millimeter-wave-systems-for-5g/.

29. Richard J. Weiler, M.P., Wilhelm Keusgen, Emilio Calvanese-Strinati, *"Enabling 5G Backhaul and Access with millimeter-waves"*, in *European Conference on Networks and Communications*. 2014, IEEE.

30. Tracy, P., *"5G New Radio – Emerging Spectrum Bands"*, in *Millimeter-wave: The 5G enabler?* 2016.

31. Medbo, S.J.M.P.K.S.W.K.J., *"5G Channel Models in mm-Wave Frequency Bands "*, in *European Wireless 2016; 22th European Wireless Conference; Proceedings of*. 2016, VDE: Oulu, Finland.

32. Theodore S. Rappaport, F.G., Eshar Ben-Dor, *"Broadband Millimeter-Wave Propagation Measurements and Models Using Adaptive-Beam Antennas for Outdoor Urban Cellular Communications"*, in *IEEE Transactions on Antennas and Propagation*. 2013, IEEE.

33. Shu Sun, T.S.R., Rimma Mayzus, *"Millimeter Wave Mobile Communications for 5G Cellular: It Will Work!".* 2013: p. 335 - 349.

34. Ilario Filippini, V.S., Francesco Devoti, Antonio Capone, *"Fast Cell Discovery in mm-wave 5G Networks with Context Information".* IEEE Transactions on Mobile Computing, 2017. **17**.

35. Wonil Roh, J.-Y.S., Jeongho Park, *"Millimeter-wave beamforming as an enabling technology for 5G cellular communications: theoretical feasibility and prototype results"*, in *IEEE Communications Magazine*. 2014, IEEE.

36. eira, F.P.r.F.n.a.P.M.o.E., *"Modeling the Wireless Propagation Channel A Simulation Approach with MATLAB1"*. Wiley Series on Wireless Communications and Mobile Computing. 2008: John Wiley & Sons Ltd.

37. Mainak Chowdhury, A.B., *"Wireless Communication: Theory and Applications"*. Cambridge University Press, 16 Jan 2017.

38. Arag´on-Zavala, S.R.S.a.A., *"Antennas and propagation for wireless communication systems"*. 2007.

39. Isaac A. Ezenugu, H.O.E., and Uwakwe Chikwado, *"Determination of Single Knife Edge Equivalent Parameters for Double Knife Edge Diffraction Loss by Deygout Method ".* 2017. **3**.

40. Theodore S. Rappaport, G.R.M.J., Shu Sun, Hangsong Yan, and Sijia Deng, *"Small-Scale, Local Area, and Transitional Millimeter Wave Propagation for 5G Communications".* IEEE Transactions on Antennas and Propagation 2017. **PP**(99).

41. Theodore S. Rappaport, G.R.M.J., Shu Sun, Hangsong Yan, and Sijia Deng, *"Overview of Millimeter Wave Communications for Fifth-Generation (5G) Wireless Networks-with a focus on Propagation Models"*, in *IEEE Transactions on Antennas and Propagation, Special Issue on 5G*. 2017.

42. Sundeep Rangan, T.S.R., Elza Erkip, *"Millimeter-Wave Cellular Wireless Networks: Potentials and Challenges".* 2014. **102**.

43. Sijia Deng, M.K.S., Theodore S. Rappaport, *"28 GHz and 73 GHz millimeter-wave indoor propagation measurements and path loss models"*, in *Communication Workshop (ICCW), 2015 IEEE International Conference on*. 2015, IEEE: London, UK.

44. Panagopoulos, A.D., *"Handbook of Research on Next Generation Mobile Communication Systems"*. 2015: IGI Global, 2015. 605.

45. Aalto University, B., CMCC, Nokia, NTT DOCOMO, New York University, Ericsson, Qualcomm, Huawei, Samsung, INTEL, University of Bristol,, *" 5G channel model for bands up to 100 GHz".* 2nd Workshop on Mobile Communications in Higher Frequency Bands (MCHFB) in Globelcom, 2015.

46. *5G; Study on channel model for frequencies from 0.5 to 100 GHz (3GPP TR 38.901 version 14.0.0 Release 14)"* 3GPP TECHNICAL REPORT of ETSI TR 138 901, 2017.

47. Shu Sun, G.R.M., Jr., and Theodore S. Rappaport, *"Millimeter-Wave Distance-Dependent Large-Scale Propagation Measurements and Path Loss Models for Outdoor and Indoor 5G Systems"*, in *10th European*

Conference on Antennas and Propagation (EuCAP 2016), April. 2016. 2016.

48. Salous, S., *"COST IC1004 White Paper on Channel Measurements and Modeling for 5G Networks in the Frequency Bands above 6 GHz".* EUROPEAN COOPERATION IN THE FIELD OF SCIENTIFIC AND TECHNICAL RESEARCH. COST IC1004, 2016.

49. Vuokko Nurmela (Nokia), A.K.A., Antti Roivainen (UOulu), Leszek Raschkowski (Fraunhofer HHI), Tetsuro Imai (NTT DOCOMO), Jan Järveläinen (AALTO), Jonas Medbo (Ericsson),, *"Deliverable D1.4 METIS Channel Models".* Mobile and wireless communications Enablers for the Twenty-twenty Information Society (METIS), 2015.

50. Paul Ferrand, M.A., Stefan Valentin, *"Trends and Challenges in Wireless Channel Modeling for an Evolving Radio Access"*, in *IEEE Communications Magazine* 2016, IEEE.

51. Katsuyuki Hanedaa, L.T., Henrik Asplundd, Jian Lie, Yi Wange, David Steere, Clara Lif, *"Indoor 5G 3GPP-like Channel Models for Office and Shopping Mall Environments"*, in *Communications Workshops (ICC), 2016 IEEE International Conference on*. 2016, IEEE.

52. Govind Sati1, S.S., *"A REVIEW ON OUTDOOR PROPAGATION MODELS IN RADIO COMMUNICATION".* International Journal of Computer Engineering & Science, 2014.

53. Clement Temaneh-Nyah, J.N., *"Determination of a Suitable Correction Factor to a Radio Propagation Model for Cellular Wireless Network Analysis "*, in *Fifth International Conference on Intelligent Systems, Modelling and Simulation*. 2014, IEEE.

54. R.K.Singh, P.K.S., *"Comparative Analysis of Propagation Path loss Models with Field Measured Data".* International Journal of Engineering Science and Technology, 2013. **2(6)**.

55. *"Propagation Models"*. [cited 2017 24/08]; Available from: http://www.altairhyperworks.com/product/FEKO/WinProp---Indoor-and-Campus.

56. Fang, C., *"The Characterisation and Modelling of the Wireless Propagation Channel in Small Cells Scenarios"* 2015, UNIVERSITY OF BEDFORDSHIRE.

57. Aymen Ben Zineb , M.A., *"A Multi-wall and Multi-frequency Indoor Path Loss Prediction Model Using Artificial Neural Networks".* RESEARCH ARTICLE - COMPUTER ENGINEERING AND COMPUTER SCIENCE, 2016.

58. NAGY, L., *"Deterministic indoor wave propagation modeling".* 2007.

59. Franco Fuschini, E.M.V., Marina Barbiroli, Gabriele Falciasecca, and Vittorio Degli-Esposti1, *"Ray tracing propagation modeling for future small-cell and indoor applications: A review of current techniques".* Radio Science RESEARCH ARTICLE online, 2015. **50**.

60. Schneider, J.B., *"Understanding the FDTD Method"*. 2017: Creative Commons Attribution-ShareAlike 4.0 International License. 403.

61. Pajusco, P., *"Propagation channel models for mobile communication".* C. R. Physique 7 (2006) 703–714, 2006.

62. Kumar, S., *"Wireless Communications Fundamental & Advanced Concepts"*. 2015: River Publishers.

63. Lott, M. and I. Forkel. *A multi-wall-and-floor model for indoor radio propagation*. in *Vehicular Technology Conference, 2001. VTC 2001 Spring. IEEE VTS 53rd*. 2001. Rhodes, Greece, Greece: IEEE.

64. Saunders, S. and A. Aragón-Zavala, *Antennas and Propagation for Wireless Communication Systems: 2nd Edition*. 2007: John Wiley & Sons.

65. GEORGE R. MacCARTNEY, T.S.R., D SIJIA DENG, *"Indoor Office Wideband Millimeter-Wave Propagation Measurements and Channel*

Models at 28 and 73 GHz for Ultra-Dense 5G Wireless Networks. SPECIAL SECTION ON ULTRA-DENSE CELLULAR NETWORKS, 2015. **3**.

66. Valenzuela, R.A., O. Landron, and D. Jacobs, *Estimating local mean signal strength of indoor multipath propagation.* IEEE transactions on vehicular technology, 1997. **46**(1): p. 203-212.

67. REMCOM, *Wireless InSite Reference Manual*. 2017, REMCOM: State College, Pennsylvania.

68. Seybold, J.S., *Introduction to RF propagation*. 2005: John Wiley & Sons.

69. Salous, S., *Radio Propagation Measurement and Channel Modelling*. 2013: John Wiley & Sons.

70. Wahab Khawaja, O.O., and Ismail Guvenc, *"UAV Air-to-Ground Channel Characterization for mmWave Systems".* Department of Electrical and Computer Engineering, North Carolina State University, Raleigh, NC, 2017.

71. Foutz, J., A. Spanias, and M.K. Banavar, *Narrowband direction of arrival estimation for antenna arrays.* Synthesis Lectures on Antennas, 2008. **3**(1): p. 1-76.

72. Krim, H. and M. Viberg, *Two decades of array signal processing research: the parametric approach.* Signal Processing Magazine, IEEE, 1996. **13**(4): p. 67-94.

73. Zekavat, R. and R.M. Buehrer, *Handbook of position location: Theory, practice and advances*. Vol. 27. 2011: John Wiley & Sons.

74. Patwari, N., et al., *Locating the nodes: cooperative localization in wireless sensor networks.* Signal Processing Magazine, IEEE, 2005. **22**(4): p. 54-69.

75. Chen, H.-C., et al. *Determining RF angle of arrival using COTS antenna arrays: a field evaluation*. in *MILITARY COMMUNICATIONS CONFERENCE, 2012-MILCOM 2012*. 2012. IEEE.

76. Mr. ANIL KUMAR KODURI , M.V.S., Mr. M. KHALEEL ULLAH KHAN, *"Propagation Characteristics of a Mobile Radio Channel for Rural, Suburban and Urban Environments".* IPASJ International Journal of Electronics & Communication (IIJEC), 2014. **2**.

77. *"Wireless communication" Line of sight and Non-line of sight*. [cited 2017; Available from: https://www.techopedia.com/.

78. GEORGE R. MACCARTNEY, J., THEODORE S. RAPPAPORT, MATHEW K. SAMIMI, AND SHU SUN, *"A Flexible Millimeter-Wave*

Channel Sounder With Absolute Timing". IEEE JOURNAL ON SELECTED AREAS IN COMMUNICATIONS, 2017. **35**.

79. Mihajlo Stefanovic, S.R.P., Rausley A. A. de Souza, *"Recent Advances in RF Propagation Modeling for 5G Systems".* International Journal of Antennas and Propagation, 2017: p. 5.

AUTHOR PUBLICATION

LIST OF PUBLICATIONS:

1. ***Waqas Manan****, Huthaifa Obeidat, Ali Al-Abdullah and Raed A Abd Alhameed, *"Indoor to Indoor and Indoor to Outdoor Millimetre Wave Propagation Channel Simulations at 26 GHz, 28 GHz and 60 GHz for 5G Mobile Networks". International Journal of Research in Engineering and Science (IJRES), 2018.*

2. **Waqas Manan***, A.A., Huthifa Obeidat, Raed A. Abd-Alhameed, Steve M. Jones, *"Indoor/Indoor and Indoor/Outdoor Propagation Channel Simulations at 28GHz and 60GHz with Different Antenna Radiation Pattern"*, in *URSI Festival of Radio Science*. 2017: University of Bradford.(Accepted paper)

International Journal of Research in Engineering and Science (IJRES)
ISSN (Online): 2320-9364, ISSN (Print): 2320-9356
www.ijres.org Volume 5 Issue 12 | January. 2018 | PP. 01-06.

Indoor to Indoor and Indoor to Outdoor Millimetre Wave Propagation Channel Simulations at 26 GHz, 28 GHz and 60 GHz for 5G Mobile Networks

Waqas Manan*, Huthaifa Obeidat, Ali Al-Abdullah and Raed A Abd Alhameed,
Faculty of Engineering and Informatics, University of Bradford, United Kingdom
Corresponding author: Waqas Manan

ABSTRACT: In this paper the characteristics of LOS and NLOS propagations channels are intensively investigated under three mm wave frequencies; 26GHz, 28GHz and 60GHz for vertical polarized omnidirectional antenna. The simulation data achieved from the 3D shooting and bouncing Ray (SBR) tracer based on the effects of frequency dependant electrical properties of building materials and has been observed that signal is much affected by the nature of building materials and frequencies for line of sight and non-line of sight.

Keywords: 5G, Line of Sight (LOS), Non-LOS (NLOS), Delay spread, path loss.

I. INTRODUCTION

A number of changes planned for 5G networks, is the extension into high frequencies in the wave spectrum, the increasing demands of high speed data and multimedia services, need to accurately predict multipath effects of indoor environments [1]. To support highly increasing traffic capacity and high data rates, the next generation mobile network (5G) should extend the range of frequency spectrum for mobile communication that is yet to be identified by the ITU-R [2]. The mm wave spectrum is the key enabling feature of next generation cellular system, for which the propagation channel models need to be predicted to enhance the design of the transceiver system.

In mobile radio propagation studies, the qualitative description of the environment are usually using terms rural, urban, dense urban and suburban [3]. Dense urban is the area defined tall buildings, commercial building areas and multi storey office blocks, while suburban is the area contains residential houses, flats, gardens and parks. Rural areas are generally defined as with scattered buildings and agricultural fields and forests. The average signal level in suburban and rural areas is better because of the environmental effect, so the signal variation in urban areas have been discussed so far [4]. In urban areas, there is no direct line of sight (LOS) between user equipment and base station (BS) antenna. There is a number of different paths because of reflection from a tall buildings, for which signal arrive at a mobile station (MS) through many paths and the received signal over each path has a random phase and amplitude [5].

Propagation models are designed by using deterministic approach and have become a preferred technique for channel propagation simulations. Deterministic is the model that can be performed through Maxwell's equation and by ray tracing techniques shooting and bouncing ray (SBR) [6].

At present, the current 4G systems provide a universal platform for broadband mobile services; however, mobile traffic is still growing at an unprecedented rate and the need for more sophisticated broadband services is pushing the limits on current standards to provide even tighter integration between wireless technologies and higher speeds. In [7] to meet the expected growth of wireless communications traffic, both efficient transmission schemes and additional spectrum allocations are needed. To support highly increasing traffic capacity and to enable the transmission bandwidths needed to support very high data rates, 5G will extend the range of frequencies used for mobile communication including indoor propagation environments [8] [9] [10] [11]. The emerging technology 5G will use to enable mobile networks and devices to make better spectrum resources and will be expected to reach the mobile data to gigabits per second [12]. Recently the research work in propagation channel modelling is to understand the mechanisms of the propagation and the behaviour of the channel at frequencies above 6 GHz which had been published in [13-15].
Channel behaviour is identified by many parameters, in which the most important are path loss, received power and delay spread. In this paper the propagation channel behaviour is examined at three frequencies including: 26, 28 and 60 GHz using ray tracing commercial software called Wireless Insite. Channel modelling in [16] has used two frequencies: 28 and 73 GHz, however the study did not explain the propagation materials properties and different antenna radiation patterns at both transmitter and receiver.

In this paper the simulation environment for indoor-indoor propagation includes corridors in the 3rd floor Chesham building, University of Bradford, while for indoor-outdoor propagation includes route outside the Chesham building and a transmitter inside the building, which provides the comparisons of these metrics at 5.8, 26, 28 and 60GHz. The model includes the full description of buildings in terms of materials used where path loss, the received power and delay spread are evaluated.

Section II summarized the investigated wireless channel characteristics, in section III simulation setup is presented, while in section IV simulation results are discussed, and finally conclusion is drawn in section V.

II. WIRELESS CHANNEL CHARACTERISTICS

In this section the investigated propagation characteristics are introduced including: path loss model, received power and delay spread.

1. Path loss model:

Path loss is the reduction in power density of an electromagnetic wave when it propagates from transmitter to receiver. Due to differences in environments, it's difficult to make a general propagation model with detailed parameters; thus it's widely accepted to adopt a model that covers the main propagation aspects with reasonable results, this model The most simple and general path loss (PL) is the nth power law [17]:

$$PL(d)[dB] = PL(d_0) + 10n\, log_{10}(d/d_0) + X\sigma \quad (1)$$

Where n is the path loss exponent which has different values as shown in table 1. d is the distance between the transmitter and the receiver, $X\sigma$ is Gaussian-distributed random variable with standard deviation σ dB for shadowing and $PL(d_0)$ is the reference path loss, In order to exclude the near field effect of the measurements, power is measured in the far field region of the antenna at d_0 (usually at 1 m) by applying Free space Friss formula or by empirical measurements [18]. reference path loss is given by [19]:

$$PL(d_0) = 20\log_{10}\left(\frac{4\pi f}{c}\right) + 20\log_{10}(d_0) - G_T - G_R \quad (2)$$

Where f, c, G_T and G_R are respectively: operating frequency, speed of light, transmitter gain and receiver gain.

Table 1: Path Loss exponent values for different environments for (0.9 GHz and 1.9 GHz) [20] [18].

Environment	n
Free space	2
Urban macro cells	3.7-6.5
Urban microcells	2.7-3.5
Shaded urban microcells	3-5
Suburban	3-5
Indoor (single floor)	1.6-3.5
Indoor (Multiple floors)	2-6
Store	1.8-2.2
Factory	1.6-3.3
House	3

2. Received Power:

The total received power can be obtained from the combination of the power for each ray path and the time average received power is given by [21]:

$$P_R = \sum_{i=1}^{N_P} P_i \quad (3)$$

Where in equation (3) N_P is the number of paths and P_i is the time average power for the i^{th} path, other methods including the effect of each path phase as [21]:

$$P_R = \left|\sum_{i=1}^{N_P} \sqrt{P_i} e^{-j\varphi_i}\right|^2 \quad (4)$$

Where φ_i is ith ray phase in radian.

While other models considers the paths coming from the same path to be combined with phase [22].

3. Delay Spread:

Delay spread σ_τ is defined as the square root of the second central moment which describes how the delays are spread with respect to the mean, Although in many cases delay spread is similar to mean delay (first moment where each path contributes proportional to its power), however in cases where NLOS propagation is dominant with large delay, the mean delay will provide a misleading indicator compared to the RMS delay. That is why σ_τ is widely used as a delay spread metric [23].

σ_τ calculates the energy of power for each ray path reached in time and defined as a delay spread [24].

$$\sigma_t = \sqrt{\frac{\sum_{i=1}^{N_p}(t_i - \bar{t})^2 P_i}{P_R}} \qquad (5)$$

Where t_i is the arrival time while $\bar{t}$ is the mean time of arrival. Table 2 presents typical Median RMS delay spread in different indoor environments.

Table 2: Median RMS delay spread in different environments [2]

Frequency	Environment	Median RMS delay spread (ns)
1.9 GHz	House	70
	Office	100
	Commercial	150
2.625 GHz	Office	11
	Corridor	18.53
	Air cabin	11.89
	Factory	69.2
3.7 GHz	House	22
	Office	38
	Commercial	145
5.2 GHz	House	23
	Office	60
	Commercial	190
60 GHz	Office	1.77

4. Angle of arrival

In terms of spectral based techniques, AOA estimation methods can be classified to Beamforming techniques and Subspace techniques [25]. The idea behind beamforming is to let the array pattern to steer (using the weighting vector) to scan all possible angles, the angle which has the maximum corresponding power is considered as the AOA [26], two major algorithms are using beamforming concept in localization, Bartlett Beamformer and Capon minimum variance method [26]. Subspace techniques consider the effectiveness of the signal space and noise space, compared to beamforming techniques, subspace techniques show better performance and higher resolution estimation even with low SNR [25]. Antenna arrays can be used to detect angel of arrivals, direction of arrival is used for many application including beamforming, localization and detection [27], DOA requires the use of antenna arrays which is makes the technique more expensive and more power consumption compared to time of arrival (TOA) and received signal strength (RSS) [28]; however it requires less equipment's as only two Access Points are required to give a localization [29]. DOA is suitable in mediums with heterogeneous mediums (like water) where the velocity of waves will be different compared to those in free space, TOA and RSS will give an error in location estimation while DOA is less affected, that is why is used in biomedical localization specially in human body [27].

III. SIMULATION SETUP

Simulations are conducted in the simulated environment of the third floor of Chesham building, University of Bradford. Where the transmitter is located on the third floor with three receiver routes representing LOS, NLOS and indoor to outdoor as shown in Figure 1:

The model was evaluated for three different scenarios such as same floor LOS '*Route 3*', same floor NLOS '*Route 1*' and indoor-outdoor '*Route 2*', as shown in Figure 1. The investigated frequencies includes 26, 28 and 60 GHz (100MHz bandwidth) which are promising frequencies to be adopted for 5G networks.

The transmitter with vertically polarization omnidirectional antenna radiation pattern was fixed at 1m height from the floor. Both route 1 and route 3 had 23 receivers point each with 0.6 m separation from each other and 1 m height of the floor, each route examines different corridor of the building. Route 2 is located on the ground floor outside of the building with 23 receiver points 2 m in height from the city floor. Receiver's sensitivity threshold was set to -160 dBm.
It is to be noted that the receivers in triangular shape of Route 1 as shown in Figure 1 is moving with an average velocity of 0.5 m/s, The properties of transmitter and receivers are described in table 3.
The model completed by a detailed modelling using three types of walls: the outer concrete wall with 30cm thickness, layered dry wall with 12cm thickness and wooden wall. Two types of door used which includes wooden door (office doors) and, glass door and the type of window used, glass made window. The floor and ceiling is 3m above the floor and the second ceiling is simulated 2.5m above the floor with 3cm thick made of dielectric material.

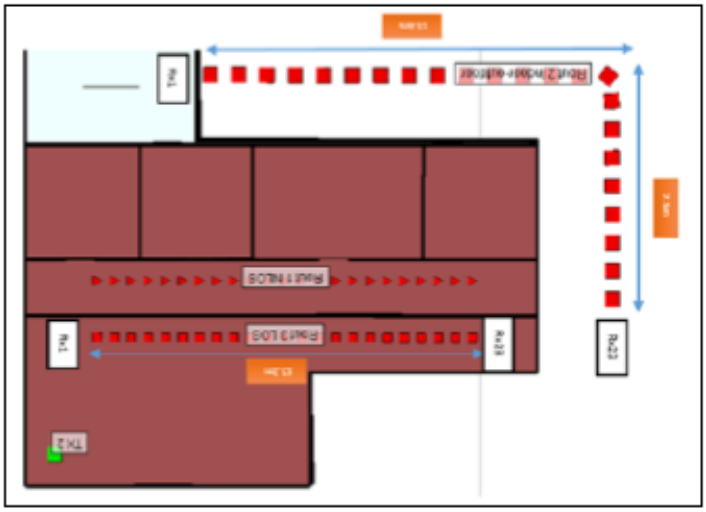

Figure 1: Floor layout with simulation routes and its dimensions.

Table 3: Properties of Transmitter and receiver antenna.

Properties	Transmitter antenna	Receiver Antenna
	Omnidirectional	Omnidirectional
Gain (dBi)	1.8	
Polarization	Vertical	Vertical
Waveform	Sinusoid	Sinusoid
Input Power (dBm)	23.0	-
E-Plane Half power bandwidth	90	
Temperature (K)	293.00	293.00
VSWR	1.00	1.00
Receiver Threshold	-160.00	-160.00

Received power are varying for each frequency due to path loss and due to reflection and transmission losses of material where its electrical properties are function of frequency, in table 4 material properties values with frequency is presented according to the ITU recommendations [2]. The ray tracing settings are set as in table 5.

Table 4 Material properties with frequency [2].

Frequency (GHz)	Concrete		Glass		Wood		Drywall	
	ε_r	σ	ε_r	σ	ε_r	σ	ε_r	σ

26	5.31	0.4557	6.27	0.1898	1.99	0.1544	2.94	0.1163
28	5.31	0.4838	6.27	0.2287	1.99	0.1672	2.94	0.1226
60	5.31	0.8967	6.27	0.5674	1.99	0.3784	2.94	0.2102

Table 5: Wireless Insite settings for the investigated scenario.

Property	Setting
Number of reflections	6
Number of transmissions	4
Number of diffractions	1
Number of reflections before first diffraction	3
Number of reflections after last diffraction	3
Number of reflections between diffractions	1
Number of transmission before first diffraction	2
Number of transmission after last diffraction	2
Number of transmission between diffractions	1
Ray tracing method	SBR
Propagation model	Full 3D

IV. RESULTS AND DISCUSSION

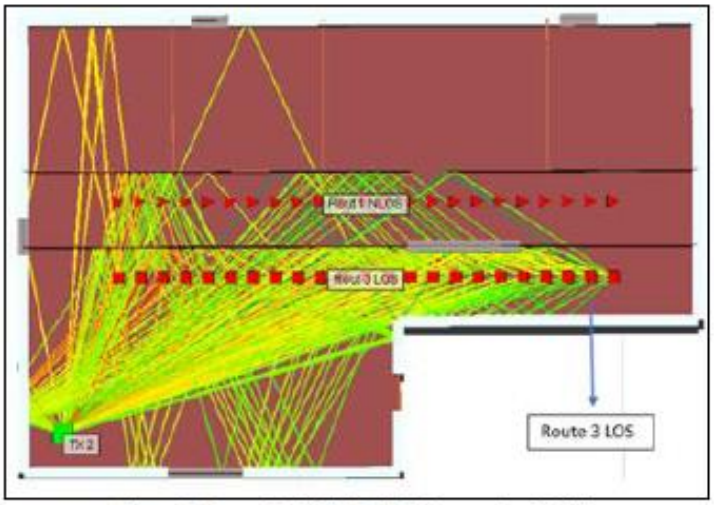

Figure 2: Route 3 (LOS) 3D SBR Propagation Model.

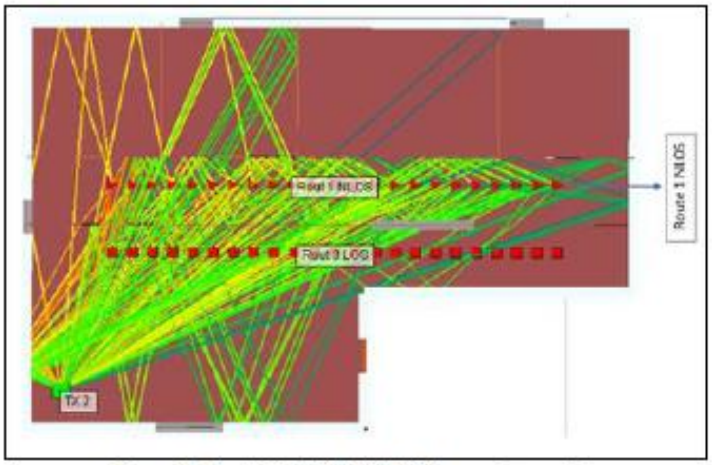

Figure 3: Route 1(NLOS) 3D SBR Propagation model

It is clear from the ray tracing in Figure 2 and Figure 3 that different materials interact with of rays differently. Some materials have less effect on signal attenuation compared to others. The low ratio of ray attenuation is from glass and layered dry wall. Comparatively for concrete walls, ray attenuations increases noticeably depending on wall thickness and the incident angle. In Figure 4 propagation paths for the indoor-outdoor scenario is presented, as expected longer paths tend to have lower signal strength.

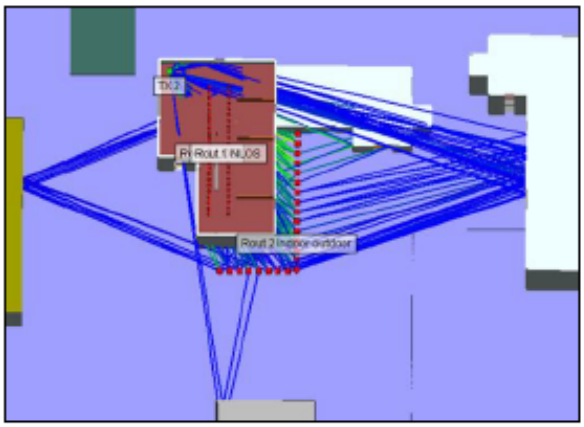

Figure 4: Route 2 (Indoor to outdoor) 3D SBR Propagation model.

Figure 5 illustrates the path loss against the Tx-Rx separation distance. The path loss data in Figure 5 (a-c) is route 3 between -68 dB to -96 dB, route 1 -71 dB to -99 dB and route 2 is -89 dB to -116 dB. The path loss here increases because of the position of the receiver routes, distance between Tx-Rx and multipath channel propagation.

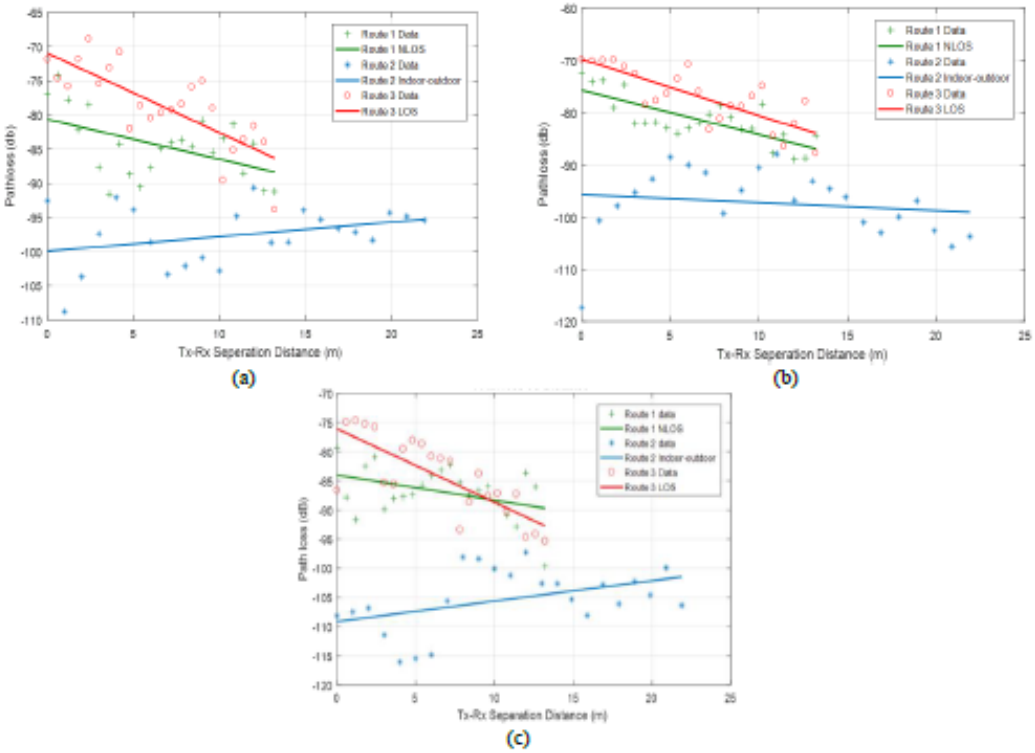

Figure 5: Path loss vs Tx-Rx separation distance for LOS, NLOS, Indoor-outdoor at (a): 26, (b): 28 and (c): 60GHz

A simple slop channel model (solid lines) which represents polynomial fitting was adopted to summarise the results in Figure 5. It is shown in the simulated results that the path loss maximum variation (in dB) found for route 3, route 1, route 2 respectively are between ±4, ±5 and ±8 at 26 GHz, ±4, ±3 and ±6 at 28 GHz and GHz ±6, ±7 and ±8 at 60.

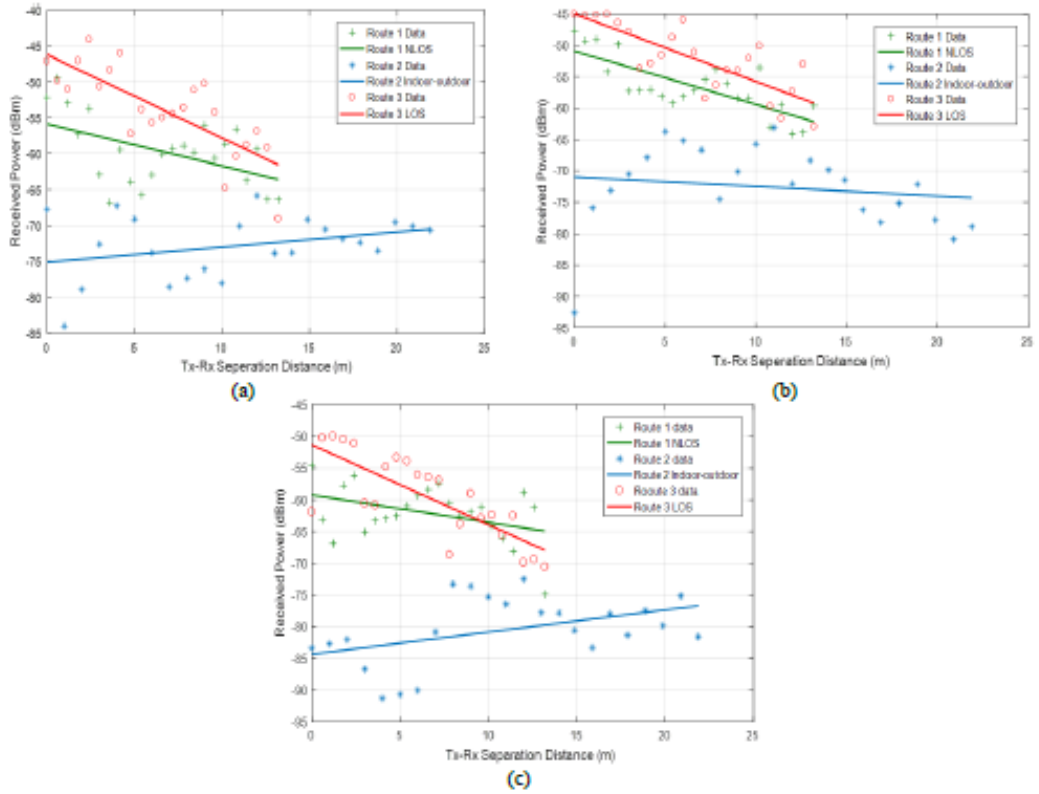

Figure 6: Received power vs Tx-Rx separation distance for LOS, NLOS, Indoor-outdoor at (a) 26 GHz, (b) 28 GHz and (c) 60GHz.

Figure 6 shows the received power at each receiver point against the Tx-Rx separation distance. The average result with curve fitting for route 3, the received power data in Figure 6 is between -44 dBm to -70dBm, route 1 -48 dBm to -75 dBm and for route 2 is -62 dBm to -92 dBm. The average power here at each receiver point is decreases because of the distance, nature of frequency and multipath channel propagation.

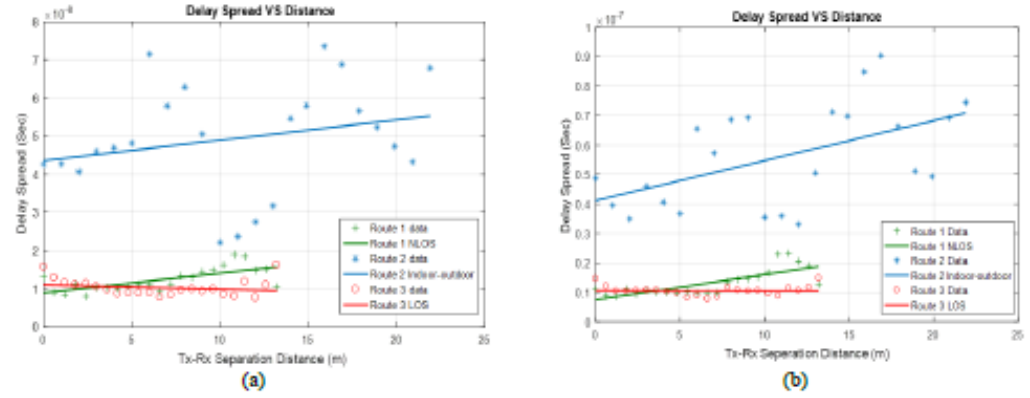

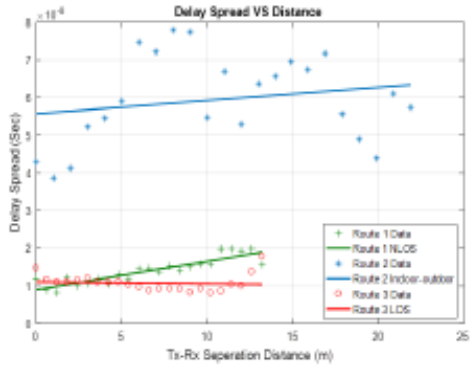

(c)

Figure 7: Delay Spread vs Tx-Rx separation distance for LOS, NLOS, Indoor-outdoor at (a) 26 GHz, (b) 28 GHz and (c) 60GHz.

Figure 7 shows a comparison between the performance of the three different frequencies using omnidirectional antenna for route 3, route 1 and route 2. It can be observed that at 26GHz the delay spread is higher than at 28 GHz and 60GHz especially for route 2. The delay spread for route 2 is much higher as compared to route 3 and 1 because of the height of the transmitter and large number of materials assumptions used between them. The initial rise is due to the position of the receivers with respect to the transmitter antenna. For LOS at higher separation distance the travel time of all multipath components are mostly the same, resulting much smaller delay spread between each receiver point.Figure 8 shows a comparison between the mean direction of arrival of the examined frequencies using omnidirectional antenna for route 3, route 1 and route 2. Figure 8(a) presents the arrival direction at 26 GHz in which the true angle found where the ray arrives at the receiver point in simulation is 70-160 degrees, 75-160 degrees and 80-160 degrees respectively. Followed the same procedure the direction of arrival for 28GHz and 60 GHz is found in Figure 8(b) and Figure 8(c).

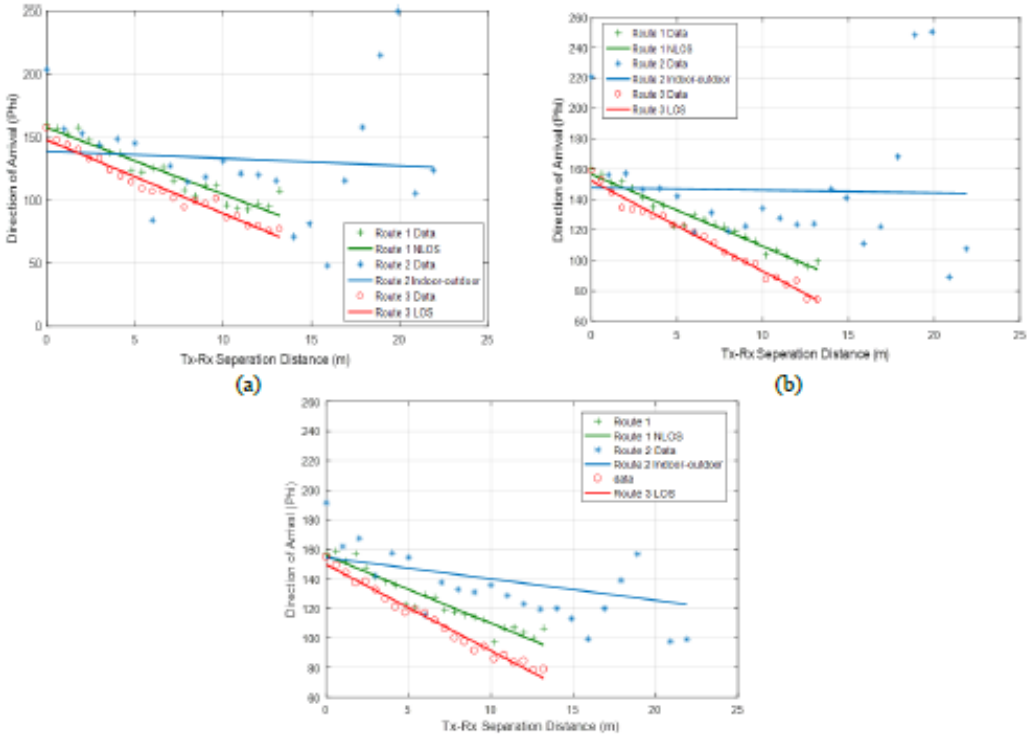

(a) (b)

(c)

Figure 8: Mean Direction of Arrival vs Tx-Rx Separation distance(m) for LOS, NLOS, Indoor-outdoor with linear fitting and at frequencies (a) 5.8GHz, (b) 26GHz, (c) 28GHz and (d) 60GHz.

V. CONCLUSIONS

Indoor-indoor and indoor-outdoor including line of sight (LOS) and Non-line of sight (NLOS) propagation channel are investigated for three different mm wave spectrum. The effect of building materials, multipath effects and channel characteristics such as path loss, received power, direction of arrival and delay spread at separation distance in (m) from transmitter (Tx) to receiver (Rx) has been presented. It has been observed that signal is much more effected by concrete walls, also reacting differently for LOS and NLOS at each particularized frequency. Another important aspect is the position of the receivers, transmitter antenna directivity and the distance between TX-RX. The results shown that path loss behaves at higher frequency and due to the number of obstructions while the received power and delay spread decreases by increasing frequency.

REFERENCES

[1] K. Chandra, Z. Cao, T. M. Bruintjes, R. V. Prasad, G. Karagiannis, E. Tangdiongga, *et al.*, "mCRAN: a radio access network architecture for 5G indoor communications," in *Communication Workshop (ICCW), 2015 IEEE International Conference on*, 2015, pp. 300-305.

[2] I. T. U. ITU, "Propagation data and prediction methods for the planning of indoor radiocommunication systems and radio local area networks in the frequency range 900 MHz to 100 GHz," in *Recommendation ITU-R P.1238-7*, ed. Geneva: ITU, 2012.

[3] L. W. Barclay, *Propagation of radiowaves* vol. 502: Iet, 2003.

[4] R. Janaswamy, *Radiowave propagation and smart antennas for wireless communications*: Springer Science & Business Media, 2001.

[5] M. V. S. Mr. ANIL KUMAR KODURI , Mr. M. KHALEEL ULLAH KHAN, ""Propagation Characteristics of a Mobile Radio Channel for Rural, Suburban and Urban Environments"," *IPASJ International Journal of Electronics & Communication (IIJEC)*, vol. 2, 2014.

[6] H. Ling, R.-C. Chou, and S.-W. Lee, "Shooting and bouncing rays: Calculating the RCS of an arbitrarily shaped cavity," *IEEE Transactions on Antennas and propagation,* vol. 37, pp. 194-205, 1989.

[7] K. B. J. Medbo, K. Haneda , V. Hovinen, T. Imai, J. Järvelainen, T. Jämsä, ""Channel Modelling for the Fifth Generation Mobile Communications"," presented at the Antennas and Propagation (EuCAP), 2014 8th European Conference on, The Hague, Netherlands, 2014.

[8] Z. Cao, X. Zhao, F. M. Soares, N. Tessema, and T. Koonen, "38-GHz Millimeter Wave Beam Steered Fiber Wireless Systems for 5G Indoor Coverage: Architectures, Devices and Links," *IEEE Journal of Quantum Electronics,* 2016.

[9] M. K. Samimi and T. S. Rappaport, "Characterization of the 28 GHz millimeter-wave dense urban channel for future 5g mobile cellular," *Technical Report, TR 2014-001,* 2014.

[10] G. R. Maccartney, T. S. Rappaport, S. Sun, and S. Deng, "Indoor Office Wideband Millimeter-Wave Propagation Measurements and Channel Models at 28 and 73 GHz for Ultra-Dense 5G Wireless Networks," *IEEE Access,* vol. 3, pp. 2388-2424, 2015.

[11] A. A. AlAbdullah, N. Ali, H. Obeidat, R. A. Abd-Alhmeed, and and S. Jones, "Indoor millimetre-wave propagation channel simulations at 28, 39, 60 and 73 GHz for 5G wireless networks," presented at the Internet Technologies and Applications (ITA), Wrexham, United Kingdom, 2017.

[12] S. Sun, G. R. MacCartney, and T. S. Rappaport, "Millimeter-wave distance-dependent large-scale propagation measurements and path loss models for outdoor and indoor 5G systems," in *Antennas and Propagation (EuCAP), 2016 10th European Conference on*, 2016, pp. 1-5.

[13] M. K. S. Sijia Deng, Theodore S. Rappaport, ""28 GHz and 73 GHz millimeter-wave indoor propagation measurements and path loss models"," presented at the Communication Workshop (ICCW), 2015 IEEE International Conference on, London, UK, 2015.

[14] T. S. R. Shu Sun, Rimma Mayzus, ""Millimeter Wave Mobile Communications for 5G Cellular: It Will Work!"," pp. 335 - 349, 2013.

[15] T. S. R. Sundeep Rangan, Elza Erkip, ""Millimeter-Wave Cellular Wireless Networks: Potentials and Challenges"," vol. 102, 2014.

[16] T. S. R. GEORGE R. MacCARTNEY, D SIJIA DENG, ""Indoor Office Wideband Millimeter-Wave Propagation Measurements and Channel Models at 28 and 73 GHz for Ultra-Dense 5G Wireless Networks," *SPECIAL SECTION ON ULTRA-DENSE CELLULAR NETWORKS*, vol. 3, 2015.

[17] M. Lott and I. Forkel, "A multi-wall-and-floor model for indoor radio propagation," in *Vehicular Technology Conference, 2001. VTC 2001 Spring. IEEE VTS 53rd*, Rhodes, Greece, Greece, 2001, pp. 464-468.

[18] T. S. Rappaort, *Wireless communications: principles and practice*, 2 edition ed. Upper Saddle River, NJ, USA: Prentice Hall, 2002.

[19] S. Saunders and A. Aragón-Zavala, *Antennas and Propagation for Wireless Communication Systems: 2nd Edition*: John Wiley & Sons, 2007.

[20] A. Goldsmith, *Wireless communications*: Cambridge university press, 2005.

[21] R. A. Valenzuela, O. Landron, and D. Jacobs, "Estimating local mean signal strength of indoor multipath propagation," *IEEE transactions on vehicular technology*, vol. 46, pp. 203-212, 1997.

[22] REMCOM, "Wireless InSite Reference Manual," 3.1.0 ed. State College, Pennsylvania: REMCOM, 2017.

[23] J. S. Seybold, *Introduction to RF propagation*: John Wiley & Sons, 2005.

[24] S. Salous, *Radio Propagation Measurement and Channel Modelling*: John Wiley & Sons, 2013.

[25] J. Foutz, A. Spanias, and M. K. Banavar, "Narrowband direction of arrival estimation for antenna arrays," *Synthesis Lectures on Antennas*, vol. 3, pp. 1-76, 2008.

[26] H. Krim and M. Viberg, "Two decades of array signal processing research: the parametric approach," *Signal Processing Magazine, IEEE*, vol. 13, pp. 67-94, 1996.

[27] R. Zekavat and R. M. Buehrer, *Handbook of position location: Theory, practice and advances* vol. 27: John Wiley & Sons, 2011.

[28] N. Patwari, J. N. Ash, S. Kyperountas, A. O. Hero III, R. L. Moses, and N. S. Correal, "Locating the nodes: cooperative localization in wireless sensor networks," *Signal Processing Magazine, IEEE*, vol. 22, pp. 54-69, 2005.

[29] H.-C. Chen, T.-H. Lin, H. Kung, C.-K. Lin, and Y. Gwon, "Determining RF angle of arrival using COTS antenna arrays: a field evaluation," in *MILITARY COMMUNICATIONS CONFERENCE, 2012-MILCOM 2012*, 2012, pp. 1-6.

URSI Festival of Radio Science (FRSci-2017), Faculty of Engineering and Informatics, University of Bradford, 10am – 5pm on 5 December 2017, Session 2, paper No. 5.

Indoor/Indoor and Indoor/Outdoor Propagation Channel Simulations at 28GHz and 60GHz with Different Antenna Radiation Pattern

Waqas Manan, Ali Abdullah, Huthifa Obeidat, Raed A. Abd-Alhameed, Steve M. Jones
Faculty of Engineering and informatics, University of Bradford, United Kingdom

As 5G will be the new technology that will enable networks and devices for better spectrum resources and it is expected to reach several Gbits/s data rates in supporting the mobile and wireless applications. Recently more work on the propagation channel modelling was applied to understand the mechanisms of the propagation and the behaviour of the channel at frequencies above 6GHz [1-3]. In addition the channel modelling in [4], two frequencies 28 and 73GHz were investigated, in which the study did not include the propagation materials properties and antenna radiation patterns at both transmitter and receiver. In this paper the propagation channels behaviour at two frequencies: 28 and 60GHz are intensively investigated using ray tracing software package.

The characteristics of indoor and indoor-outdoor channels are investigated for vertical polarized directional, omnidirectional and isotropic antennas pattern under two proposed mm-wave frequencies. Chesham building at Bradford University was considered as a model for this study. Various routs were considered, these are Route 1 non-line of sight (NLOS), Route 2 indoor-outdoor scenarios and Route 3 line of sight (LOS) as shown in Figure 1. The simulated data achieved from the 3-D Wireless Insite (Software Package) based on the effect of frequency dependant electrical properties of building materials stated in [5]. These include reflections, penetrations and diffractions of walls and objects. It has been observed that signal is much affected by the nature of building materials, frequency and radiation pattern for LOS and NLOS. A simple slope channel model was adopted to summarize the results as shown in Figs 2 and 3. It is clearly shown that the maximum variations of the received power for example at 28 GHz found approximately between ±3dBs, ±6.5dBs and ±10dBs respectively to LOS rout 3, NLOS rout 1 and NLOS rout 2. Similarly, the max power variations for 60 GHz were computed as ±4dBs, ±4.3dBs and ±11dBs respectively to rout 3, rout 1 and rout 2. The delay spread also found to follow similar tone of changes for both 28 and 60 GHz.

Figure 1: Office building with simulation Routes

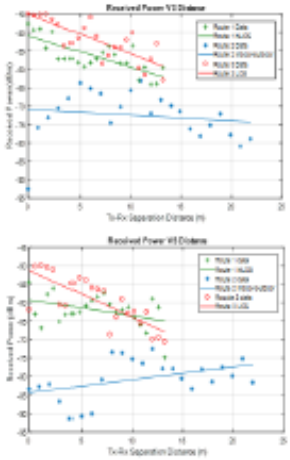

Figure 2: Received power versus distance at 28GHz (top) and 60GHz (below)

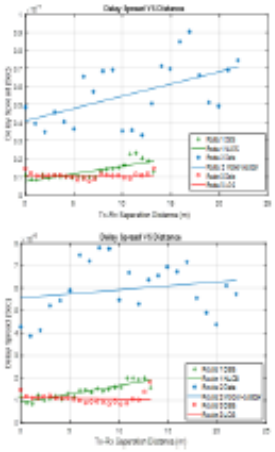

Figure 3: Delay spread versus distance at 28GHz (top) and 60GHz (below)

1. Sijia Deng, M.K.S., Theodore S. Rappaport, *"28 GHz and 73 GHz millimeter-wave indoor propagation measurements and path loss models"*, in *Communication Workshop (ICCW), 2015 IEEE International Conference on*. 2015, IEEE: London, UK.
2. Sundeep Rangan, T.S.R., Elza Erkip, *"Millimeter-Wave Cellular Wireless Networks: Potentials and Challenges"*. 2014. 102.
3. Theodore S. Rappaport, G.R.M.J., Shu Sun, Hangsong Yan, and Sijia Deng, *"Overview of Millimeter Wave Communications for Fifth-Generation (5G) Wireless Networks-with a focus on Propagation Models"*, in *IEEE Transactions on Antennas and Propagation, Special Issue on 5G*. 2017.
4. GEORGE R. MacCARTNEY, T.S.R., D SIJIA DENG, *"Indoor Office Wideband Millimeter-Wave Propagation Measurements and Channel Models at 28 and 73 GHz for Ultra-Dense 5G Wireless Networks*. SPECIAL SECTION ON ULTRA-DENSE CELLULAR NETWORKS, 2015. 3.
5. *"5G; Study on channel model for frequencies from 0.5 to 100 GHz (3GPP TR 38.901 version 14.1.1 Release 14)"* ETSI TR 138 901, 2017.